Volcanology of the Owharoa and Waikino ignimbrites, Waihi, Coromandel Volcanic Zone

A thesis submitted in partial fulfilment
of the requirements for the degree
of
Masters of Science (Technology)
in Earth Sciences
at
The University of Waikato
by

Hannah Alice Julian

The University of Waikato
2016

THE UNIVERSITY OF
WAIKATO
Te Whare Wānanga o Waikato

Abstract

The Waihi Caldera (Coromandel Volcanic Zone) is defined by a 15 km diameter gravity anomaly, which was active during the Pliocene and has been infilled by a 1.5 km-thick succession of volcanic deposits and lake sediments. The Owharoa and Waikino ignimbrites are both suspected to have been a product of the Waihi Caldera (Brathwaite & Christie, 1996). The aim of this study was to determine and compare the eruption and emplacement processes of the Owharoa and Waikino ignimbrites.

The ignimbrites were characterised in the field by facies analysis and dated by U-Pb zircon dating using laser ablation inductively coupled plasma mass spectrometry. Their petrographic characteristics were described by optical microscopy, scanning electron microscopy and X-ray powder diffraction. Geochemical characteristics were identified by electron microprobe analysis (on minerals and glass shards) and X-ray fluorescence spectrometry (on pumice and bulk ignimbrite).

The Owharoa Ignimbrite (3.76 ± 0.05 Ma, Vincent, 2012) is poorly sorted with variable degrees of welding degrees. Facies identified include pumice-rich and lithic-rich facies (O1), flattened pumice rich facies (O2), lithic rich, pumice poor facies (O3), dark grey, densely welded, fiamme rich facies (O4) and pumice rich facies (O5). Juvenile clasts include creamy rounded woody-textured pumice in the east, and dark to black, lensoidal, glassy fiamme in the west with quartz and plagioclase phenocrysts. Lithic clasts include volcanic lithics (rhyolite, andesite, and ignimbrite), and occasional sedimentary lithics (sandstone/siltstone).

The Waikino Ignimbrite (3.48 +/- 0.19 Ma) is a finer-grained, relatively well sorted, massive, glass shard matrix-rich (~93%) ignimbrite that is separated into two facies, W1, a softer, massive yellow basal facies; and W2 a grey, well welded, massive facies. The pumice within the Waikino Ignimbrite (1%) was no larger than coarse ash-sized, white fragments. The Waikino Ignimbrite had plagioclase, quartz, biotite (larger than the Owharoa Ignimbrite) and opaque minerals. Geochemically the Waikino Ignimbrite was rhyolitic with higher alkali content than the Owharoa Ignimbrite.

The Owharoa Ignimbrite represents the deposit of an intra-caldera, pulsating depositional pyroclastic flow that shows subtle variations in pumice and lithic

abundance. The massive nature of the Waikino Ignimbrite indicates a consistent, steady pyroclastic flow, derived from an intensely fragmented magma to form a glass shard-rich, pumice-poor deposit. Both ignimbrites were sourced from the Waihi Caldera due to their proximity to the caldera, the lithic characteristics and their similar geochemistry and mineralogy. The closeness in age of the ignimbrites signifies the relationship between the deposits, and relationship they have with the Waihi Caldera. It is possible that the Waikino Ignimbrite was the last major eruption from the Waihi Caldera, therefore the end of the duration of the caldera can be identified as after the Waikino Ignimbrite eruption at 3.48 +/- 0.19 Ma.

Acknowledgements

Thank you to all the dedicated people who contributed to this study.

Adrian Pittari – Thank you for being my supervisor for this study. Thank you for your constant patience and understanding throughout this process. I am grateful for all the assistance you provided.

Also thank you Roger Briggs for being an invaluable source of knowledge and information about my field area and being a constant support when a hand was required.

Thanks to Elizabeth Cook for being a great field companion, co-pilot and supporter through our studies.

Thank you to Renat Radosinsky, Annette Rogers, Ian Schipper (Victoria University of Wellington), Helen Turner and Kirsty Vincent for their technical support and vital advice during the duration of this study.

Thank you to Jasmine Robinson for her assistance in the field and comical relief.

Thank you to Damian Beachen for his assistance in the field and being the primary rock crusher.

Thank you to my family and friends who have supported me through this time.

I would also like to extend my thanks for the Broad Memorial Fund Scholarship, the Waikato Graduate Women's Masters Study Award and University of Waikato Masters Research Scholarship for their contributions towards this study

Table of Contents

List of Figures

Chapter 1: Introduction

Chapter 2: Literature review

Chapter 4: Stratigraphy and facies description

Chapter 5: Petrography

Chapter 6: Geochemistry

Chapter 7: Discussion

List of Tables

Chapter 5: Petrography

Chapter 7: Discussion

Chapter 1: Introduction

1.1. Overview

The Coromandel Volcanic Zone (CVZ) was the precursor volcanic region to the Taupo Volcanic Zone (TVZ) within New Zealand. The CVZ was active between 18 to 1.8 Ma (Nicholson *et al.*, 2004) and underwent bimodal andesitic-dacitic-rhyolitic volcanism. Silicic caldera centres are identified in the CVZ, dominantly along the eastern Coromandel peninsular (Briggs *et al.*, 2005).

A major focus of previous studies of the CVZ has been based on the gold-bearing andesitic host rock found in the area (e.g. Brathwaite *et al.*, 2006, Brathwaite *et al.*, 1989, Bell & Fraser, 1912), and the wider tectonic-forming processes including those associated with the migration of volcanism to the current TVZ (e.g. Briggs *et al.*, 2005, Cole, 1990, Brathwaite, 1989, Skinner, 1986). A significant knowledge gap lies within understanding the volcanological processes of the younger, felsic volcanic units and how these deposits contribute to the volcanic history of the area. These volcanic units include the ignimbrites of the Ohinemuri Subgroup (of the Whitianga Group), including the Owharoa and Waikino ignimbrites which are the focus of this study.

An important volcanic structure in the southern CVZ is the Waihi Caldera which has provided an underlying structure for the Waihi Basin, recently identified using gravity surveys by Smith *et al.*, (2006). This caldera is one of the southernmost, younger silicic centres in the CVZ. The Waihi Caldera has been buried by three kilometres of sediment. It is likely that the Owharoa Ignimbrite and/or the Waikino Ignimbrite are deposits from the Waihi Caldera and these deposits could give insight into the formation, structure and volcanic processes of the caldera.

The Owharoa and Waikino ignimbrites are found throughout the south-east of the Karangahake Gorge and through the surrounding Waihi area. The area was most recently mapped and described by Brathwaite and Christie (1996). The Owharoa Ignimbrite is a densely welded, pumice and fiamme-rich member of the Ohinemuri Subgroup (Braithwaite & Christie, 1996). The Waikino Ignimbrite is a fine grained, welded ignimbrite with little pumice. The Owharoa Ignimbrite directly underlies the Waikino Ignimbrite, which is the youngest of the Ohinemuri Subgroup deposits. Furthermore the Owharoa and Waikino ignimbrites show

significant differences between their composition, texture and appearance. The reason why there are two contrasting ignimbrites from the same caldera system is not known.

1.2. Objectives

This study aims to interpret the volcanic processes of the Owharoa and Waikino ignimbrites, to better understand the volcanic history of the Waihi-Waikino area, associated with the Waihi Caldera. This study will attempt to make correlations between the evolution and volcanic processes that occurred at the Waihi Caldera. The Waihi Caldera is presumed to have been active between 4.5 - 3 Ma (Briggs *et al*., 2005) and is related to the younger CVZ activity occurring within the Waihi-Waikino area. The caldera is the most likely source for the Owharoa and Waikino ignimbrites. The Owharoa Ignimbrite has been dated by Vincent (2012) to be 3.76 ± 0.05 Ma using U-Pb zircon dating, and the Waikino Ignimbrite's age is unknown.

Rhyolitic ignimbrite deposits from calderas in the CVZ are comparable to other examples of rhyolitic volcanism within New Zealand dominantly in the TVZ. The geology of the wider Waihi area has been mapped on both 1:250,000 (Edbrooke, 2001) and 1:50,000 scale (Braithwaite & Christie, 1996), however the internal stratigraphy and facies characteristics of individual volcanic units are not known. The objectives for this study therefore are;

- To document the stratigraphic relationship and facies architecture of the Owharoa and Waikino ignimbrites.
- To date the Waikino Ignimbrite using the U-Pb zircon dating method.
- To document the petrographic characteristics of the deposits
- To analyse the geochemical composition of the deposits

The objectives will be carried out on the Owharoa and Waikino ignimbrites at multiple sites throughout the Waihi-Waikino region, and each objective will be addressed in separate chapters within this study.

1.3. Location

This study is being undertaken within the Waihi-Waikino district, located within the North Island of New Zealand (Figure 1.1). An important region of focus within the field area is the Karangahake Gorge, which is comprised of gold bearing andesite and overlying ignimbrites – one of these ignimbrites is the Owharoa Ignimbrite. The Waikino Ignimbrite is found further east dominantly on the farming plains of the Waihi Basin which overlies the Waihi Caldera.

Figure 1.1. Map highlighting the sector of the North Island encompassing the field area (Google Earth 2016). Red outlined box highlights the field area.

1.3.1. Land use

Within the Karangahake Gorge (Waikino area) to the west of the field area, the land is a rugged, hillscape terrain. The area is a part of the Hauraki Gold Trail walk and cycle way which uses the old gold mining excavation. The Owharoa Falls (a type section in this study) is a sight-seeing spot for travellers along the trail.

Further east in the field area farming dominates the landscape. Waihi is dominantly a farming and mining community. Martha Gold mine is central to the township. The township covers approximately 7 km^2, and the rest of the area is farmland. Farming practices includes beef, sheep and dairy.

1.4. Thesis outline

Chapter two will cover the regional geology and previous research carried out on the Owharoa and Waikino ignimbrites. Chapter three will describe the methods used within the study. Chapter four will cover the stratigraphy and facies architecture identified within the field and include a new U-Pb zircon age for the Waikino Ignimbrite. Chapter five will follow on from Chapter four, covering the petrographic analysis and mineralogical descriptions. Chapter six will then discuss the results from the geochemical analyses. Chapter seven will discuss the volcanic processes of the Owharoa and Waikino ignimbrites, and the volcanic history of the Waihi Caldera.

Chapter 2: Literature Review

2.1 New Zealand tectonic setting

New Zealand occurs along an oblique, convergent plate boundary zone between the subducting oceanic Pacific plate and the over-riding Indo-Australian continental plate (Davey *et al.*, 1994). This results in a migrating arc volcanic environment within in the North Island (Stevens, 2010) and forms the Coromandel Volcanic Zone (CVZ) as the predecessor to the currently active Taupo Volcanic Zone (TVZ).

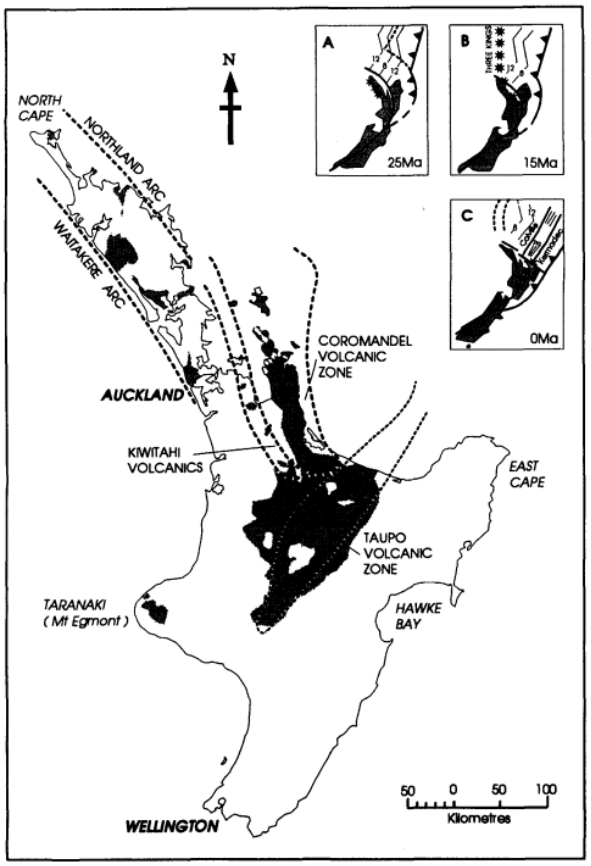

Figure 2.1: Map of the North Island, New Zealand, highlighting the three volcanic zones and the plate boundary migration over the last 25 million years (Adams et al., 1994).

The subduction zone boundary within New Zealand has moved over time, and can be constrained into three major time and spatial groups, along with a south eastward progression (Figure 2.1). The Northland Volcanic Zone (NVZ) was active between 25 and 15 Ma and was dominated by basaltic-andesitic eruptives. The CVZ was active between 16 and 2 Ma and was dominated by andesitic-rhyolitic volcanism. The currently active TVZ began volcanic activity 2 Ma, (Figure 2.1) is also dominated by andesitic and rhyolitic eruptives.

2.2 Coromandel Volcanic Zone and the associated geology

The CVZ is the largest and longest lived area of andesitic-rhyolitic volcanism within New Zealand, active from approximately 16 Ma to 1.8 Ma (Skinner, 1986). The north northwest-trending CVZ is a basement horst structure hosting arc volcanism related to the west northwest-dipping Pacific Plate beneath the Indo-Australian Plate (Skinner, 1986) which has resulted in a convergence subduction zone. The CVZ is therefore a product of Neogene arc volcanism over a fundamental horst structure (provided by the basement Jurassic deposits) on which both the volcanism and Neogene tectonics have been superimposed (Skinner, 1986).

The initiation of the CVZ occurred as the Indo-Australian and Pacific plate migration moved south-eastwards from the Northland Arc between 14 and 12 Ma (Nicholson, 2004) and caused a rapidly evolved volcanic arc setting (Booden *et al.*, 2012). As a result of the convergent subduction margin a mechanism for extension across the back arc region was created, causing an active Miocene arc with bimodal andesitic and rhyolitic volcanism (Nicholson, 2004).

The CVZ was active for approximately 14 million years and in that time created the volcanic rocks in the Coromandel peninsula preserved today, with parts of the extinct CVZ having being inundated (de Ronde *et al.*, 2005). To the west of the CVZ is the Hauraki Rift zone, a zone of crustal thinning, which is associated with the Hauraki Graben. The central region of the CVZ is the Coromandel Peninsula, which is comprised of andesitic mountain ranges through the central region of the peninsula and transitions into the dominantly andesitic Kaimai Ranges further south. East of the CVZ, along the coast line and low-lying areas of the Coromandel Peninsula and Tauranga, silicic centres have formed (Booden *et al*., 2012), including collapsed calderas which were initially suggested from satellite photography (Skinner, 1986). These calderas are associated with ring faulting and ignimbrite eruptions (Skinner, 1986). The CVZ continues offshore and has been researched using seismic analysis (Thrasher, 1986).

The Coromandel subduction zone can be associated with the westward-dipping Benioff zone, to depths up to 120 km beneath the Hauraki-Coromandel area (Hatherton, 1969). Brothers (1986) suggests that the north westward Hikurangi subduction orientation was responsible for the CVZ volcanism and its orientation. The focus of the CVZ has moved irregularly until the TVZ volcanism began

(Nicholson *et al.*, 2004). Changes in the pole of rotation of the Pacific plate (King, 2000) realigned the zones, and by 2 Ma the northeast-trending TVZ had established (Wilson et al., 1995).

The volcanic stratigraphic succession of the CVZ (Figure 2.2) was initially deposited on top of meta-sedimentary Mesozoic basement greywacke of the Waipapa Terrane (Booden *et al.*, 2012). The basement material has undergone extension, being faulted into a series of fault-angled depressions and grabens (Thrasher, 1986). The fault patterns within the CVZ are NNW- and NE-trending, and these fault trends are inherited from and were controlled by the Jurassic basement during the early Cretaceous period (Skinner, 1986).

On the surface of the CVZ, three dominant volcanic groups have covered the basement material, including the Mercury Basalts, the Coromandel Group and the Whitianga Group (Figure 2.2). The Mercury Basalts are not found within the main field area of this study and therefore will not be further discussed here.

CVZ volcanism began 18 Ma producing intermediate to mafic volcanism, dominantly in the north of the CVZ. While the Coromandel Peninsula was undergoing volcanic activity, so to was the offshore submarine Colville Ridge, spreading north-eastwards to the east of the Coromandel Peninsula (Cole *et al.*, 2015). Throughout the Miocene, volcanism along the Coromandel Peninsula was accompanied by volcanic activity along the Colville Ridge, which extends offshore to the northeast. Coromandel Peninsula was accompanied by volcanic activity along the Colville Ridge, which extends offshore to the northeast.

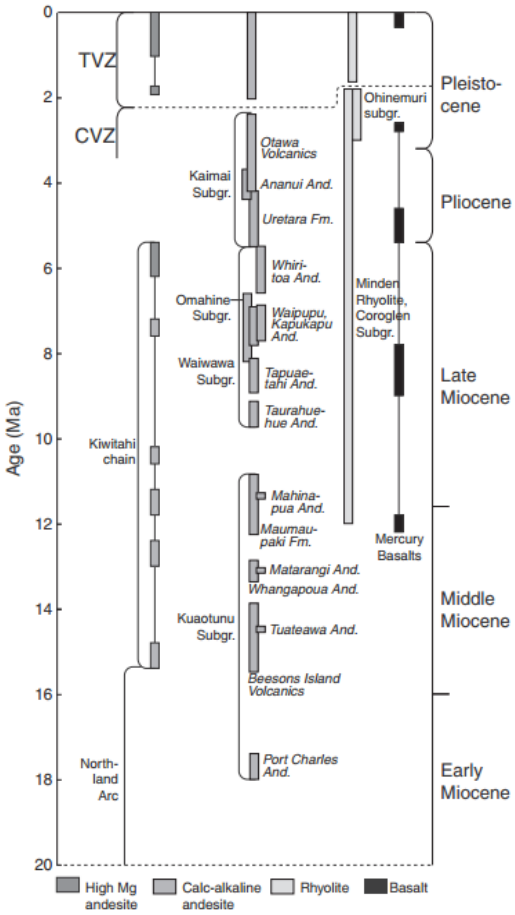

Figure 2.2: Volcanic stratigraphy of the Coromandel Volcanic Zone (Booden et al., (2012), based on Skinner (1986), Adams et al., (1994), Brathwaite & Christie (1996), Nicholson et al., (2004), Briggs et al., (2005))

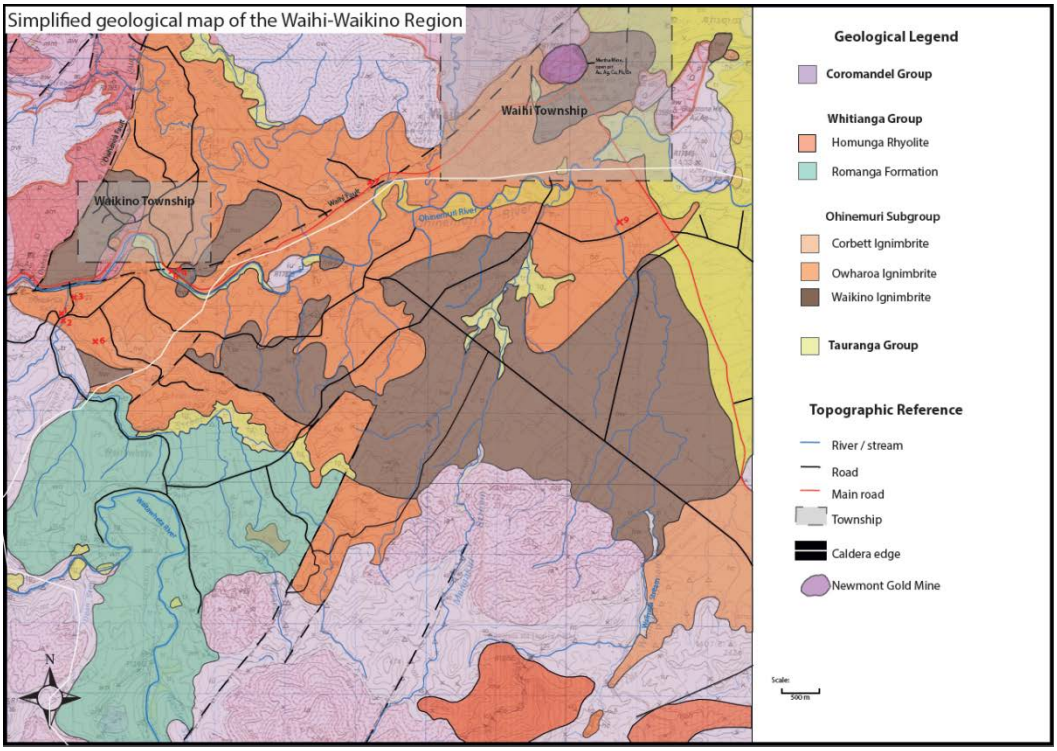

Figure 2.3: Simplified geological map derived from Brathwaite & Christie (1996). This map highlights the dominant deposits within the region, along with faults and main anthropogenic features.

Around 12 Ma rhyolitic volcanism began in the CVZ, probably as a result of progressive heating and melting of the crust associated with earlier andesitic volcanism and crustal extension (Cole *et al.*, 2015). The focal point of volcanism moved southwards towards the centre and south of the CVZ and began depositing the Coromandel Group. The Coromandel Group (Figure 2.3) consists of dominantly pyroxene or pyroxene-hornblende andesite with lesser dacite and rhyodacite (Skinner, 1986, 1993). This andesitic-dacitic volcanic sequence formed a continental volcanic arc more than 200 km long by 35 km wide (Black and Skinner 1979).

7-6 Ma was a dynamic stage for the CVZ which became the host to geothermal systems similar to those seen in the TVZ (Cole *et al.*, 2015). Mineral deposits (including gold and silver) were formed throughout the Waihi and Karangahake areas, which created the largest gold extraction sites in New Zealand (Figure 2.2). The hydrothermal activity ended around 6-5 Ma, before the deposition of the lake deposits in the Waihi region.

The Pliocene represents a very active volcanic stage for the CVZ. 5 Ma saw a change of activity through the wider CVZ where the Colville Ridge had separated

from the Kermadec Ridge, forming the Havre Trough in between the two ridges. The Havre Trough began to open due to the clockwise ration of the Hikurangi Margin. This produced a major change in the orientation of the plate boundary with subduction and its related volcanic activity shifting from the north trending Coromandel Arc to the northeast-trending TVZ (Cole *et al.*, 2015). The activity between the Colville and Kermadec Ridge matches the activity occurring between the CVZ and the TVZ (Cole *et al*., 2015).

In the late Miocene the focus of volcanism shifted from west to eastern central CVZ, moving south, with a change from composite stratovolcanoes to rhyolitic calderas, typified by widespread ignimbrite sheets and rhyolite dome complexes (Adams *et al.*, 1994). Bimodal basaltic-andesitic and rhyolitic volcanism was active from 12 to 7 Ma (Nicholson *et al.*, 2004), and was associated with the early deposits of the Whitianga Group.

Volcanism in Waihi occurred around 7-3 Ma, during in which a caldera formed and explosive rhyolitic volcanism occurred, which deposited thick welded ignimbrite deposits (Ohinemuri Subgroup, including the Owharoa and Waikino ignimbrites studied here). The volcanism in the CVZ ended just after 2 Ma (Carter *et al*., 2003), which is when the volcanism in the TVZ began.

Rhyolitic centres form an irregular north-south-trending (southward younging) volcanic chain (Booden *et al.*, 2012). Between ~6 – 2 Ma, the Whitianga Group (Figure 2.2) was deposited, and is comprised of the Minden Rhyolite, the Coroglen Subgroup (which consists of ignimbrites, pumice breccia and associated sediments) and the Ohinemuri Subgroup (which contains the Corbett, Owharoa and Waikino ignimbrites) (Brathwaite and Christie, 1996). These units can be seen in Figure 2.2, and dating through this study will constrain the upper time unit of the Ohinemuri Subgroup.

Lastly the Tauranga Group (Figure 2.3) consists of late Pleistocene alluvial and estuarine sediments, ignimbrite and tephra, post glacial sand dunes, estuarine deposits and alluvial fans which fill the Tauranga Basin (Brathwaite and Christie, 1996).

The transition from CVZ to TVZ (4-2 Ma) is considered to have occurred as a ‘seamless’ transition with no distinct changes or hiatuses, nor obvious changes in major element geochemistry, suggesting that either a continuation or overlapping interval occurred when both the CVZ and TVZ were active (Carter *et al.*, 2003).

2.3 Geology of the Waihi-Waikino region

The geology of the Waihi-Waikino region (Figure 2.3) is dominantly comprised of volcanic and hydrothermally altered deposits and sedimentary basin deposits. Seven million years ago there was active hydrothermal activity, forming substantial gold and silver deposits throughout the region. The volcanism in the Waihi region lasted through to approximately two million years ago (which is the literature-derived estimate for the Waikino Ignimbrite – the last deposit of the Ohinemuri Subgroup from Brathwaite and Christie (1996)), creating a range of andesite and rhyolite lavas and pyroclastic density current deposits.

Also there is an occurrence of a major magnetic anomaly centred seven kilometres southeast of the Waihi gravity anomaly (see Section 2.3.1), which may represent a buried intrusion at depth (Couper and Lawton, 1978; Stagpoole *et al*., 2001).

2.3.1 Waihi Caldera and associated Waihi Basin

Several calderas have been identified throughout the CVZ as large circular negative gravity anomalies (Skinner, 1986; Malengreau *et al.*, 2000), which are formed from regional extension and crustal thinning, a similar process seen in the TVZ. The Waihi Caldera was formally identified by Smith *et al*., (2006) using gravity anomaly data. The Waihi Caldera is associated with the initial formation of the Waihi Basin but had been previously suggested by Brathwaite and Christie (1996), Bromley (1991), Skinner (1986), Hunt and Syms (1977) and Woodward (1971). The Waihi Caldera is located just south of Waihi, and is defined as an asymmetric trapdoor caldera (Smith *et al*., 2006). The Waihi caldera site has a large concentration of post-rhyolite pyroxene andesite dykes and flows (Henderson and Bartrum, 1913; Skinner, 1986).

The Waihi Caldera is an approximately 15 km diameter negative gravity anomaly (Figure 2.4), with steep north and west sides and shallow east and south sides which has been infilled with relatively young volcanic material, including the Romanga Formation and Ohinemuri Subgroup ignimbrites forming the infill of the Waihi Basin (Smith *et al*. 2006). The basin is a semi-rectangular shape and has a deep floor which, when combined with the lighter density lake sediments and ignimbrite fill, could be associated with the fault-controlled Waihi caldera structure. The western scarp of this basin is defined by the Mangakino Fault, and the south dipping boundary coincides with the Waihi Fault (Smith *et al.*, 2006).

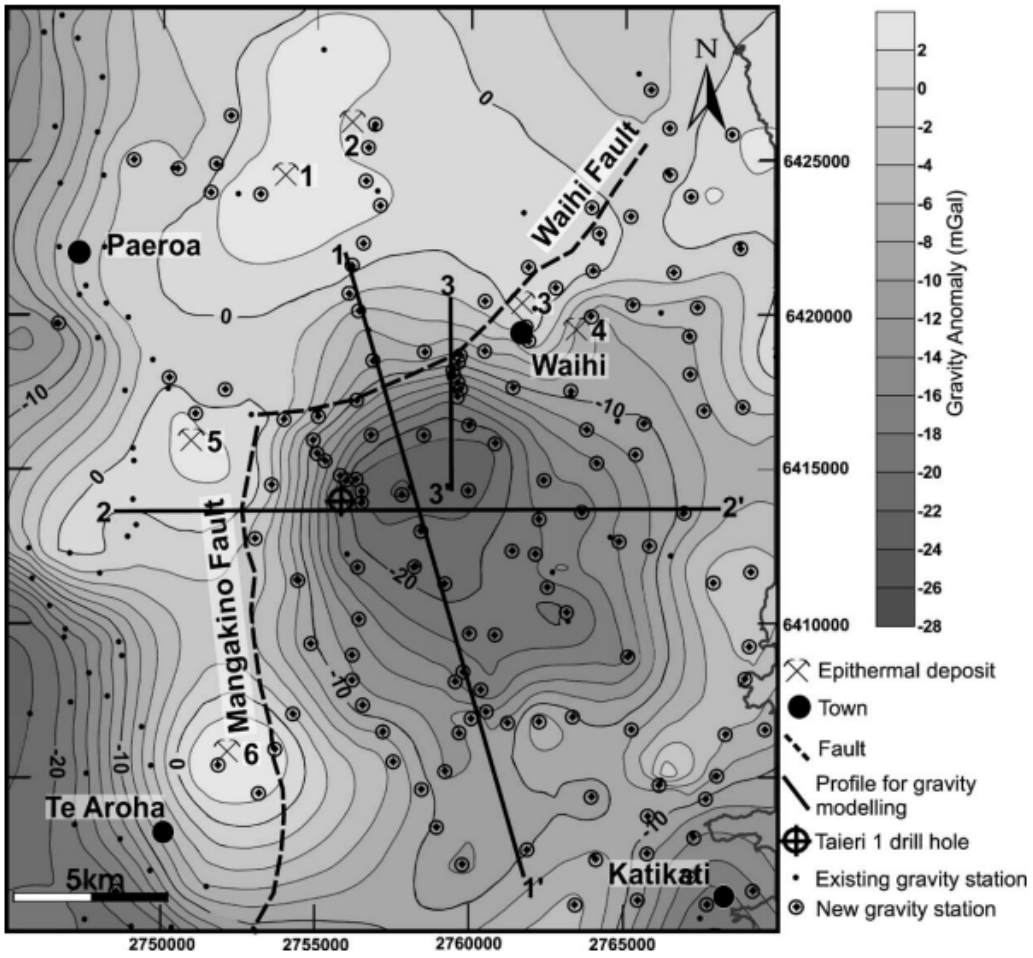

Figure 2.4. Gravity anomaly (mGal) map highlighting the infill material within the Waihi Caldera from Smith et al. (2006).

Subsidence of the caldera is suggested to have been caused by regional faults Brathwaite and Christie, 1996), as there appears to be a circle-like arrangement of faults which could indicate the rim of the caldera, identified within Figure 2.4.

Limited research on the Waihi Caldera has taken place as its burial beneath 3 km of sediment and volcanic deposits (Smith *et al.,* 2006) makes it inaccessible, however its confirmed presence could result in significant structural control on hydrothermal systems and the associated mineral deposition which have occurred throughout the area.

The Romanga Formation and Uretara Formation lake sediment deposits are also found in the Waihi region and may represent a lake that existed within the Waihi Caldera (Smith *et al.,* 2006). The Romanga Formation is the underlying unit underneath the Ohinemuri Subgroup ignimbrites (Brathwaite and Christie, 1996).

Magmatic sources discussed by Smith *et al.*, (2006) and suggests that if there is a magnetic anomaly that resulted from a pluton, it may have been the magma source for the caldera-forming eruption and the large volume of volcanic rocks filling the Waihi Basin, although the pluton must be at least 7 km south-east of the proposed caldera. Alternatively this magmatic anomaly may be related to the Ananui andesties, and there is another deeper body which postdates the formation of the Uretara Formation and Waihi Basin.

2.3.2 Faulting

There are several important faults located within the Waihi- Karangahake region which influence the geology of the area. These faults include the Waihi Fault, the Owharoa Fault, the Mangakino Fault and several small unnamed faults.

The Waihi Fault (seen in Figure 2.4) cuts the main body of the Owharoa Ignimbrite and parts of the Waikino Ignimbrite. It has a NNE trend (Braithwaite and Christie, 1996) although this is mainly inferred, and has a distinct topographical low in the landscape. The fault is displaced from 70 to 250 m.

The Mangakino Fault (seen in Figure 2.4) marks a clear boundary between these units; however, the location of the contact along the Waihi Fault is obscured by sheets of younger ignimbrites of the Whitianga Group (Brathwaite and Christie, 1996).

The Owharoa Fault is considered an important fault found within the ignimbrites by Rabone (1975). While the Owharoa Fault appears to be a single fault however it may be a more complex fault zone. West of the fault are local dacites and andesites and to the east, the younger ignimbrites.

Several small faults offset the ignimbrites and along these, immediately east of the Waikino Hotel, the faults are cut off to the south against an ENE-striking fault running parallel to the Ohinemuri River (Rabone, 1975).

The age of the fault that occur through the ignimbrites is poorly constrained however it is assumed that the activity was continuous from the mid Tertiary to the late Pleistocene (Rabone, 1975). Recent uplift at Karangahake Gorge and faulting of the late Pleistocene ignimbrites at Owharoa testify to the persistence of fault movements into very recent times (Rabone, 1975).

Fault ages are constrained based on evidence of hydrothermal activity. Smith *et al.*, (2006) summarised that most hydrothermal deposits are dated between 6-7 Ma.

There is no alteration in the Uretara Formation which formed 5.6 – 4.3 Ma, it indicates that hydrothermal systems were active prior to this deposition. The proximity of these deposits to the Ohinemuri and Mangakino Faults suggests that these faults pre-date or formed at the same time as the major hydrothermal phase, and before the caldera formation. Epithermal deposits and their associated alteration halos are not directly aligned along these faults.

2.4 Ohinemuri Sub-Group

The Ohinemuri Subgroup is part of the wider Whitianga Group, encompassing the Late Pliocene to Early Pleistocene ignimbrites of the Waihi Basin, including the Corbett, Owharoa and Waikino ignimbrites (Rabone, 1975). The Corbett Ignimbrite is the oldest of the Ohinemuri Subgroup ignimbrites, but is not included in this study.

Prior to 1975 the Owharoa and Waikino ignimbrites were classified as part of the wider Whitianga Group (Skinner, 1986), however Rabone (1975) highlighted a significant age difference between the units within the Whitianga Group (which were hydrothermally altered) which were distinctly different to the unaltered Owharoa and Waikino ignimbrites, and suggested a change, which prompted the formation of the Ohinemuri Subgroup by Brathwaite and Christie (1996).

2.5 Owharoa Ignimbrite

The Owharoa Ignimbrite has been recognised under different names since the first reference of the Owharoa ‘Wilsonite’ (Morgan, 1910). Names include the Owharoaite, the Tridymite rhyolite and the present Owharoa Ignimbrite (Marshall, 1935; Ewart and Healy, 1965; Rabone, 1971; Skinner 1986). In Marshall (1935), the Owharoa Ignimbrite was the unit in which Marshall first introduced the term ‘ignimbrite’ (Latin origin, ign (is) fire + imbr (is), imber shower of rain) into geological terminology.

2.5.1 Distribution

Earlier distribution mapping had been carried out by Bell and Fraser (1912), Morgan (1924), and most recently by Brathwaite and Christie (1996), and can be seen in Figure 2.3. The first clear description of the Owharoa Ignimbrite was

made by Marshall (1935) who stated that the Owharoa Ignimbrite was ‘composed of relatively large fragments of glass embedded in a matrix of stony appearance in which many clear and colourless crystals of feldspar and quartz can be distinguished’.

The Owharoa Ignimbrite has outcrops in the western and northern parts of the Waihi Basin, and is well exposed in the Owharoa area (Brathwaite and Christie, 1996). An isolated outcrop near Awangaro Stream, seven kilometres northwest of Owharoa indicates that the ignimbrite originally extended further west (Brathwaite and Christie, 1996) however this site was not located in this study. In the south of the basin, the ignimbrite is up to 80 m thick and overlies the Romanga Formation (Brathwaite and Christie, 1996).

2.5.2 Significance of the deposit

The Owharoa Ignimbrite represents the last phase of volcanism within the Waitekauri Valley (located within the Karangahake Gorge), causing infilling from the east into the base of the valley (Haworth, 1993). The Owharoa Ignimbrite is assumed to be sourced locally within the Waihi Basin making it an important deposit for the geological history of the area. It is well exposed naturally at sites such as the Owharoa Falls, and through mining and quarrying sites such as the Owharoa Quarry and the Waikino Quarry.

2.5.3 Identified characteristics

The Owharoa Ignimbrite was described by Brathwaite and Christie (1996) as a moderately to strongly welded, pumice rich, plagioclase-quartz-biotite lenticular ignimbrite which overlies the late Pliocene Romanga Formation lake sediments and underlies the Waikino Ignimbrite.

The Owharoa Ignimbrite contains small lithics of andesite, rhyolite and siltstone. There is also minor magnetite crystals present (Brathwaite and Christie, 1996).

The Owharoa Ignimbrite has reverse polarity (Brathwaite and Christie, 1996) and has been dated at 3.69 Ma by U-Pb on zircon (Hoskin *et al.*, 1998), and recently dated by Vincent (2012) using U-Pb dating at 3.76 +/- 0.05 Ma. Fission track/glass ages that resulted in 2.89 ± 0.38 Ma for the Owharoa Ignimbrite (Kohn 1973) which are significantly younger and are now considered incorrect (Briggs *et al.*, 2005). Therefore the more recent date of Vincent (2012) will be used for this study.

2.5.4 Unit and facies description

The lithological characteristics of the Owharoa Ignimbrite have been described in depth by Bull and McPhie (2007) and Rabone (1975). The Owharoa Ignimbrite was described as undeformed and consisting of four layers (Bull and McPhie, 2007):

- A lower, altered 'lenticulite' (breccia comprising of lenticle-shaped clasts) at least several meters thick (obscured base).
- A 4 m thick non-lenticle-bearing, fine grained layer of predominately flattened glass shards; vitric-rich tuff with minor plagioclase and hypersthene crystals (Rabone, 1975).
- A massive 15 m thick, jointed and devitrified layer.
- Remnants of a second 'lenticulite' layer which is weathered and poorly exposed, but is at least 16 m thick and is pumice rich (Rabone, 1975).

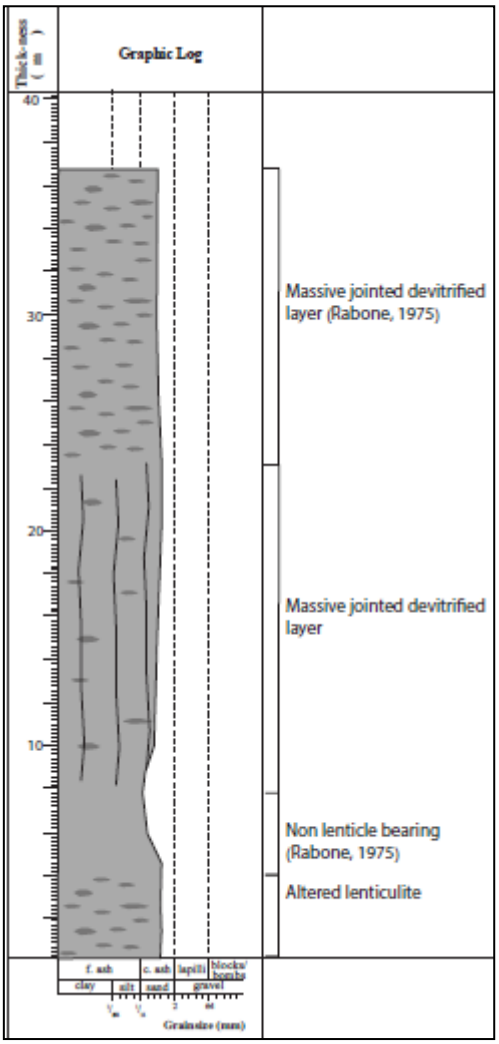

Figure 2.5. Stratigraphic column of the Owharoa Ignimbrite based on the observations of Rabone (1975).

White (1995) described a 175 + m section over three drill holes in the lower Waitekauri Valley:

- An upper, moderately welded ignimbrite/lithic vitric lapilli tuff, 50+ m thick.
- A moderate to strongly welded lenticular ignimbrite unit, up to 58 + m thick.
- A lower, moderately welded ignimbrite/lithic vitric lapilli tuff, 75 + m thick.
- A fine grained vitric tuff unit, up to 18 m thick.

The lenticulite layers were described as containing “abundant flattened pumice lenticles in a matrix of flattened shards and fresh interstitial glass” (Rabone, 1975). Pumice within the Owharoa Ignimbrite comprises 76.5 - 77.3% SiO_2, consistent with rhyolitic mineralogy (Ewart and Healy, 1965).

2.5.5 Fiamme

Fiamme are of interest towards this study because they can highlight compaction and welding processes. Fiamme texture occurs in both volcaniclastic facies and coherent parts of lavas, and in both subaerial and subaqueous volcanic successions. This texture is not uniquely diagnostic of any particular origin (Bull and McPhie, 2007).

Bull and McPhie (2007) have described the fiamme within the Owharoa Ignimbrite as elongated, 2 mm to 2 cm long, have length to thickness ratios of 4:1 to ≥15:1, with typically ragged, feathery ends and wrap around lithic clasts and crystals and are aligned parallel to bedding. The fiamme contain sparse quartz and/or plagioclase phenocrysts, and have an internal striated or fibrous texture that is parallel to the clast elongation direction and bedding, interpreted to be compacted tube vesicle texture. There are also angular, equant, tube pumice clasts, up to 3 cm in diameter, in which the tube vesicles are perpendicular to bedding (Bull and McPhie, 2007).

2.6 Waikino Ignimbrite

The Waikino Ignimbrite is the youngest of the three ignimbrites within the Ohinemuri Subgroup. The Waikino Ignimbrite forms the near horizontal surface of the central part of the Waihi Basin (Brathwaite and Christie, 1996). According to Brathwaite and Christie (1996) it was probably originally more widely distributed but has since been eroded.

The Waikino Ignimbrite as described by Brathwaite and Christie (1996) as a fine grained, moderately to strongly welded, plagioclase-hypersthene vitric-crystal ignimbrite. It is rhyolitic in composition. Sparse lithic fragments occur within the unit, consisting of andesite, rhyolite, and crystal-lithic tuff. Pumice fragments, and quartz and biotite crystals occur only in the lower part of the formation. The Waikino Ignimbrite is described as strongly welded with a thin zone of non-welded basal ash, which identifies with an intra-caldera ignimbrite facies with a

near source vent. This unit has a normal polarity (contrasting the Owharoa Ignimbrite) and has been previously dated at 1.5 ± 0.23 Ma though fission track/glass ages (Kohn, 1973).

The basal contact of the Waikino Ignimbrite is upon the Owharoa Ignimbrite. This contact is erosional, and locally marked by lenses of fluvial andesite gravels in drill holes on the east side of Waihi (Rabone and Keal, 1985).

Chapter 3: Methods

3.1 Field methods

Field research was carried out to determine the stratigraphic and facies variation of the Owharoa and Waikino ignimbrites within the field area. Initial sites were identified using the Brathwaite and Christie's (1996) geological distribution map and more sites were identified as field area familiarity expanded. Site variation was important for differentiating characteristics and topographic influences of the two ignimbrites. The vertical and lateral changes in ignimbrite characteristics were based on outcrop appearance, degree of welding, componentry abundance and texture. The different site coordinates for this study can be found in Appendix I.

Stratigraphic columns were constructed at multiple sites to demonstrate internal characteristics, changes within the componentry and the different facies of the ignimbrites (Chapter 4). Contacts between the two ignimbrites were identified are important to map as they have the ability to show paleo-landscapes and erosion that may have occurred between the depositions of units. The ignimbrites were described based on variation of grainsize, pumice abundance and variations (including aspect ratio), lithic abundance and variations, componentry abundance (percentages) and degree of welding.

Field sketches were drawn to show lateral extent of contacts and internal deposit characteristics.

Representative samples of the units, their facies and components were collected during field work for further analysis within the laboratory. Samples ranged in diameter from 5-10 cm to 50 cm in size and with varying weights. Samples mostly came intact however some disaggregated. The sample list can be seen in Appendix I.

3.2 Geochronology

U-Pb zircon dating was undertaken for the Waikino Ignimbrite. The Owharoa Ignimbrite already had a U-Pb zircon date obtained by Vincent (2012). The sample preparation and age determination of this material was undertaken by laboratory technicians at the University of Waikato.

Zircons were extracted for dating with this process because "Zircons are assumed to be robust enough that they will not be broken during sample crushing, nor is any bias caused by the Gemini Table or heavy liquid separation (Fedo *et al.*, 2003)" (Vincent, 2012).

Separation to obtain zircons:

3 kg of bulk, unweathered, fresh outcrop was sampled. This sample was crushed to 500 µm using a jaw crusher and Bico mill. The powdered sample was then separated by weight using a Gemini Table (sample tray at 55 Hz, table at 22 Hz). The heavy mineral fraction was then oven-dried and the magnetic components were separated using a vertical Frantz Isodynamic magnetic separator (at 1.0 A). The non-magnetic fraction was processed through sodium polytungstate (SPT) (density 3.0 $g.cm^3$). The resultant air-dried heavy mineral fraction was processed on an inclined Frantz separator (15 ° front-to-back, 10 ° side-to-side, 0.5 A) to produce a final non-magnetic, heavy mineral fraction.

The ideal 50-100 zircons (where possible) were selected using a stereo microscope with reflected and/or transmitted light ('ideal' meant free of inclusions/cracks, whole/intact, wider than 60 µm). They were then mounted on double sided tape on a glass slide to be made into a polished block. Using a camera mounted on a stereo microscope, image(s) were taken of the sample, so that the 'best of the best' grains could be pre-selected/identified/mapped for dating.

Laser ablation inductively coupled plasma mass spectrometry

U-Pb isotopes ^{204}Pb, ^{206}Pb, ^{207}Pb, ^{208}Pb, ^{232}Th, ^{235}U, ^{238}U were measured using a RESOlution SE series excimer laser (193 nm) and an Elan 6100 DRCII inductively coupled plasma mass spectrometer in the Faculty of Science and Engineering, the University of Waikato.

Data was acquired using laser software called Geostar v8.50, and the ICPMS software was Elan v3.4.

"Two analytical standards and a zircon of known age were used as a check against the data for a sample of unknown age (i.e. the crystals being dated in this study). The NIST610 is a glass standard that is completely homogeneous in 61 trace elements and was used as a base check for the concentration of elements in the unknown samples (Richards, 2009). The second standard, GJ1, is a large homogenous zircon of gem quality (Jackson et al., 2004) obtained from the

School of Earth and Planetary Sciences, Macquarie University, Australia. The GJ1 is used as a calibration to correct for any mass discrimination by the ICP-MS and has a TIMS age of 608.5 ± 0.4 My (Jackson *et al.*, 2004).

Temora2 zircon crystals were used as a zircon of known age (416.78 ± 0.33 Ma) and as a method check (Black *et al.*, 2004). Temora2 zircons are from the Middledale Gabbroic Diorite of the Paleozoic Lachlan Orogen in eastern Australia (Black et al., 2004)." (Vincent, 2012).

NIST610 analysed twice at start and at end of session, GJ1 analysed at start and end, and twice between every 9-12 unknowns and Temora2 analysed twice at start and twice at end of session.

The Waikino Ignimbrite age determination is based on the method of Solari et al., 2010:

- 30 µm spot size for standards and unknowns (60 µm on NIST610) and
- Laser firing at 5 Hz, energy on spot = ~0.042 mJ, at 25 % power to achieve an energy density (fluence) on sample of ~6 J.cm^2.

Data was reduced using Iolite v3.1 with the 'U-Pb Geochronology 4' data reduction scheme, and histograms were plotted with KDE (Kernel Density Estimation) using 'Density Plotter' (Vermeesch, 2012).

3.3 Petrographic methods

A variety of different thin sections were made for different sites of the two ignimbrites. At the Owharoa Falls (locality 1 and 2) and McHardy Stream (locality 9C) sites had multiple thin sections prepared through the section to provide petrographic information vertically through the Owharoa Ignimbrite. Thin sections were made, 63 were cover slipped and 9 were polished.

Petrographic analysis was undertaken using the following methods:

Optical microscopy - Thin sections were used to identify and describe the different components and textures of the ignimbrite including:

- Variations in the proportions and texture of the different ash to very fine lapilli size particles (i.e. the matrix),
- Variation in lithic - lapilli or block based on colour and texture (e.g. andesite, various rhyolites, greywacke, ignimbrite and sandstones).

- Variations in pumice based on colour, vesicle textures, crystallinities, or degree of flattening (including fiamme).

Point counting was also undertaken to quantify the percentage componentry. Eight slides were point counted at 800 points per slide at quarter inch increments. Thin sections provided the stepping stone to identify requirements for further investigations using geochemical analyses.

Scanning electron microscopy (SEM) was used due to increased resolution and control of magnification compared to traditional microscopy. The machine was the Hitachi S-4700 Field Emission Scanning Electron Microscope (SEM) with Quorum Technologies Cryo-system, used at the University of Waikato. Specs that were used for the secondary electron function was 20 kV, and the EDS was 15 kV at varying magnifications. Samples that underwent SEM analysis are recorded in Appendix IV.

The secondary electron function of the SEM was used to investigate the micro-textures and components of the two ignimbrites, as well as look closer at the components individually. The SEM revealed important information regarding pumice textures, phenocrysts, lithic textures and flow banding within the fine grained material (matrix). The matrix texture was not able to be seen in detail with an optical microscope and required a stronger magnification provided by the SEM. EDS analysis/element map functions were also used on the SEM. This was used to gain elemental information on points or create larger elemental maps to show elemental changes over a space. EDS results can be seen in Appendix V.

X-ray powder diffraction (XRD) was used to further identify the mineralogy of the ignimbrites. This helped identify primary and alteration mineralogy. The results for the XRD analysis can be seen in Appendix VI.

XRD analysis was carried out by obtaining multiple bulk samples from the Owharoa and Waikino ignimbrites. Approximately 10 grams of each sample was dried and crushed into a fine powder using the tungsten-carbide ring mill.

The prepared samples were then processed through the Panalytical Empyrean XRD at the Faculty of Science and Engineering, University of Waikato. The prepared samples were run for 2-80°2Θ, at 50 seconds per step.

The results from these samples were then processed using the Highscore Plus program which generated XRD traces according to their crystallographic structure and a mineral was chosen that matched the graph (to the nearest degree).

3.4 Geochemical methods

Electron microprobe analysis was used for identifying individual mineral composition. EMPA looked at single spot analyses compared to XRF (below) which looked at whole rock.

Polished thin sections were taken down to Victoria University of Wellington, where the samples were coated in carbon and put into the JEOL JXA-8230 Electron Microprobe Analyser. For the crystal analysis the acceleration voltage was 15.0 kV, the abs current was 1.01×10^{-8}, probe current of 12 nA and a spot diameter of 1 µm. For glass analysis the same methods and machine was used as in the petrography section, however the probe current was lower at 8 nA and had a spot diameter of 10 µm.

EMPA analysis was carried out at Victoria University of Wellington. Analyses included those of individual crystals, including plagioclase, biotite, ilmenite, magnetite; and glass within the matrix and within pumice clasts. Results for the EMPA analysis can be found in Appendix VIII.

X-ray fluorescence spectrometry (XRF) was used for whole rock geochemical analysis, focusing on the pumice, as well as some bulk samples. Bulk samples were taken where pumice samples could not be extracted – i.e. the ignimbrite was too welded and the pumice couldn't be extracted well, or in the Waikino Ignimbrite's case, there was no pumice to extract.

Samples were selected for major and trace element geochemical analysis using the Bruker S8 Tiger XRF machine at the University of Waikato. The results for these geochemical tests are in Appendix VII.

To minimise sample contamination and analyse only the pumice, the samples were drilled out as mentioned, and soaked overnight in distilled water and washed using distilled water to remove further contaminants to get clean pumice sample. For XRF testing, material that was ideal for the analysis was just the pumice as it is a result from magmatic material during the eruption. The pumice fragments

were extracted using a diamond bit dremel to minimise contamination. Samples were then washed with distilled water at least three times, then oven dried and crushed using the tungsten carbide ring mill into a fine powder.

Once the sample material was prepared, fusion disks were made by measuring 0.9 g of sample material and combined with 9 g of LM100 flux (PURE 100% Li-metoborate). This was then sent to another site where it was processed and results were returned.

Loss of ignition (LOI) was calculated by measuring ~20 g of sample into a crucible and heating up to ~1000°C and measuring the weight difference.

Pressed pallets were formed by adding approximately 8-9 g of sample and 15 drops of PVA binder then pressed into an aluminium cup using a hydraulic press. The pressed pellets were then heated for approximately 2 hours at 70°C to evaporate off the binder.

Chapter 4: Stratigraphy and facies description

4.1 Overview

The Owharoa and Waikino ignimbrites (members of the Ohinemuri Subgroup) were both deposited within the Waihi-Waikino region, illustrated by Figure 4.1. In this chapter, the distribution of stratigraphic relationships and facies architecture of each of the ignimbrites is described using field results and stratigraphic columns.

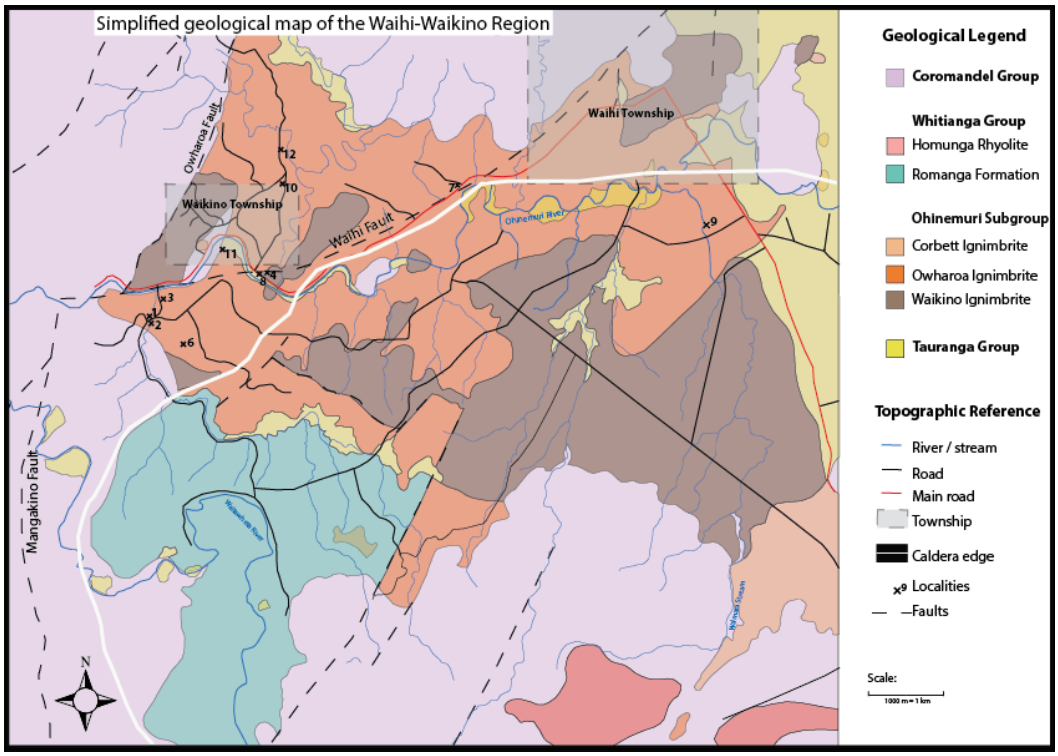

Figure 4.1: Simplified geological map of the Waihi-Waikino region (adapted from Brathwaite and Christie 1996). The map indicates localities from this study area and the caldera rim from the

The Owharoa Ignimbrite was quarried in the early 1900s. At different mining sites the Owharoa and Waikino ignimbrites have been overburden to the gold-bearing andesite and therefore often removed or partially removed (e.g. Martha Mine, Waihi).

4.2 Exposure and geomorphology

The Waihi-Waikino region has a unique and diverse geomorphology. The landscape ranges from the eastern beaches to an infilled basin which has created flatlands and low/foothills. Further west hills dominate the landscape. Steep cliffs within the Karangahake Gorge have been cut out by the Ohinemuri River.

The exposure of the Owharoa and Waikino ignimbrites in the study area is limited due to the steep terrain and thick bush within the Karangahake Gorge and the flat rolling landscape of the Waihi Basin. Areas which have good exposure occur along the Waitawheta River, Ohinemuri River, and previously excavated areas such as the Waikino Quarry and the Owharoa Quarry.

Road cuttings provide access to outcrop however several were located on the state highway (Figure 4.1) and therefore secondary roads were safer for extended periods of time.

The Owharoa Ignimbrite is non to densely welded and has prominent exposures in the landscape. It forms waterfalls and

Figure 4.2: The main type section is the Owharoa Falls (lower) which is 13 metres high. The Owharoa Ignimbrite forms large cliffs within the landscape.

Figure 4.3. Photo of the lowlying areas of the Waihi area, including plains used for farming, and the low hills to the left.

large open faces (Figure 4.2), as seen in the Karangahake Gorge. It also forms steep scarps and hills throughout the Waikino-Waihi region.

Throughout the rolling foothills (Figure 4.3) of the Waihi area, to the east of the gorge, the Owharoa Ignimbrite appears as low hills.

The Waikino Ignimbrite is non to moderately welded and due to its poor induration has been subjected to weathering and erosion, resulting in few natural exposures in the field. The Waikino Ignimbrite is found at the eastern end of the Karangahake Gorge and covers the low-lying farming areas towards the coast. The Waikino Ignimbrite appears to infill topographic lows and create smooth rolling landscapes, which has been cut by many streams.

4.3 Distribution

The distribution of the Owharoa and Waikino ignimbrites has been recorded within mapping projects over the last century, most recently by Brathwaite and Christie (1996). The simplified distribution can be seen in Figure 4.1.

The preserved deposit of the Owharoa Ignimbrite is dominantly distributed in an E-W orientation, and varies in thickness from 1.5 metres (Locality 6) to up to 80 m thick in drill holes (Brathwaite and Christie, 1996) within the Waihi Caldera. The major deposits extend from the Owharoa Falls in the Karangahake Gorge to the Waihi Township, 10 kilometres from east to west, and five kilometres north to south, either side of the Ohinemuri River (Figure 4.1).

Several sites identified on the Brathwaite and Christie (1996) geological map that record outcrop of the Owharoa Ignimbrite were no longer exposed at the time of this study, such as along the Awangaro Stream (northwest of Figure 4.1, at the western end of the Karangahake Gorge). At Samson Road (Locality 9) the Owharoa Ignimbrite, as identified by Brathwaite and Christie (1996) was found here and is overlain by a minor pebble conglomerate unit. However at Samson Road the site’s deposits may have been moved or altered due to road construction/earth works. This could have potentially formed an artificial deposit or just cutting the rock face exposing the deposit.

The Waikino Ignimbrite deposits are distributed to the south-east and north-west of the exposed Owharoa Ignimbrite in the low-lying hills and stream catchment basin of the Waihi area. The Waikino Ignimbrite extends west from the eastern

side of the Karangahake Gorge (at isolated sites, including the old Waikino Quarry, Locality 4, and along road cuttings, Locality 12) to the Waihi Basin. Drill holes on the eastern side of Waihi township suggest that the total Waikino Ignimbrite thickness is up to 75 metres (Rabone and Keal, 1985).

4.4 Contacts

The basal contact for the Owharoa Ignimbrite is only found at locality 6 (Figure 4.6 A), where the Owharoa Ignimbrite it is underlain by a dark, organic rich layer (Figure 4.6. B), possibly of the Romanga Formation. The Romanga Formation is defined as a lacustrine siltstone, mudstone and tuffaceous sandstone (Brathwaite and Christie, 1996).

The upper contact of the Owharoa Ignimbrite is found at locality 4 (Waikino Quarry), where the Owharoa Ignimbrite is overlain by the younger Waikino Ignimbrite with a sharp contact (Figure 4.4). The contact is irregular and unconformable indicating erosion of the Owharoa Ignimbrite prior to the emplacement of the Waikino Ignimbrite. The contact dips down towards the Ohinemuri River, suggesting that the river may have been present between the two ignimbrite forming events (Figure 4.5).

Figure 4.4: Photo of the upper Owharoa – lower Waikino Ignimbrite contact. The contact follows the iron staining.

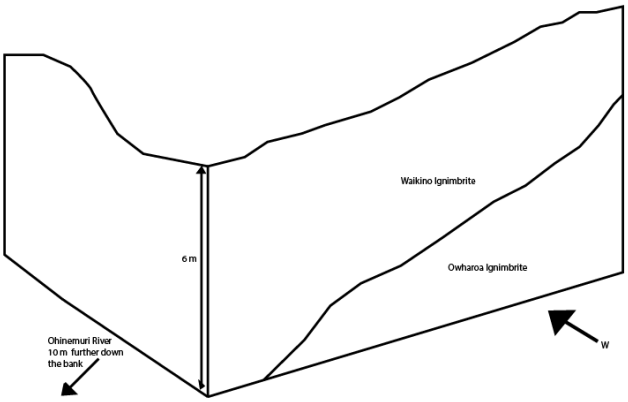

Figure 4.5: Waikino Quarry (Locality 4) schematic showing the Owharoa and Waikino ignimbrite in their stratigraphic orientation and contact orientation.

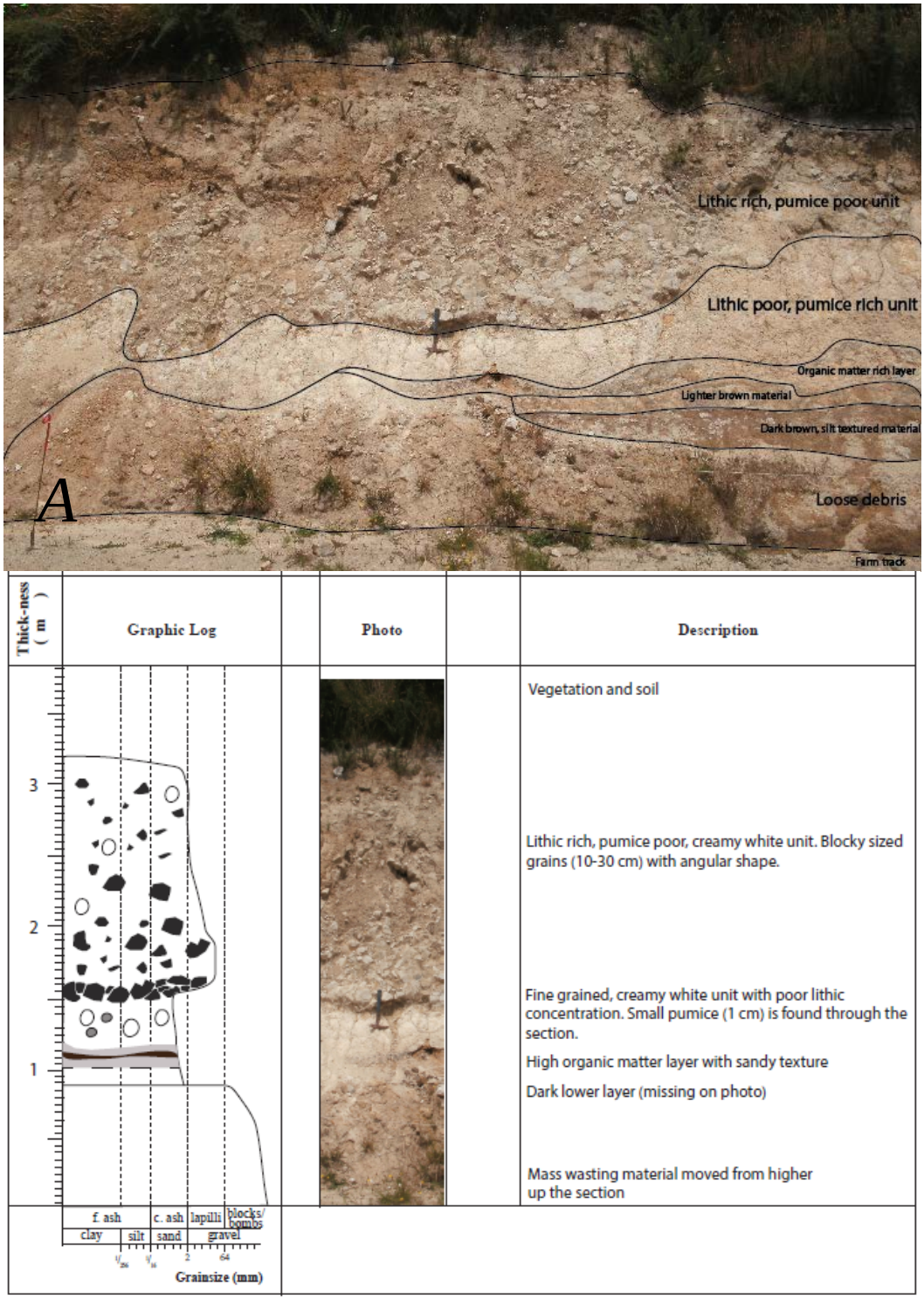

Figure 4.6 A: Annotated photograph of the basal Owharoa Ignimbrite at site 6. The organic rich layer is Romanga Formation which is overlain by the Owharoa Ignimbrite – including the fine grained, creamy white pumice rich unit and the lithic rich pumice poor unit above. B: a stratigraphic column of the basal contact of the Owharoa Ignimbrite at the same site.

Rabone and Keal (1985), in drill holes identified andesite pebbles within the contact between the Owharoa and Waikino Ignimbrite, which is indicative of a high energy depositional environment, such as a river. This means that during the time between the deposition of the Owharoa and Waikino ignimbrites there were two different circumstances occurring at two different sites – an erosional environment leaving no material within the contact, and a depositional environment leaving andesitic pebbles.

The Waikino Ignimbrite is the uppermost stratigraphic unit at Waihi-Waikino. The top surface of the Waikino Ignimbrite is therefore exposed and has been eroded, and it is suggested that it was much more widely distributed (Brathwaite and Christie, 1996). The only overlying sedimentary deposit to the Waikino Ignimbrite is the Matua Subgroup (0.84-0.22 Ma) comprised of terrestrial and estuarine sediments from an ephemeral braided river environment (Brathwaite and Christie, 1996).

4.5 U-Pb zircon ages

The Ohinemuri Subgroup is comprised of three pyroclastic density current deposits – the Corbett, Owharoa and Waikino ignimbrites. The oldest of the Ohinemuri Subgroup ignimbrites is the Corbett Ignimbrite which has been studied by Cook (2016). The Owharoa Ignimbrite is the second oldest of the three ignimbrites, dated at 3.76 ± 0.05 Ma using U-Pb zircon dating (Vincent, 2012). The contact between the Owharoa and Waikino ignimbrites has also been identified, supporting the relative positions of the older Owharoa and the younger Waikino Ignimbrite.

The Waikino Ignimbrite is the youngest of the three Ohinemuri Subgroup ignimbrites, dated in this study at 3.48 +/- 0.19 Ma using U-Pb zircon dating (Figure 4.7). Figure 4.7 shows the spread of zircon ages used to define the age of the Waikino Ignimbrite.

Figure 4.8 is an extended version of Figure 7.4 and shows the complete range of zircon ages identified within the ignimbrite from between 2.8 to 84 Ma.

Zircons with the ages from 10 – 20 Ma were most likely formed with the emplacement of Coromandel Group Miocene andesites and basalts. These

deposits were laid down in the Waihi region through the Miocene period. One zircon was dated at 28 Ma, during the Oligocene. This may be from earlier deposits in the CVZ which ended up down in the Waihi area, or from the NVZ. There was also one zircon dated at 58 Ma, during the Paleocene, one zircon from 69 Ma and 84 Ma, during the Cretaceous period.

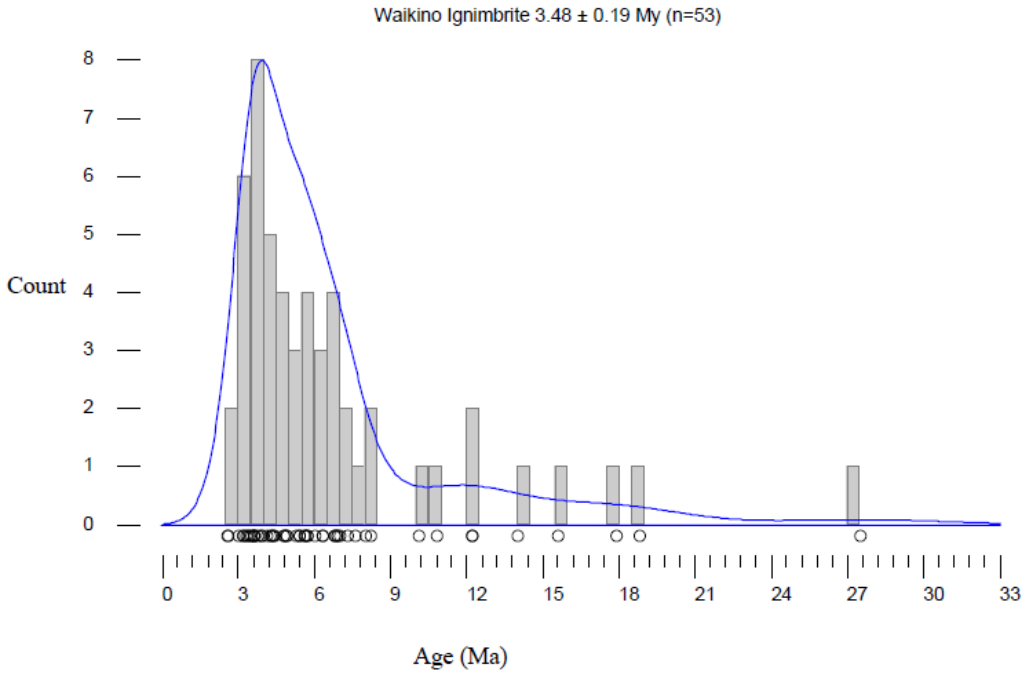

Figure 4.7. Histogram of zircon count verses U-Pb zircon age highlighting the age identified for the Waikino Ignimbrite.

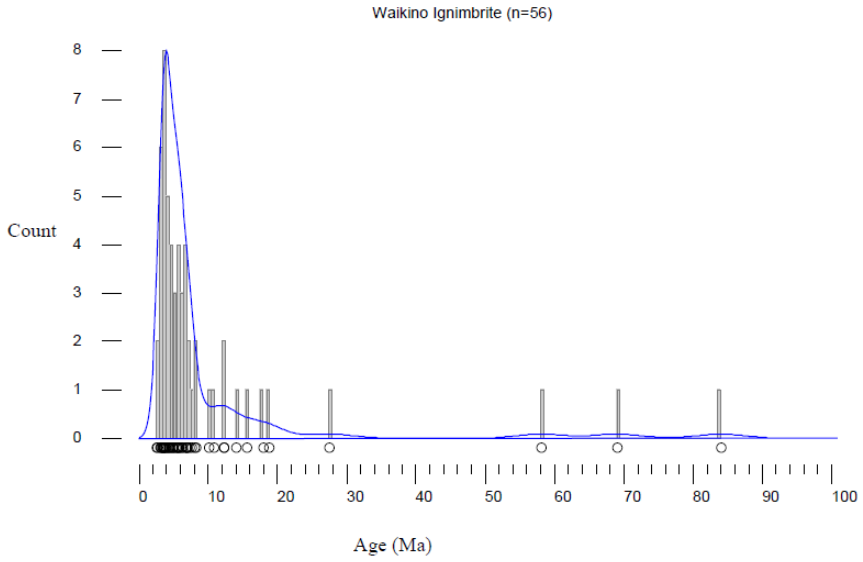

Figure 4.8. Histogram of zircon count verses U-Pb zircon age, which includes the data from Figure 4.7 as well as older zircons within the Waikino Ignimbrite.

4.6 Owharoa Ignimbrite

The Owharoa Ignimbrite is a non- to densely-welded, creamy white to grey, pumice-rich ignimbrite. The ignimbrite is poorly sorted, has variable lithic content (~1-30%), is pumice rich (~5-30%) and has crystals present (~1-5%), including plagioclase, quartz and biotite. As seen in Figure 4.9, the Owharoa Ignimbrite fluctuates in grain size within the matrix, but still within the range of coarse ash. The matrix consists of glass shards and fine grained inter-granular material. The percentage of lithics and pumice vary at different localities, which defines several of the facies described here. The relationship between pumice and lithic content appears to be inversely proportional to each other (Figure 4.9). The unit also exhibits prominent vertical columnar jointing which is widely spaced (1-3 metres), seen dominantly at locality one (Figure 4.9).

The ignimbrite contains a range of different types of juvenile clasts, including dark lensoidal fiamme throughout the welded sections of the ignimbrite, and rounded, white woody pumice in moderately welded to non-welded sections. The juvenile clasts have phenocrysts of quartz, plagioclase, biotite and opaques.

The type section for the Owharoa Ignimbrite is the Owharoa Falls (Figure 4.9), where it is moderately welded to densely welded and is 13 meters thick. A further, higher section of the falls, comprises over 30 meters of section. This site is the most western site.

Figure 4.9 also shows the variation of juvenile clast aspect ratio, and juvenile clast and lithic content. The column highlights the lithic-poor, pumice-rich zones (i.e. 5 m) and pumice-poor lithic-rich zones (0 m), indicating a change of componentry. The aspect ratio of the pumice also changes throughout the stratigraphic column, with the highest aspect ratio to be at 10 and 24 metres. This increase in aspect ratio is indicative of an increase of welding of the section.

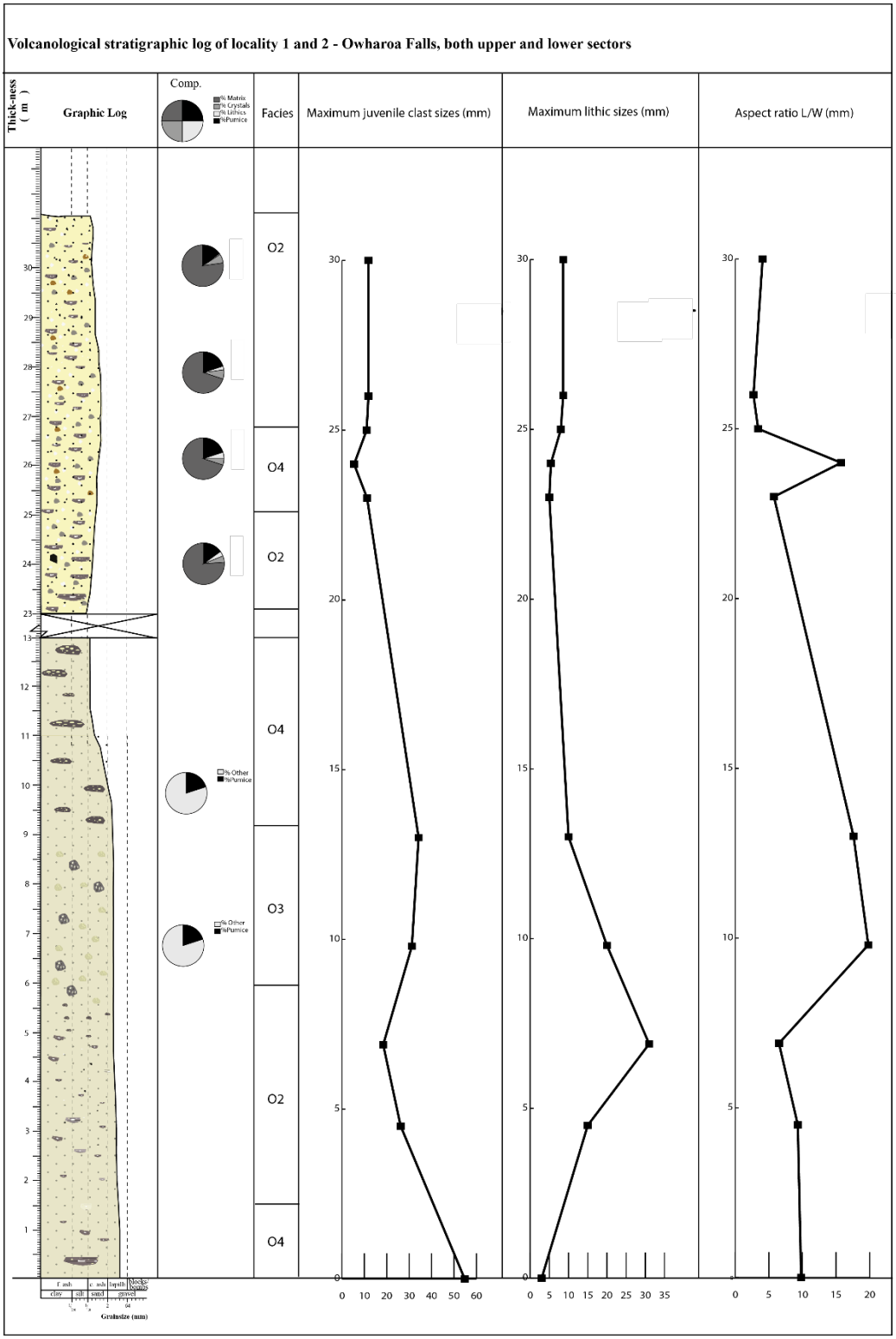

Figure 4.9. Stratigraphic column of the Owharoa Falls section of the Owharoa Ignimbrite. This stratigraphic column also shows maximum pumice and lithic content, and aspect ratio of pumice.

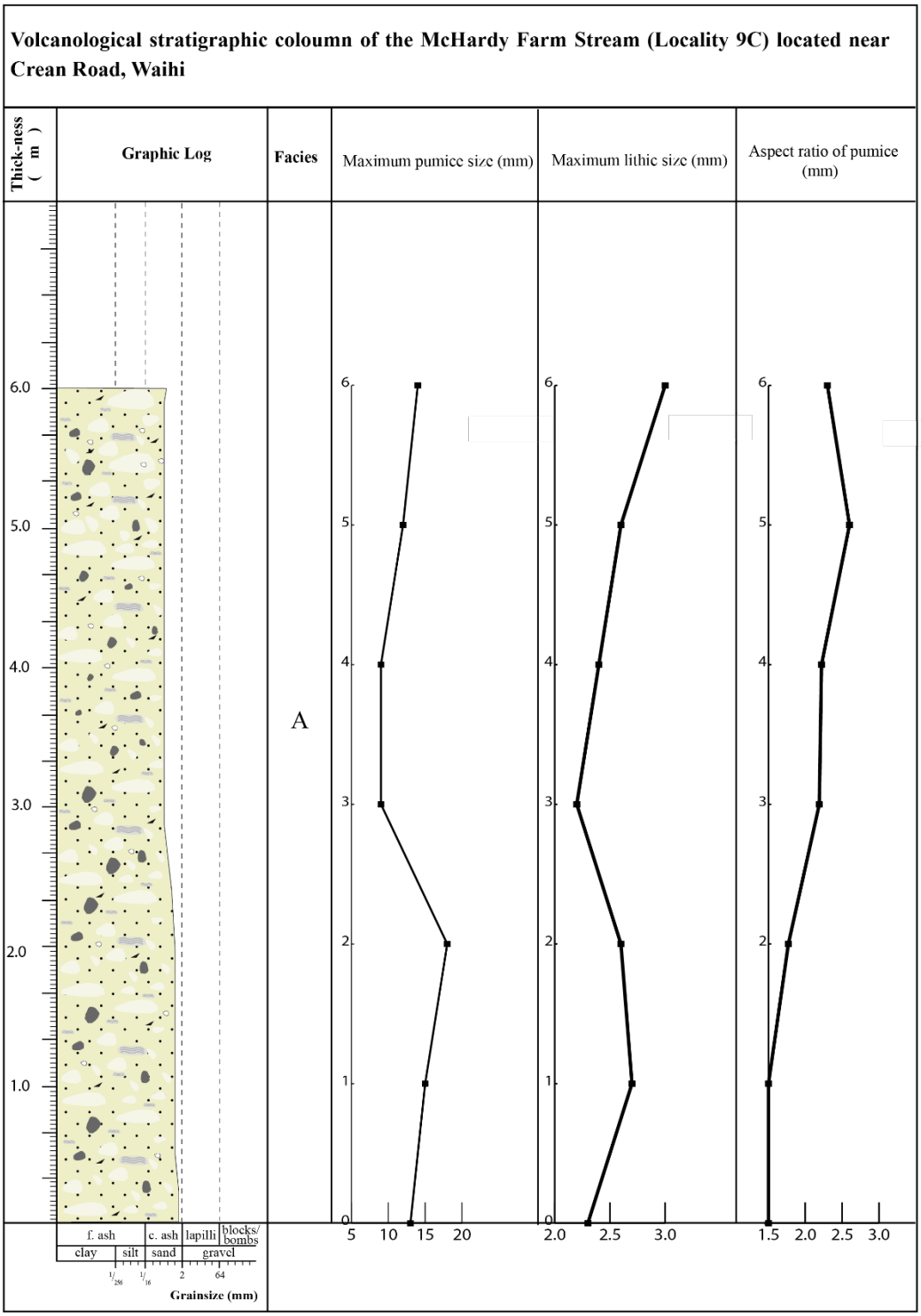

Figure 4.10. Stratigraphic column of the McHardy stream site (Owharoa Ignimbrite) on Crean Road, Waihi. This stratigraphic column also shows maximum pumice, lithics and aspect ratios of the components.

The McHardy stream site (Figure 4.10) is located on Crean Road, just outside the Waihi township, and is the most easterly locality of this study. This site exhibits a pumice-rich deposit, with varying pumice aspect ratios (Figure 4.10) and lithics present in small percentages (2-5%). The pumice at this site is rounded, exhibits a woody texture and is far more abundant than at the western site of the Owharoa Falls.

The varying pumice shapes are of interest to this study as it is one of the defining characteristics of the Owharoa Ignimbrite. Flattened pumice and associated fiamme occur throughout the unit, although the concentrations vary in ranges of 5 - 30%. Pumice ranges in colour (creamy white to dark grey/black) and many have a woody to glassy textures. Phenocrysts of quartz and plagioclase are present though comprise only a small percentage of the pumice. The vesicles within the pumice vary in size (2 - 0.2 mm) and shape (thin and tubular to round and shallow). Pumice clast morphology ranges from being rounded to flattened fiamme. Fiamme tend to be lensoidal and have a concave base (Figure 4.9 exhibits this well). The flattened pumice are orientated horizontally in the field (with very little angle or tilting) and when observed vertically, they are round.

4.6.1 Facies description

From the field analysis of the Owharoa Ignimbrite six different ignimbrite facies identified, and they are described below.

Figure 4.11. Facies O1 sample from sections of the Owharoa Ignimbrite.

Facies O1 is a **pumice-rich facies** (Figure 4.11). This facies is found at locality 6, 9 and 11 (Figure 4.1). Its thickness ranges from 1 metre to over 7 m. It is a creamy white facies exposured within farm land and at the McHardy waterfall (locality 9). Facies O1 is weakly to moderately welded with a coarse ash matrix, and is lighter in colour than the other facies. Crystal phases include plagioclase, quartz,

hornblende and biotite. Jointing is present at locality 1, 2 and 3. This facies is lithic (10-20%) and pumice (30-40%) rich, and has rounded pumice rather than flattened fiamme. Pumice has a low aspect ratio, indicating a relatively low degree of welding.

Figure 4.12. Facies O2 from block samples

Facies O2 is a **flattened pumice-rich facies**, which is characterised at locality 1 (Figure 4.12). It is a creamy light grey facies that is flattened pumice/fiamme-rich (10-40%) and lithic poor (5-7%). Biotite and plagioclase are dominant crystals throughout the unit. This facies has large pumice aspect ratios, and has a mixture of black and grey glassy fiamme and white, woody-textured pumice (woody appearance). Small lithics are present throughout facies O2.

Figure 4.13. Facies O3 from block samples cuts of the Owharoa Ignimbrite. .

Facies O3 is a **lithic-rich, pumice-poor facies**, found throughout locality 1, alternating with facies O2 (Figure 4.13). This facies has a moderately coarse ash matrix, and is lithic-rich (10%) and pumice poor (5-15%). The thickness of this facies ranges from tens of centimetres to several metres. There is flattened pumice/fiamme throughout the unit. Larger lithics are 2-3 centimetres in diameter.

Figure 4.14. Facies O4 from block samples cuts of the Owharoa Ignimbrite.

Facies O4 is a **dark grey, densely welded, fiamme-rich facies**, found at locality 1.6. (Figure 4.14). Its thickness ranges from tens of centimetres to

Figure 4.15: Photograph of facies O5 of the Owharoa Ignimbrite.

several metres. It contains black glassy fiamme (~40%) and is densely welded. There are very few small lithics and crystals (1-2%). It is darker in colour.

Facies O5 is a **pumice-rich facies**, only found at locality 4 (Figure 4.15). This is the same as Facies A, but with an increased concentration of pumice at the Owharoa-Waikino ignimbrite contact (30%). Lithic componentry also increases to 5-10%. The thickness of this facies is 10-15 cm, and is located approximately 5 cm from the Owharoa-Waikino ignimbrite contact.

Facies O6 occurs at locality 7 (Samson Road). This facies underlies the pebble conglomerate, and has a weathered, pink to beige colour with a coarse ash matrix, irregular, angular lithics (grey, black, white and pink) and small black crystals (biotite and opaques). It is 1-2 m thick and the site has been subject to road/earth works and this may have disrupted the deposit(s) at this site, therefore will not be taken into consideration for the larger study.

4.7 Waikino Ignimbrite

The Waikino Ignimbrite is a creamy beige to grey, fine to medium coarse ash, poorly welded, well sorted, massive ignimbrite (Figure 4.16). It contrasts to the Owharoa Ignimbrite as it is well sorted with low concentrations of pumice (~1%), crystals (1-6%) and lithics (~2%). The pumice within this ignimbrite is difficult to identify within the surrounding matrix, and the few that are visible appear rounded and vary in size (1-2 mm) and are only distinctive in hand samples. The

lithics tend to be dark grey and crystals include quartz, plagioclase and black angular biotite, ranging in size from 1-6 mm. The Waikino Ignimbrite is massive, has no distinct grading and is dominantly comprised of a coarse ash, glass-rich matrix.

The deposit has weathered jointing which varies in width from site to site from 50 cm to 2 m. Horizontal and vertical jointing is present however there is no consistency with their positioning.

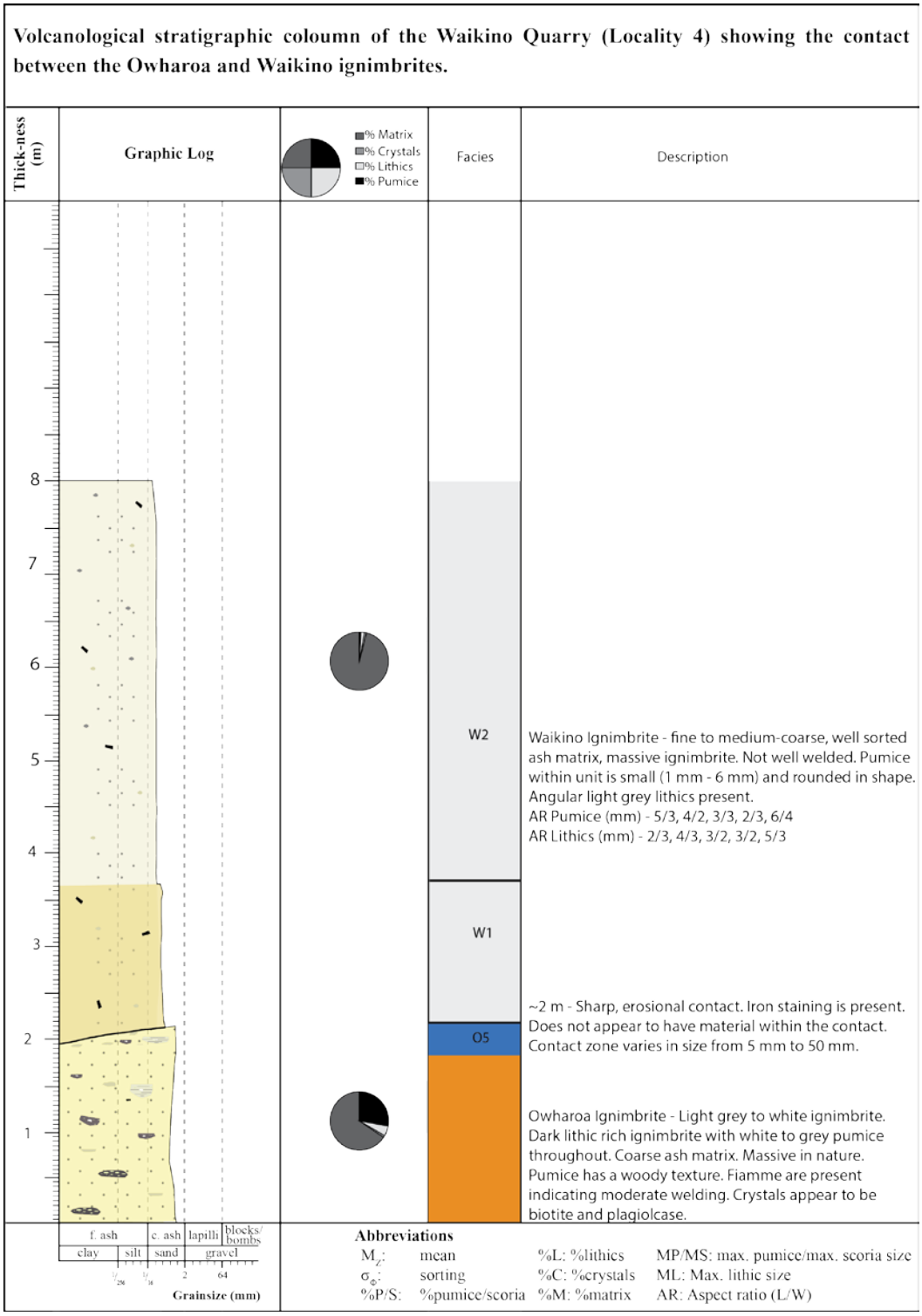

Figure 4.16. Stratigraphic column of the Waikino Ignimbrite at the Waikino Quarry, Waikino. This stratigraphic column also identities facies within the Waikino Ignimbrite.

Facies description

There are two facies of the Waikino Ignimbrite – a weakly welded, dark yellow-brown, soft, coarse ash, basal layer (Facies W1, Figure 4.17 A) and a moderately welded, finer ash-textured, grey massive deposit (Facies W2, Figure 4.17 B). These facies were found at localities 4 and 8.

Figure 4.17: A: Facies W1 – the soft basal facies of the Waikino Ignimbrite (from the Waikino Quarry, Locality 4). B: Facies W2 – the moderately welded facies of the Owharoa Ignimbrite.

Brathwaite and Christie (1996) and Ewart and Healy (1965) describe the Waikino Ignimbrite as a strongly welded ignimbrite with a thin zone of basal ash, which aligns well with these facies descriptions. This study describes the Waikino Ignimbrite as moderately welded in comparison to the strongly welded deposits of the Owharoa Ignimbrite.

4.8 Pebble conglomerate

The moderately sorted pebble conglomerate (Figure 4.18 A) is found throughout the Karangahake Gorge area (near locality 5, locality 7 and Jackson Road) and occurs above the Owharoa Ignimbrite in several locations, including Samson Road.

Figure 4.18: A: Photo of the pebble conglomerate within the field area. Jackson Road, near Paeroa. B: Close up photo of the rounded clasts within the pebble conglomerate.

The pebble conglomerate unit has a rubbly surface, small (1 cm) pebbles, cobbles and gravel sized clasts (40%) amongst a sandy creamy white grey matrix/cement (60%) (Figure 4.18 B). The large clasts within the matrix (>50 cm) are rounded and sub-rounded. The surface is highly weathered covering most of the exposed surface. There is no grading within the unit and it is poorly sorted.

The pebble conglomerate was studied in detail at locality 7 – Samson Road. This site is not marked on Brathwaite and Christie's (1996) geological map, however the pebble conglomerate may be a unit from the Ruahihi Formation. The Ruahihi Formation consists of a range of matrix-and clast-supported gravels and gravelly sands containing sub-angular to rounded boulders derived principally from the Kaimai and Waiwana subgroups. In Braithwaite and Christie (1996) the Ruahihi Formation occurs a few hundred metres south of the locality, next to the Ohinemuri River, therefore this deposit is the most likely geological unit to match the pebble conglomerate.

4.9 Facies architecture

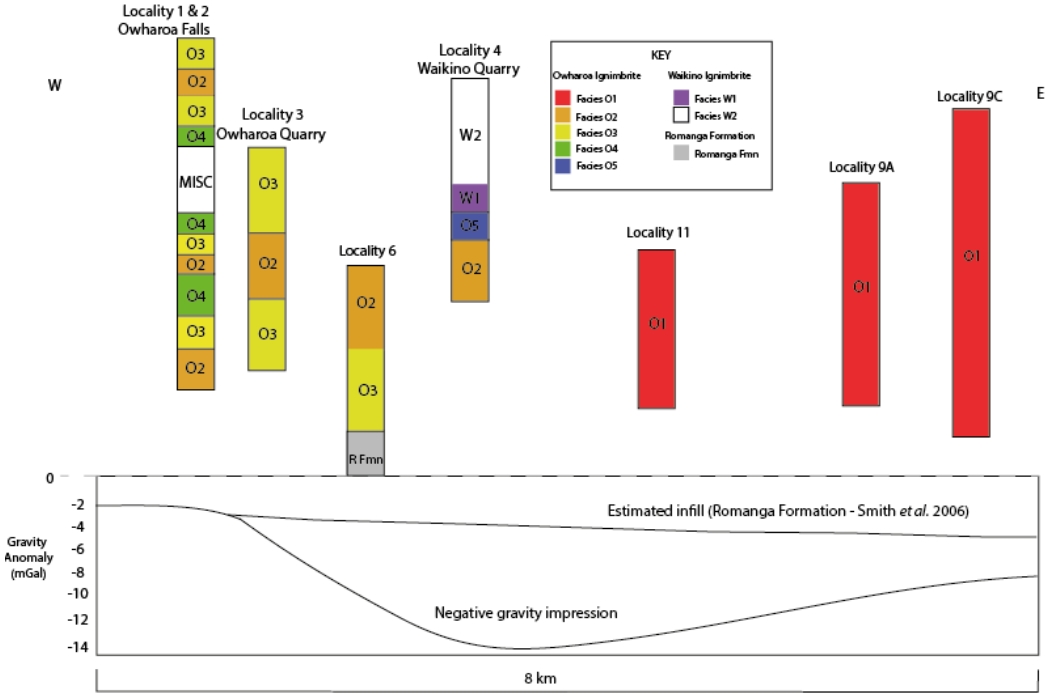

Figure 4.19: Owharoa and Waikino ignimbrites facies architecture, showing the relationship of the different facies of the ignimbrites in comparison to the underlying caldera paleo-surface as indicated by gravity anomaly data from Smith et al. (2006).

Figure 4.19 highlights the facies variations found at several Owharoa – Waikino ignimbrite sites from east to west, and indicates their location in relation to the negative gravity depression. It is important to remember that this gravity low represents the dense rock surrounding the lower density basin-fill, before the present time, rather than the pre-deposition landscape of the ignimbrite(s).

Facies vary in relation to the depth of the gravity anomaly. There are alternating facies such as facies B and C found near the assumed caldera rim. Facies A only occurs from the middle to the eastern side of the caldera.

Figure 4.19 shows that there are alternating facies within the Owharoa Ignimbrite. The alternation between lithic rich and pumice rich occurs, along with varying degrees of welding. On the western side of the caldera structure facies O2, O3 and O4 are all strongly to densely welded deposits which alternate, particularly seen at the Owharoa Falls site. Pumice-rich deposits alternate with lithic-rich deposits, which could be indicative of different flow deposits. On the eastern side of the caldera structure the deposit is moderately to weakly welded with rounded

pumice and abundant lithics as described in section 4.6, and is comprised of facies O1. This shows a lateral W-E variation of depositional units, dominantly controlled by welding. Facies O5 is only found at the contact of the Owharoa and Waikino ignimbrites. It is likely that this facies is another alternating deposit, but the higher deposits have been eroded away

Chapter 5: Petrography

This chapter discusses the petrographical characteristics of the Owharoa and Waikino ignimbrites, identifying component proportions, characteristics, and textures. Methods included optical microscopy, scanning electron microscopy, electron microprobe analysis and XRD analysis. The results obtained here will aid in identifying differences and similarities between the two ignimbrites and in the understanding the eruption and emplacement processes of each unit.

5.1 Owharoa Ignimbrite

The Owharoa Ignimbrite is a vitriclastic, eutaxitic, poorly sorted ignimbrite, comprised of pumice, lithics (including rhyolitic, andesitic, ignimbrite and sandstone/siltstone lithics), crystals, glass shards and optically unresolvable fine grained interstitial matrix.

Component proportions

The results of point counting are shown in the table below. These results represent the matrix-sized components only. Samples with 'oversized components' (any component considered 'abnormally large' in comparison to the rest of the components within the thin section) were excluded from point counting.

Table 5.1. Table of point counting results as percentages for different thin sections of the Owharoa Ignimbrite.

Component	**Percentage (%) per thin section**					
Sample	**1.1.1**	**1.4.2**	**1.6.1**	**2.1.2**	**2.7.1**	**9.1.7**
Pumice	46.36	26.7	37.8	41.37	38.2	45.13
Lithics	5.77	0.76	5.88	0.99	4.99	9.63
Matrix (unresolvable)	28.35	35.09	26.3	27.01	36.79	19.38
Glass shards	15.72	30.48	24.9	25.12	14.97	20.5
Free crystals						
Plagioclase	1.99	5.46	3.1	4.68	1.95	3.5
Quartz	0.59	1.82	1.5	0.29	1.27	1.5
Biotite	0.39	0.38	0.09	0.09	0.39	0.25
Hornblende	0	0.095	0.09	0	0.19	0
Opaques	0.09	0.32	0.18	0.09	0.58	0.125

Figure 5.1. Chart of the Owharoa Ignimbrite point counting results.

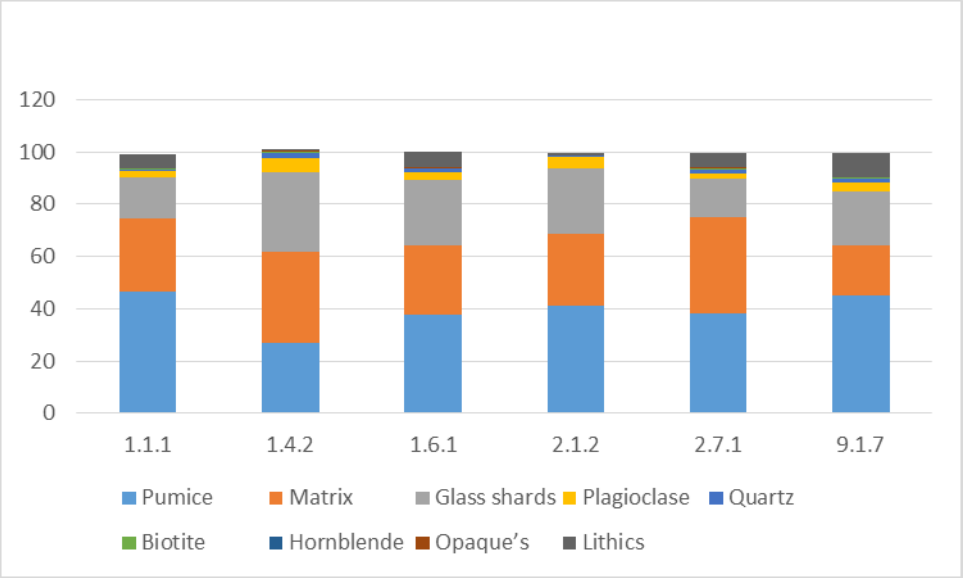

Table 5.1 and Figure 5.1 indicate the component proportions under optical microscopy, which aids in separating the different facies. Pumice percentages range from ~20% to over 40%, making the Owharoa Ignimbrite a significantly pumice rich ignimbrite in sites. Glass shards range from ~15 – 30%, and lithic percentages range from ~0.7 – 6% (Figure 5.1). The unresolvable matrix ranges from ~26- 37%, making up a substantial proportion of the Owharoa Ignimbrite's componentry.

5.1.1 Mineralogy of free crystals

Plagioclase and quartz are abundant throughout the Owharoa Ignimbrite, with hornblende and biotite being less common, however they are still ubiquitous. Crystals have been analysed within the field as hand samples, under optical microscopy and under the SEM.

Plagioclase

Plagioclase crystals (Figure 5.5 A) within hand samples range from anhedral to euhedral in shape, and range from 3-1 mm. Smaller crystals are present, ranging from 1 mm to 0.1 mm. Plagioclase comprises ~2-6% of the Owharoa Ignimbrite (Table 5.1).

Plagioclase (Figure 5.5 C) is the most common crystal phase and tends to form sub-rounded to sub-angular shapes. The plagioclase crystals exhibit zoning and twinning throughout a majority of the samples. Plagioclase crystals often have

worn away edges from resorbtion. SEM images of plagioclase (Figure 5.2) also reveal more intimate details of the zoning areas and the intensity of the fractures and resulting resorbtion.

Plagioclase within the Owharoa Ignimbrite is dominantly andesine, but does verge overlap with oligoclase and labradorite (Figure 5.3). There is no significant site variation of the plagioclase composition.

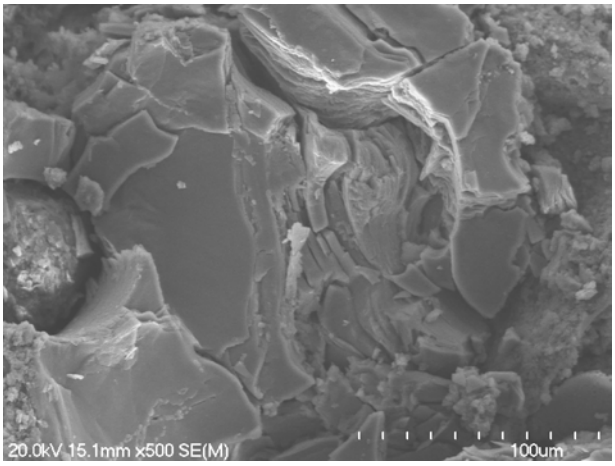

Figure 5.2.Plagioclase crystal under the SEM showing fracturing and layering of the crystal structure.

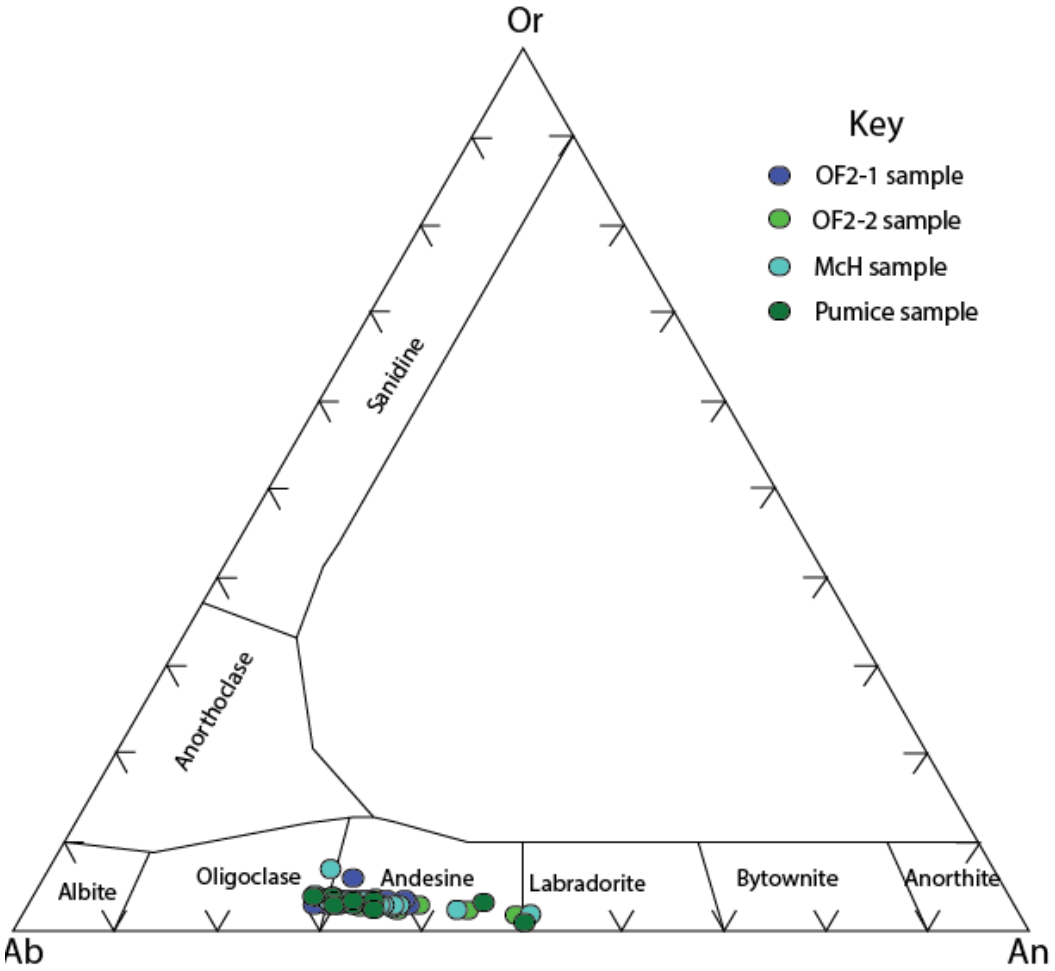

Figure 5.3. Feldspar Ternary diagram of the electron microprobe data for different sites of the Owharoa Ignimbrite.

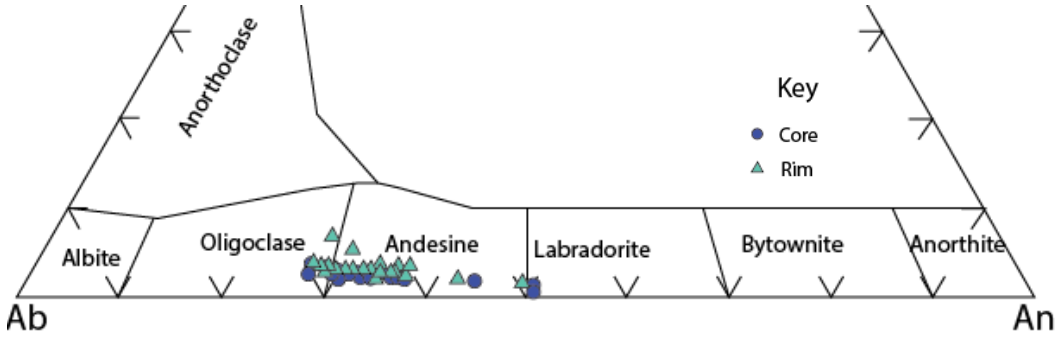

Figure 5.4. Ternary diagram of the rim and core of plagioclases within the Owharoa Ignimbrite.

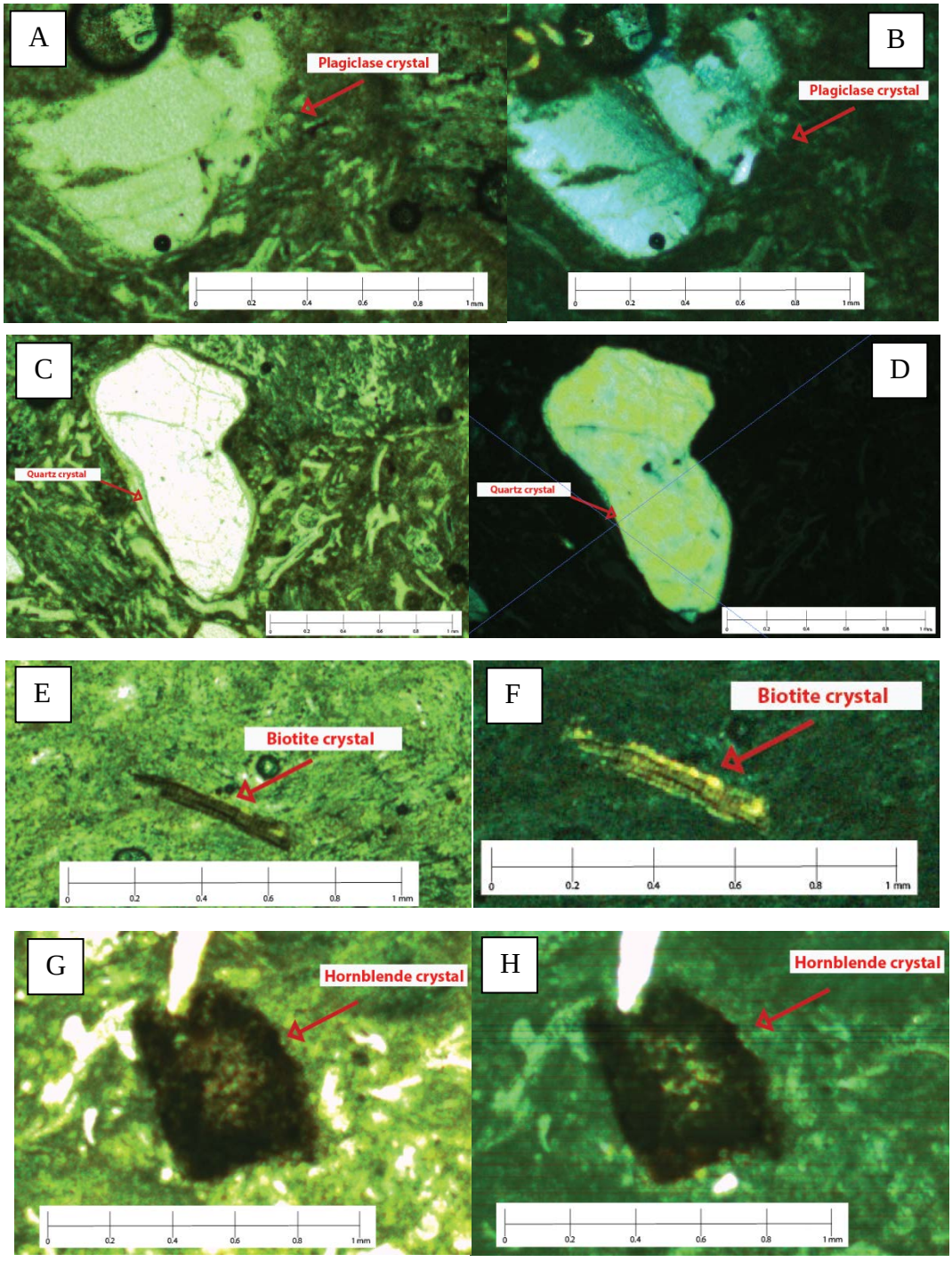

Figure 5.5. A. Plagioclase under PPL (left) and B. XPL (right), showing the embayment zones and fractures. C. Quartz crystal under PPL (left) and D. XPL (right). E. Biotite crystal under PPL. F. Biotite crystal under XPL. G. Hornblende crystal underneath PPL (left) and H. XPL (right).

Figure 5.4 highlights the different elemental composition between the core and the rim of plagioclase. There is a slight increase of potassium within rim samples compared to core samples.

Quartz

Quartz (Figure 5.5 C, D) is commonly found throughout the Owharoa Ignimbrite, typically in clusters with plagioclase. The size range for quartz is from 1-2 mm to 10 µm. Quartz comprises 0.3 – 2% of the Owharoa Ignimbrite. The quartz crystals exhibit embayment and irregular fractures throughout the samples.

Biotite

Biotite (Figure 5.5 E) is found occasionally and is a deep brown to light brown colour and exhibit pleochroism. The biotite crystals have a thin rectangular, tabular shape, and range in size from 0.1 to 1.0 mm. Biotite comprises of ~0.09-0.4% of the ignimbrite. The orientation of the crystals appear to be random unlike the orientation of the pumice and glass shards.

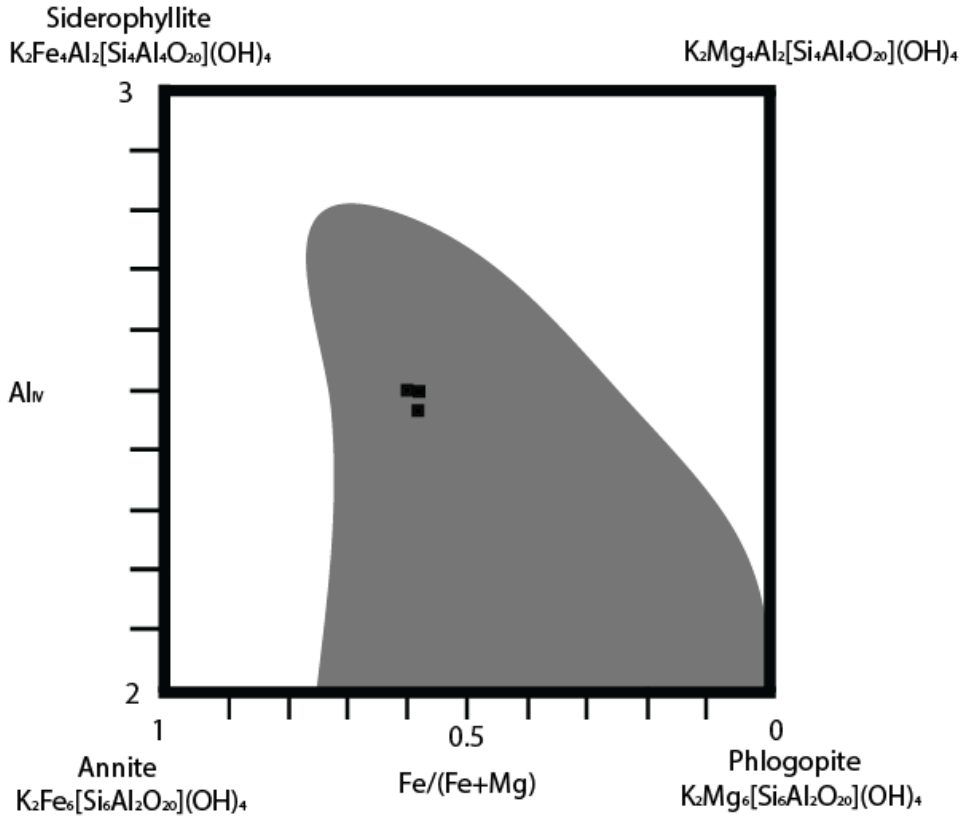

Figure 5.6. Biotite classification diagram for the Owharoa Ignimbrite for the crystals within the matrix and pumice.

Figure 5.6 is a diagram that classifies the type of biotite crystals in the Owharoa Ignimbrite. The diagram indicates that the biotites are nearly in the middle of the four biotite variations, however is closest to the annite composition.

Hornblende

Hornblende (Figure 5.5 G) is sparse, and is dominantly a dark khaki brown to green colour. The hornblende crystals tend to have an anhedral, rounded shape and the contact between the crystal and the matrix is diffuse. Hornblende crystals range in size from 0.1- 0.4 mm and comprises 0.09 – 0.9% of the Owharoa Ignimbrite.

Opaques

Opaque minerals occur occasionally (Figure 5.7) and these minerals could either be ilmenite or titano-magnetite. Square crystals are likely to be titano-magnetite.

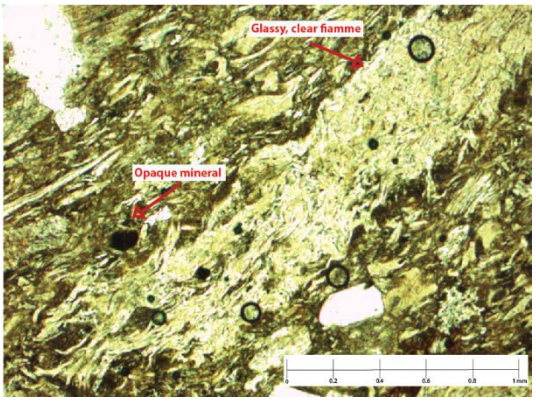

Figure 5.7. Photo of opaque mineral within the Owharoa Ignimbrite.

Table 5.2: Major element compositions of the opaque minerals using the electron microprobe and interpretation of the mineral, if it is a magnetite (Mt) or ilmenite (Il).

Owharoa Ignimbrite Opaque Minerals chemical composition using EMP							
Analysis Identifier	**OF2-1-4**	**McH1- -4-center**	**P- -2-center**	**P- -2-rim**	**P- -3-Westside**	**P- -8-east**	**P- -9**
Major Oxide							
SiO2	0.958	0.031	0.032	0.247	0	0.024	0
TiO2	17.208	48.35	48.484	48.637	48.928	48.605	48.608
Al2O3	1.483	0.065	0.093	0.079	0.076	0.054	0.088
FeO	69.848	47.502	47.178	46.179	47.201	46.982	46.986
MnO	0.398	0.676	0.689	0.692	0.756	0.716	0.749
MgO	0.356	0.767	0.762	0.779	0.76	0.75	0.778
Cr2O3	0.074	0.008	0.021	0.029	0.001	0.023	0.03
Total	90.325	97.399	97.259	96.642	97.722	97.154	97.239
Result	Mt	Il	Il	Il	Il	Il	Il

Electron microprobe analyses of the opaque minerals testing revealed only one tito-magnetite crystal and seven ilmenite crystals (Table 5.2). This could be indicative that Mt is not as abundant as Il in the Owharoa Ignimbrite samples tested.

Other minerals

Hunt (1991) also identified hypersthene and augite within the Owharoa Ignimbrite, which were not identified in this study. Rabone (1975) identified hypersthene within separate facies of the Owharoa Ignimbrite and also rare lumps of granular epidote from hydrothermal alteration.

5.1.2 Lithics

There are a variety of different lithics throughout the Owharoa Ignimbrite including volcanic lithics (rhyolite, andesite, and ignimbrite), and occasional sedimentary lithics (sandstone/siltstone) which can all be seen in Figure 5.8.

Rhyolite lithics are the most common lithics found within the Owharoa Ignimbrite. There is a large range of rhyolitic lithics, including dark rhyolite lithics (common), occasional spherulitic rhyolite (Figure 5.8 A), flow banded rhyolite (Figure 5.8 C), and occasional crystalline, crystal-rich rhyolites (Figure 5.8 D). Devitrified brown lithics are found at localities 1 and 2, and occasional aphanitic rhyolite lithics and altered hornblende rhyolites are also found. Rhyolitic lithics range from 5 cm to 0.5 mm, seen in both hand samples and thin sections, and range from sub-angular to sub-rounded in shape.

Andesite lithics (Figure 5.8 E) are common throughout the Owharoa Ignimbrite, and tend to be sub-rounded to sub-angular. The andesite lithics range in size from 5 mm to 0.4 mm and are porphyritic with variety of shapes of quartz and plagioclase.

Ignimbrite lithics (Figure 5.8 F) are not common, but were found at the Owharoa Falls (locality 1), Samson Road (locality 7) and McHardy Farm (locality 9). Ignimbrite lithics range in colour from soft pink to dark brown, sub-rounded in shape, and range in size from ~0.5 – 2.5 mm. Crystal content of the ignimbrite varies, including plagioclase, quartz, biotite and opaque minerals.

Sandstone and siltstone lithics are rare. These lithics are rounded to sub-rounded in shape, and have a range of different crystals within them, including grains of plagioclase, quartz, and opaques.

Hunt (1991) also identified small angular to sub-rounded fine grained argillite lithics, which may correspond to the siltstone lithics that have been identified within this study.

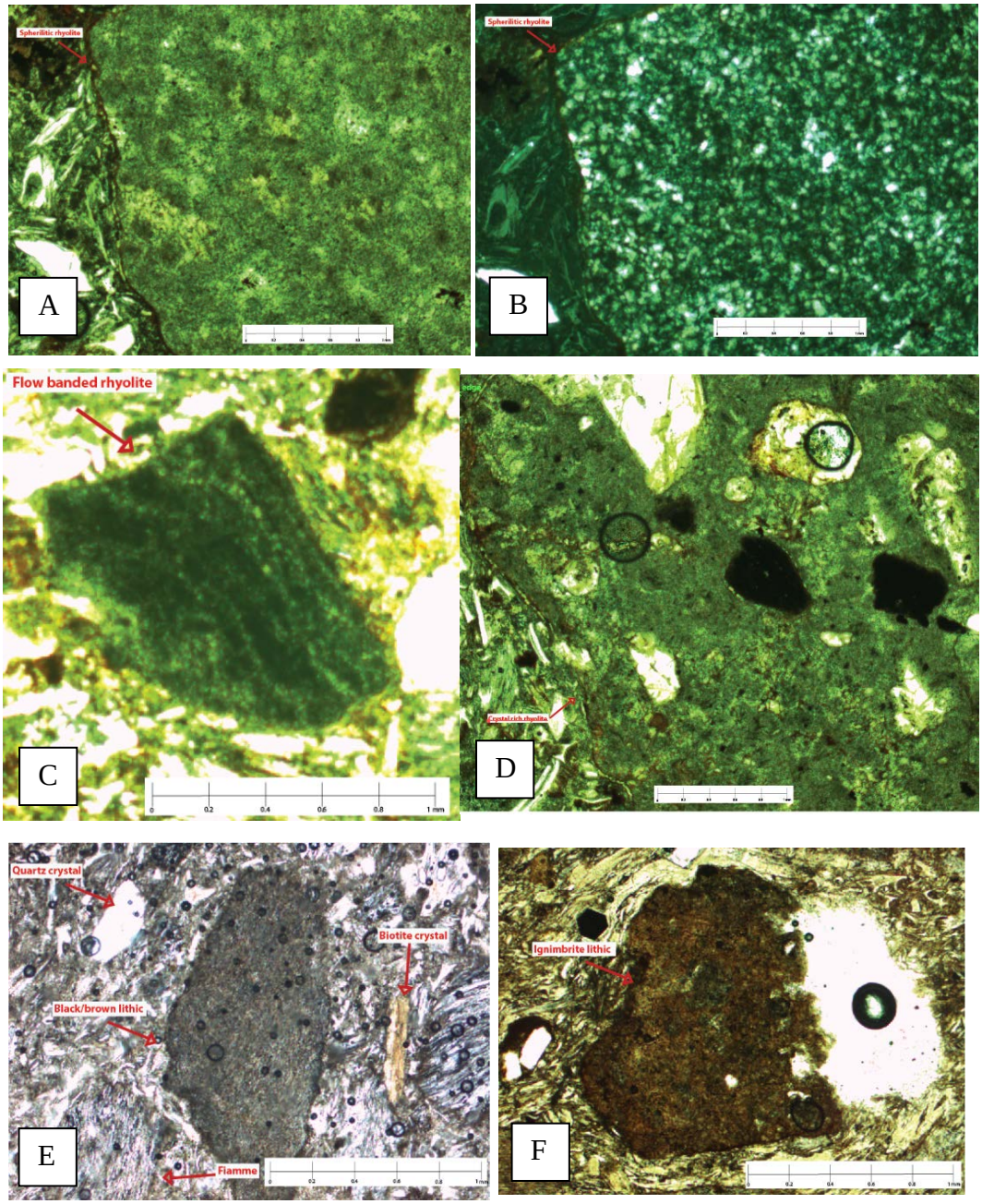

Figure 5.8. A. Spherulitic rhyolite lithic. PPL and B. XPL (right). C. Flow banded rhyolite under PPL. D. Porphyritic rhyolite lithic under PPL. Lithic has opaque, quartz and plagioclase phenocrysts and a glassy groundmass. E. Andesite lithic under PPL. Dark coloured andesite with no clear phenocrysts. F. Ignimbrite lithic (partially worn) under PPL. There are crystals within the matrix, including biotite, quartz and plagioclase.

5.1.3 Pumice

Juvenile clasts are found throughout the Owharoa Ignimbrite, varying in shape, colour, texture and phenocrysts. The size of the juvenile clasts ranges from 10 cm to 0.4 mm. Material smaller than this has been described as a glass shard/matrix appropriately. The juvenile clasts tends to have an E-W orientation which matches the orientation that they have in the field.

Juvenile clasts descriptions range from finely vesicular, rounded, white and woody to flattened, non-vesicular, black, glassy, thin, and lensoidal. Fiamme is present within the Owharoa Ignimbrite, and exhibits itself as flattened pumice with raggedy ends and a eutaxitic texture. Under optical microscopy the fiamme appears to 'flow' and wrap around crystals and lithics.

The juvenile clasts have phenocrysts including plagioclase, quartz, opaques (magnetite) and biotite. This mineral content is the same as the mineral content of the free crystals in the matrix. Phenocrysts within the juvenile clasts do not appear to be influenced by the welding as they appear to hold the sub-angular to sub-rounded shape compared to the flattened fiamme.

Pumice begins as a typically rounded shape, and then due to the heat and pressure of the ignimbrite's eruption and emplacement processes, causes the stretching, flattening and compression of the pumice, created elongated fiamme. Pumice has a fiberous texture with little to no vesicles, particularly seen within fiamme. There are five main different pumice and fiamme types found throughout the Owharoa Ignimbrite.

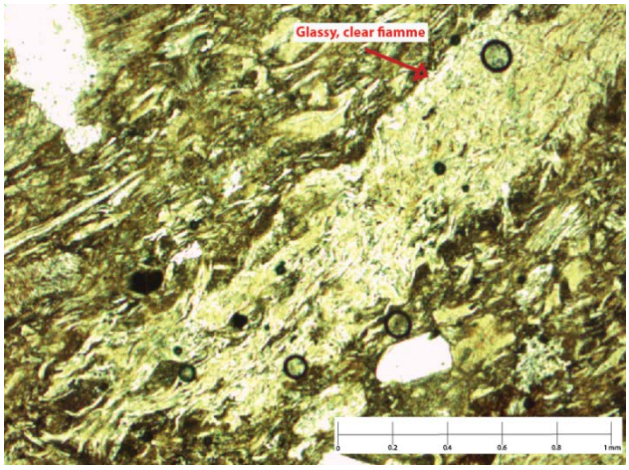

Figure 5.9. Pumice type 1: Glassy clear fiamme.

Pumice type 1 (PT1): Poorly vesicular, colourless fiamme. This pumice type is elongated, flattened and lensoidal with raggedy/flame-like ends, defining it as a fiamme (Figure 5.9). It ranges from aphyric to porphyritic, with phenocrysts of plagioclase and quartz. It is poorly vesicular, colourless and has a glassy texture.

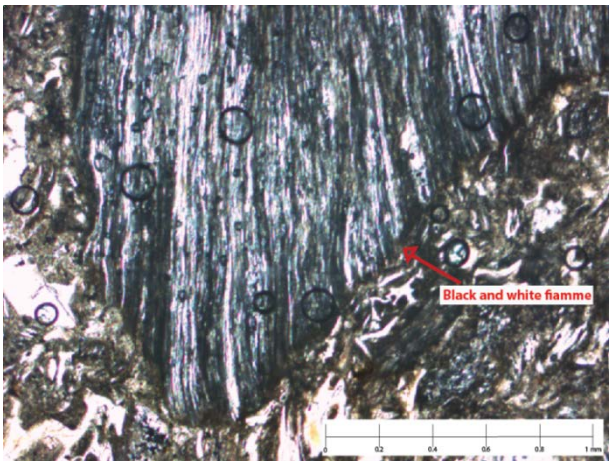

Figure 5.10. Pumice type 2: Black and white tube pumice without raggedy ends.

Pumice type 2 (PT2): Black and white pumice. This pumice type has distinct alternating black and white stripes, and appears to have horizontal layers which may be from stretched vesicles, creating tube vesicles (Figure 5.10). PT2 have rounded, joint edges. They are flattened, but not to the extent of pumice type 1. Phenocrysts include opaque minerals, biotite and quartz.

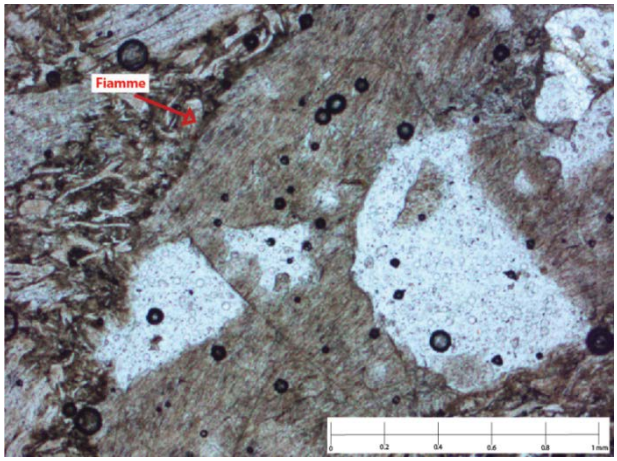

Figure 5.11. Pumice type 3: Brown and grey pumice – not as deformed as higher pumice types.

Pumice type 3 (PT3): Brown and grey pumice. The edges of this pumice type are not as defined as the PT2, and are dominantly rounded rather than flattened (Figure 5.12). PT3 exhibits more complex internal characteristics within,

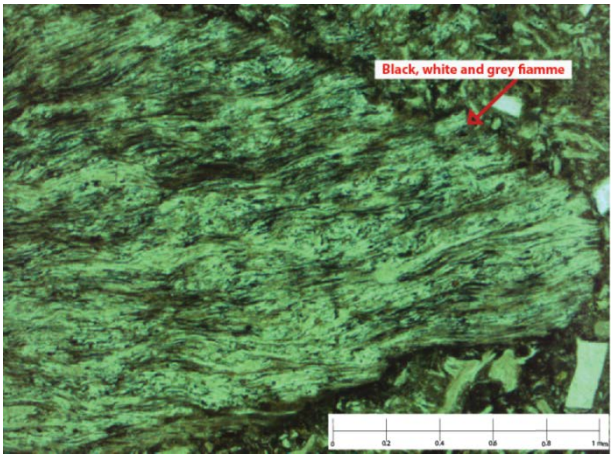

Figure 5.12. Pumice type 4: Black, white and grey fiamme.

rather than horizontal layers seen by PT2 and PT4. Occasional very fine vesicles are present. PT3 is a brown-grey colour and is more uniform.

Pumice type 4 (PT4): Black, white and grey fiamme. This pumice type is fiamme 'bow tie' ends (Figure 5.13). There pumice type has more distinct flow patterns compared to the other pumice flow patterns. The fiamme structure is flattened and exhibits a compacted shape.

Pumice type 5 (PT5): White pumice. Rounded, white woody-textured pumice, which is vesicular and contains quartz and plagioclase crystals which are visible to the naked eye. Locality 9 showed both rounded pumice and fiamme in hand samples and thin sections, whereas locality 11 showed rounded pumice in hand samples and elongated pumice in thin sections. Phenocrysts of PT5 is quartz.

Each of the different kinds of pumice has a ranging degree of elongation. Elongation of the pumice can range from little elongation, producing rounded/equant pumice (PT5) to thin, long strands producing tubular and ragged vesicle structures, creating long flattened pumice (PT1). Elongation of pumice is controlled by eruption gas extension (where, during the eruption, the gas escapes the pumice, stretching the structure with it, creating an elongated vesicle) and welding (where the vesicles are flattened during deposition).

Different vesicle shapes are also seen within the pumice ranging from rounded to elongated and tubular, with varying degrees of stretching and elongation of vesicles can be a result of eruption gas extension.

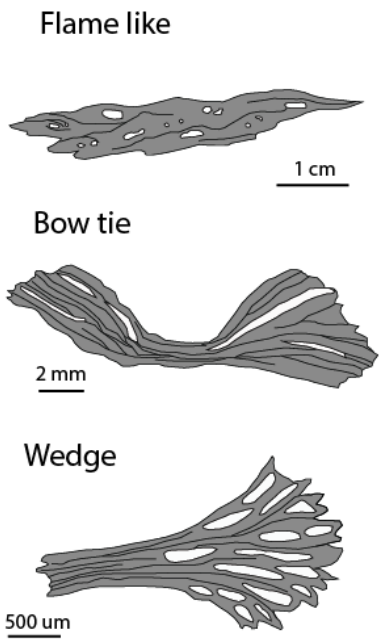

Figure 5.13. Sketches of different fiamme ends adapted from Gifkins et al. 2005.

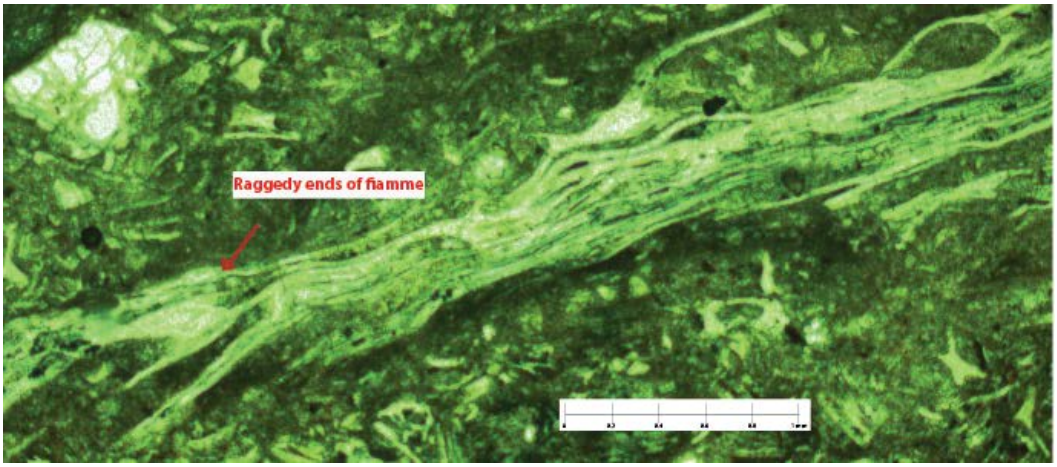

Figure 5.14. Fiamme raggedy ends of the Owharoa Ignimbrite.

Fiamme ends are of particular interest in this study due to the significant number of good examples of fiamme through the Owharoa Ignimbrite. The different kinds of fiamme and pumice are dominantly controlled by welding and eruption processes. The more welded a sample is, the darker the pumice appears. Different fiamme ends are seen within Figure 5.13, which is the basis for the descriptions of fiamme ends within the different types of pumice.

The darker fiamme like pumice are found westward, and the rounded pumice tends to be found eastwards within the field area. There is a rapid interchange between sites 1 and 2 to site 11, which turns from fiamme to pumice within a short distance. Site 11 may be higher stratigraphically than sites 1 and 2 within the Owharoa Ignimbrite unit, resulting in rounded pumice being found here. Within thin sections, fiamme tend to dominate, and found in most sites. In some sections, fiamme and pumice are both present (e.g. locality 9).

5.1.3.1 SEM of pumice

Under the SEM the pumice appear to have the similar textures and patterns as hand samples on a sub microscopic level. The SEM was able to expand on optical microscopy and reveal much more detail. Figure 5.15 A shows the flow texture of the fiamme along with vesicles which are difficult to see within optical microscopy.

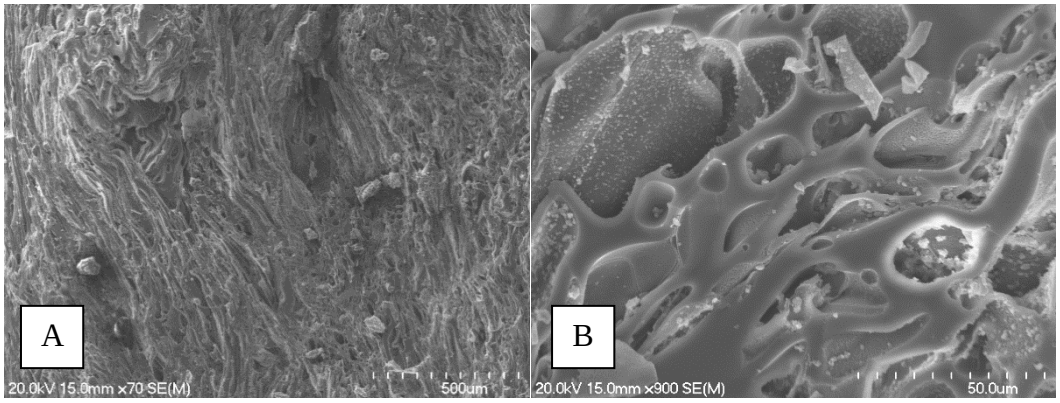

Figure 5.15. A. A SEM photo of an Owharoa Ignimbrite fiamme. B. A closer photo of the fiamme, highlighting the vesicles of the fiamme.

As seen in the Figure 5.15 B, the fiamme vesicles have not completely collapsed and appear elongated and correspond with the flow nature of the pumice. Some are rounded, some are elongated and some are broken and damaged, due to compression forces. This indicates that the bursting of bubbles that were trapped within the pumice when the magma was brittle and cause the bubbles to snap, leaving sharp ends.

Ragged ends that can be seen in thin sections can also be seen in under the SEM as seen in Figure 5.15.B. Figure 5.16 shows clearly the tubular structure of the vesicles which has created the elongated nature of the fiamme. This is indicative of the shearing nature of the magma during eruption, forming long tube structures from stretching the ductile material into thin tubes.

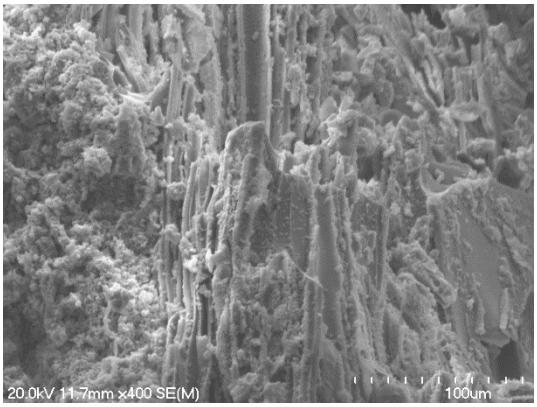

Figure 5.16. Owharoa Ignimbrite pumice sample with near straight ends.

5.1.4 Matrix

The matrix for the Owharoa Ignimbrite can be described as vitriclastic. The matrix consists of flattened glass shards and finer grained material which is unresolvable under an optical microscope.

5.1.4.1 Glass shard description

Glass shards are abundant within the matrix of the Owharoa Ignimbrite, and the variety of glass shard morphologies can be seen in Table 5.3 below. There are five main groups of glass shards and the Owharoa Ignimbrite has a range of the five groups and a mix of other glass shards which could be a result of the deformation of glass shards. Glass shard sizes range from 0.3 mm – 40 µm.

Glass shards within the Owharoa Ignimbrite align parallel to the fiamme although some wrap around lithics and crystals (Figure 5.17).

The glass shards within the Owharoa Ignimbrite are dominantly flattened (Figure 5.17) due to welding, indicating that the glass shards were still ductile when they were being flattened. A majority of glass shards also have sharp ends, indicating that bubble-bursting was occurring when the bubbles where brittle. This resulted in snapping of the bubbles into sharp glass shards. Table 5.2 shows the different shapes of glass shards.

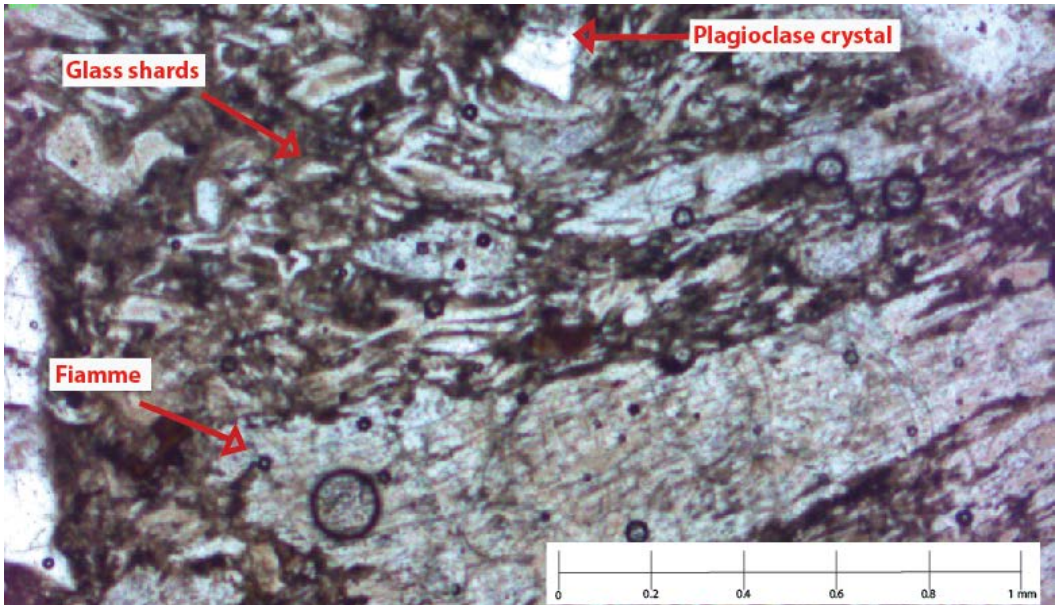

Figure 5.17. Photo of the Owharoa Ignimbrite matrix and glass shards.

Table 5.3. Glass shards table of the Owharoa Ignimbrite indicative of the different shapes that were seen through the Owharoa Ignimbrite in the produced thin sections. They are not to scale and were not quantified through shape, and are no way exclusive of the Owharoa Ignimbrite.

Cuspate	
Lunate	
Y shaped	
Platy	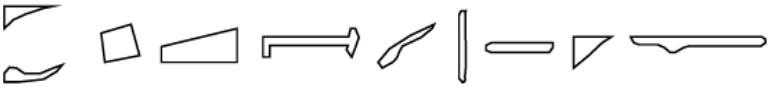
Other	

5.1.5 SEM results for fine grained matrix material

Using the SEM for the Owharoa Ignimbrite was difficult due to the nature of the chip samples – they were rough and tended to carry too much charge, making observations difficult. However, some photos were obtained of the glass shards. Glass shards are seen in Figure 5.18, and are prominent, sharper elongated shapes. Figure 5.18 B highlights the fine grained unresolvable material. It is finer than glass shards (~5 µm), and appears to be small, coarse-textured, rounded lumps. It is difficult to see at this scale as the material could be fine grained glass particles, clay material within the matrix or contamination of the sample such as dust.

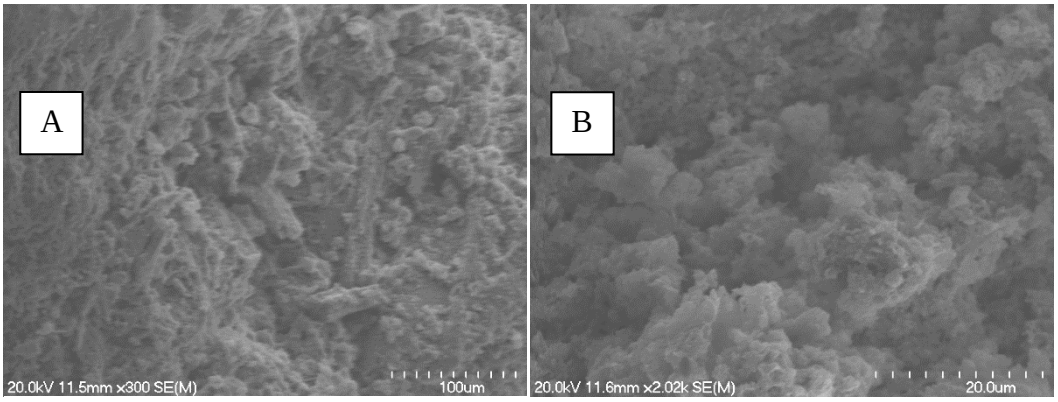

Figure 5.18. A. SEM photo of the Owharoa Ignimbrite glass shards. B. Photo from the under secondary electron showing the fine grained material at 20 µm.

Backscattered SEM elemental analysis on a polished sample was undertaken and revealed the microtexture of the unresolvable matrix material (Figure 5.19). Table 5.4 shows the results of this analysis and does not show any significant difference between the compositions of the two analysis points. Aluminium and iron are the most significant differentials between the different points.

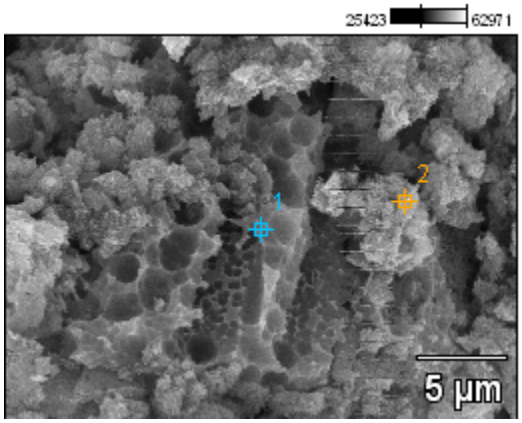

Figure 5.19. Back scatter image of the OI matrix at 15.0 kV of Base (7) – Owharoa Ignimbrite matrix.

Table 5.4: Elemental analysis of sample 'Base(7)' on two points, Base(7)_pt1 and Base(7)_pt2. Base 7 is a spot of the Owharoa Ignimbrite matrix.

Owharoa Ignimbrite glass and matrix elemental analysis (wt %)		
Analysis Identifier	**Base(7)_pt1**	**Base(7)_pt2**
Major oxides		
Si-K	37.28	34.34
Al-K	6.37	14.10
Fe-K		3.87
C-K	7.97	
Na-K	1.42	1.02
O-K	43.46	42.45
K-K	3.50	2.63
Cl-K		1.58

5.1.6 XRD results

The XRD results did not contribute significantly to the mineralogy that had already identified using optical microscopy. The results for these XRD tests can be found within the Appendix VI.

Minerals identified by the XRD include cristobalite (OI 1.1), quartz and plagioclase.

5.2 Waikino Ignimbrite

The Waikino Ignimbrite is a fine grained, massive ignimbrite. It is glass shard rich and pumice and lithic poor. This ignimbrite is uncharacteristically low in pumice, making it difficult to describe and interpret as pumice is a diagnostic feature of eruption and emplacement processes.

Component proportions

A point count analysis for the Waikino Ignimbrite was undertaken and the results are as shown in Table 5.5 and shown graphically in Figure 5.20.

Table 5.5. Table showing the point counting results of the Waikino Ignimbrite in percentages.

Component	W2
Pumice[1]	**0**
Matrix[2]	**88.3**
Total abundance of free crystals	**4.154**
Plagioclase	2.46
Quartz	0.94
Biotite	0.094
Opaques	0.66
Lithics	**2.18**
Iron oxyhydroxides	**3.03**

[1]*visual field estimates suggest <2%*

[2]*include glass shards and unresolvable fine grained material*

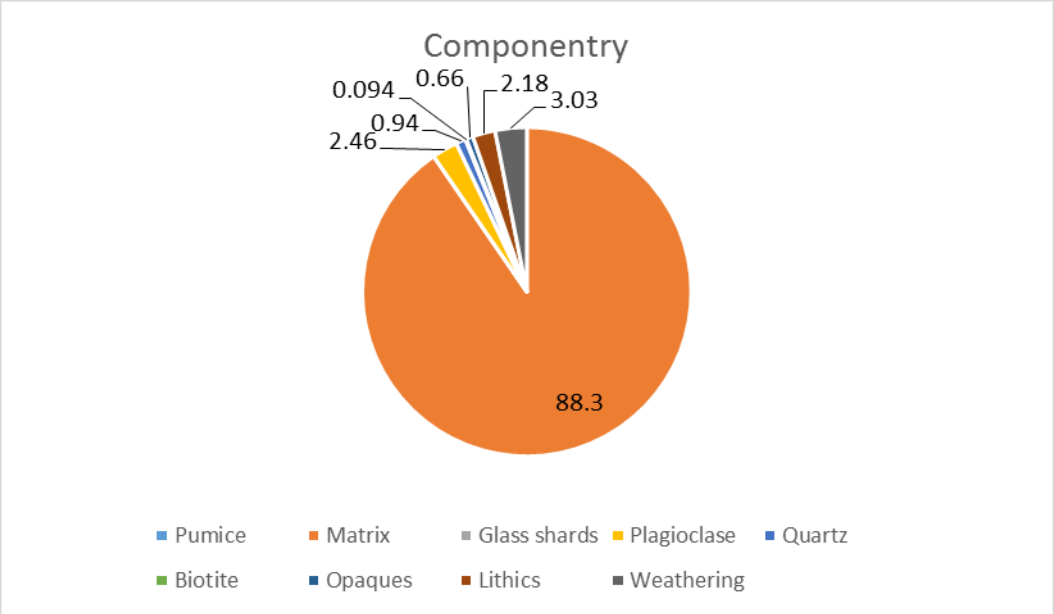

Figure 5.20. Pie graph of the Waikino Ignimbrite componentry.

This indicates that the Waikino Ignimbrite is an ash rich ignimbrite.

5.2.1 Mineralogy of the free crystals

The Waikino Ignimbrite crystal content is dominated by plagioclase, quartz and biotite with occasional occurrence of opaque minerals and hornblende.

Plagioclase

Plagioclase crystals within the Waikino Ignimbrite have a size range from 1.5 to 0.2 mm. The abundance of plagioclase within the ignimbrite is ~ 2.5% (Figure 5.20). The plagioclase crystals tend to be rounded to sub angular, but dominated by a sub angular rectangular shape. The centres of some of the plagioclase crystals tend to be worn away from resorbtion. Plagioclase also has irregular fractures. Embayment and twinning are both characteristic of plagioclase within this ignimbrite.

Electron microprobe analysis was used to determine the elemental composition of plagioclase further (Figure 5.21).

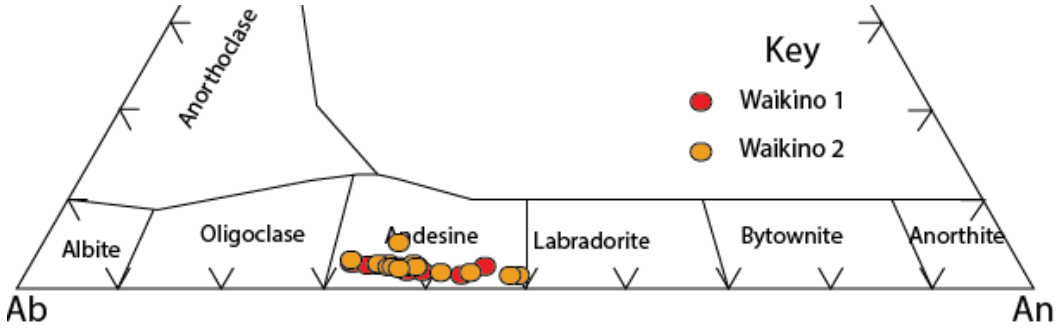

Figure 5.21. Ternary diagram of plagioclase for the Waikino Ignimbrite.

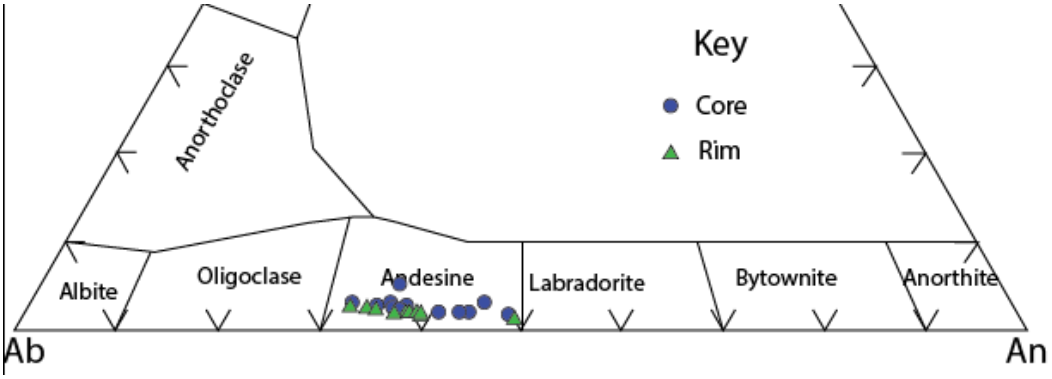

Figure 5.22. Ternary diagram of the Waikino Ignimbrite core and rim of plagioclase

Figure 5.21 shows that the plagioclase cyrstals of the Waikino Ignimbrite are constrained to andesine. This is more constrained than the Owharoa Ignimbrite indicating the Waikino Ignimbrite has less chemical variation within the plagioclase.

In Figure 5.22 above, core and rim analysis of the plagioclase was undertaken. There is a slight difference, with core samples being more potassium rich.

Quartz

Quartz (Figure 5.23) is a common crystal facies within the WI. Quartz tends to be rounded to sub-angular with small embayments forming from resorption or emplacement processes (i.e. weathering on emplacement). The size of quartz crystals ranges from 0.7 to 0.05 mm, and their is abundance is ~ 1%.

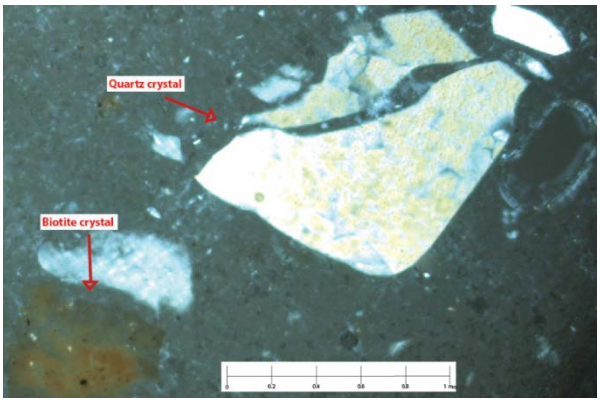

Figure 5.23. Quartz crystal and biotite crystal within the Waikino Ignimbrite. The slide is slightly thick, creating the dark brown colour of the biotite.

Biotite

Biotite crystals (Figure 5.23) are larger in the Waikino Ignimbrite compared to the Owharoa Ignimbrite. The size ranges from 1.5 mm to 0.2 mm, and have a ~0.1% abundance. Altered and non-altered biotite are present. The biotite also tend to be longer and more fibrous than those in the Owharoa Ignimbrite.

Table 5.6. Waikino Ignimbrite EMPA mineral analysis of the biotite crystals.

Waikino Ignimbrite biotite electron microprobe analysis results		
Biotite Sample	**WAI1-Biotite-1**	**WAI1-Biotite-1a**
Major oxide		
SiO2	48.261	45.216
TiO2	0.03	0.04
Al2O3	18.661	18.397
FeO	19.499	18.589
MnO	0.004	0
MgO	0.293	0.287
CaO	16.103	17.951
Na2O	0.09	0.106
K2O	0.335	0.299
Cr2O3	0	0.034
Total	103.276	100.919

Table 5.6 indicates the different elemental compositions of two of the Waikino Ignimbrite biotite crystals.

Opaque minerals

Opaque crystals (Figure 5.24) a larger in size compared to the Owharoa Ignimbrite from 0.5 to 0.1 mm and an abundance of ~0.66%. The shapes of the opaques range from sub angular to sub-rounded, and square to long 'stringy' shapes (which could be an alteration mineral).

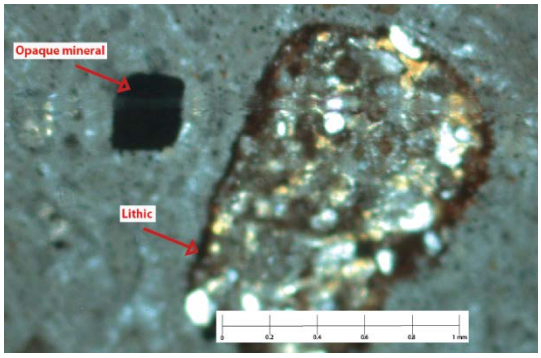

Figure 5.24. Opqaue mineral and lithic.

Table 5.7. Table showing the mineral analysis of opaque minerals in the Waikino Ignimbrite.

Waikino Ignimbrite Opaque Minerals							
Opaque Sample	**WAI1-1-center**	**WAI1 - 1.1-center**	**WAI1-4-center**	**WAI1-6-center**	**WAI1 - 9-center**	**WAI1 -10-center**	**W3 -6**
Major oxides							
SiO2	9.589	20.003	23.425	0.028	0	16.62	0.117
TiO2	8.129	14.803	28.284	47.911	50.166	29.234	22.491
Al2O3	0.486	0.438	0.229	0.054	0.003	0.326	0.402
FeO	71.457	57.068	41.624	47.55	44.955	46.545	66.094
MnO	0.535	0.558	0.975	0.852	1.138	0.978	0.992
MgO	0.271	0.422	0.76	0.558	0.658	0.753	0.819
Cr2O3	0.051	0.018	0.006	0	0.08	0.002	0
Total	90.518	93.31	95.303	96.953	97	94.458	90.915
Result	Mt	Mt	Mt	Il	Il	?	Mt

Mt = magneite and Il = Ilmenite

The elemental compositions of a number of opaque minerals within the Waikino Ignimbrite were determined by EMPA. Table 5.7 shows these results. The Waikino Ignimbrite has a higher number of magnetite crystals probed, which may mean that there are more magnetite crystals compared to ilmenite crystals.

Hornblende

Hornblende is also found within the Waikino Ignimbrite, however it is rare and was not within the point counted sample. They were small crystals (0.1 – 0.2 mm) and were subangular to subrounded.

Ewart and Healy (1965) identified hypersthene and magnetite within the Waikino Ignimbrite, but were not identified in this study.

5.2.2 Lithics

Lithics comprise ~2-3% of the Waikino Ignimbrite. There are several different lithic types present including; beige, glassy rhyolite lithics; rounded brown-pink lithics; glassy devitrified lithics (Figure 5.25); ignimbrite lithics; and black-grey to brown and pale grey lithics with biotite.

Glassy rhyolite lithics contained quartz crystals. These lithics range from 0.5 – 0.8 mm and have a sub angular to sub rounded shape. Rounded brown pink lithics which appear to be rhyolite lithics have a low crystal content and are approximately 0.5 – 1.5 mm and are sub-angular in shape. Light and dark speckled rhyolite lithics are present with plagioclase and quartz phenocrysts. These lithics range from 0.4 – 0.8 mm and are rounded to sub-angular in shape.

Dark grey andesite crystals were identified with a mid to dark grey matrix and crystal contents including plagioclase. They are sub-rounded in shape and range from 0.4 - 0.2 mm. Light grey andesite lithics are also present, however have few indistinguishable crystals, however biotite is identifiable. These lithics range from 0.3 – 0.5 mm in size and are sub-rounded in shape.

Devitrified lithics (Figure 5.25) were identified, including a range of dark brown, rounded lithics around 0.5- 1 mm. A range of rhyolitic devitrified speckled lithics with low crystal contents (including biotite, quartz and opaque crystals) were also identified.

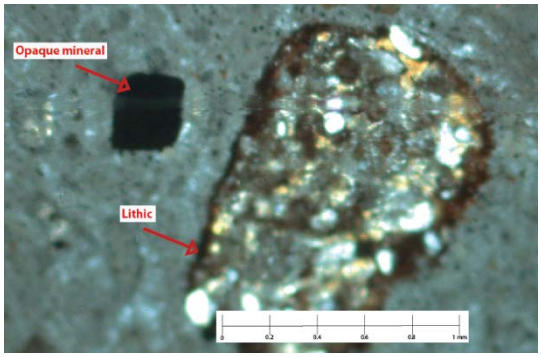

Figure 5.25. Devitrified lithic within the Waikino Ignimbrite.

Ignimbrite lithics range in size from 0.3 – 1.0 mm, and are rounded in shape. The ignimbrite lithics contain white, grey, brown and black ‘specks’/clasts. Crystal content includes quartz and plagioclase.

Volcanic lithics are pink-coloured, and have long thin plagioclase laths within at a high percent (~30%). These lithics range from 1 -0.3 mm and are rounded to sub rounded in shape.

Sandstone lithics (Figure 5.26) tend to be rounded, 1 to 5 mm in size with sand sized clasts and sub-rounded quartz crystals. Sandstone lithic clasts range from white/clear, black, yellow to brown in colour.

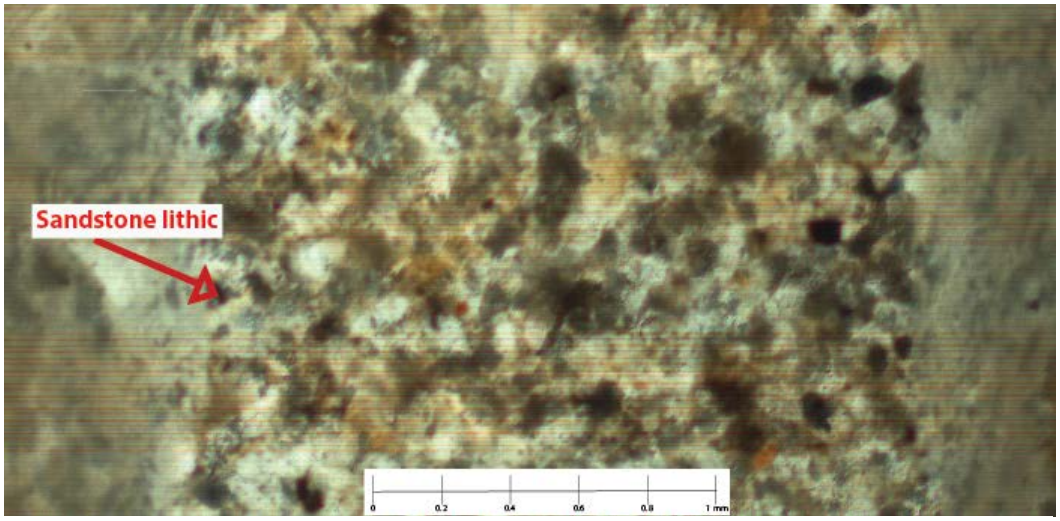

Figure 5.26. Large sandstone lithic within the Waikino Ignimbrite, showing grainsize and variety of different clasts, including quartz minerals.

Siltstone lithics were rare, and contained light to dark-coloured silt-sized clasts, with a much less variety of colours compared to the sandstone lithics. Siltstone lithics were subrounded and ranged in size from 0.5 mm – 0.1 mm.

An unidentified black to grey lithic with biotite was found, however it was weathered and difficult to identify. A light to dark brown lithic with no diagnostic features was also identified.

Ewart and Healy (1965) highlight lithics within the Waikino Ignimbrite to be greywacke, siltstones and ignimbrite(s), which is consistent with the present findings.

5.2.3 Pumice

Pumice comprises less than 2 vol. % of the bulk deposit. Coarse ash-sized, white (0.5 mm) pumice fragments are seen in hand samples, but are difficult to identify in thin sections. Their edges are not well-defined within the glass shard-rich matrix.

5.2.4 Matrix and glass shards

The matrix of the Waikino Ignimbrite is comprised of light grey to dark grey, very fine grained glass shards and unresolvable material under optical microscopy. When weathered, the matrix appears yellow, and fresh matrix material appear light to dark grey.

Glass shards in the Waikino Ignimbrite are typically larger than the Owharoa Ignimbrite. The different morphologies of glass shards include platy, lunate, cuspate and forked. The shards are prominent and appear long, thin and stringy (Figure 5.27). Figure 5.27 highlights the range of different sizes between the different glass shards (i.e. 1 mm – 50 µm).

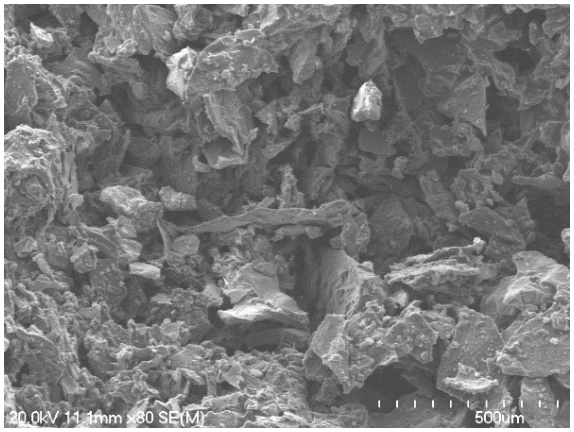

Figure 5.27. Waikino Ignimbrite SEM photo showing the glass shards within the matrix.

5.2.5 SEM elemental analysis

The SEM was used as an alternative method of mineral and matrix identification and elemental analysis. Using the SEM and secondary electron scanning and back scatter methods, there was some differentiation of mineral and matrix compositions within the Waikino Ignimbrite.

The mineral in Figure 5.28 has a high concentration of titanium and iron. This would suggest that the mineral in the photo is either ilmenite or titanomagenitite. However, due to the ‘eaten’ nature of the mineral, it is difficult to differentiate. As the shape of the mineral is more ‘compact’ and evenly sized, I would be inclined to suggest it is a titanomagnite rather than the regularly rectangular ilmenite.

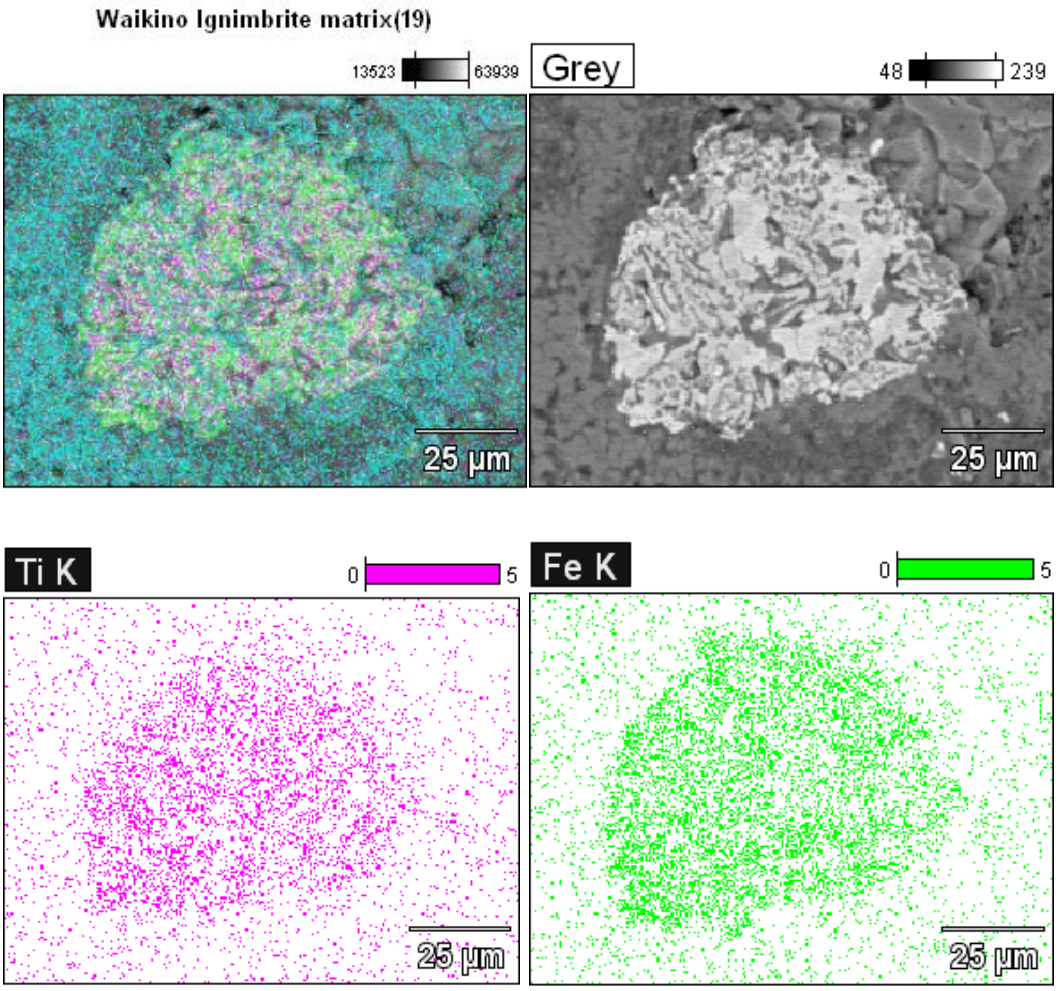

Figure 5.28. The elemental back scatter diagrams of an unidentified mineral. Data Type: Counts Mag: 1000 Acc. Voltage: 15.0 kV. The light blue spots are indicative of silica, and due to the 'eaten' nature of the material, the silica is showing through the mineral more than it typically would if the material was complete.

Figure 5.29 highlights the elemental analysis of a crystal (point 1), an opaque mineral (point 2) and unresolvable, fine grained matrix material (point 3). Point 1 (pt1) indicates a high silica content, resulting in a quartz/plagioclase crystal. Point 2 (pt2) exhibits iron and titanium as the two dominant elements. It is particularly high in iron, indicating it is magnetite. Point 3 (pt3) is high in potassium, silica and carbon.

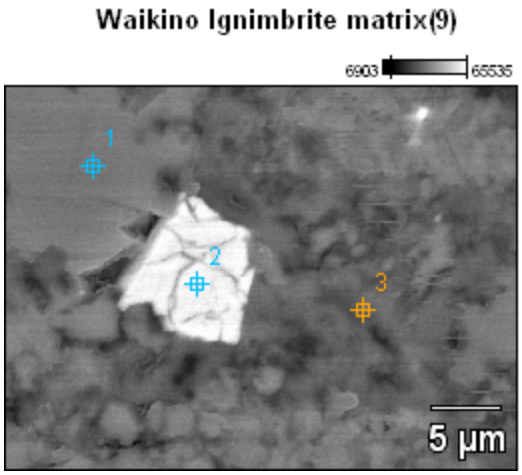

Waikino Ignimbrite matrix and mineral analysis (9) using the SEM						
	C-K	***O-K***	***Al-K***	***Si-K***	***Ti-K***	***Fe-K***
Waikino Ignimbrite matrix(9)_pt1	6.89	32.74		60.37		
Waikino Ignimbrite matrix(9)_pt2	1.87	8.19		0.71	2.51	86.72
Waikino Ignimbrite matrix(9)_pt3	24.82	27.50	18.72	28.96		

Figure 5.29. SEM elemental analysis of a crystal within the Waikino Ignimbrite and associated table with the results of the analysis.

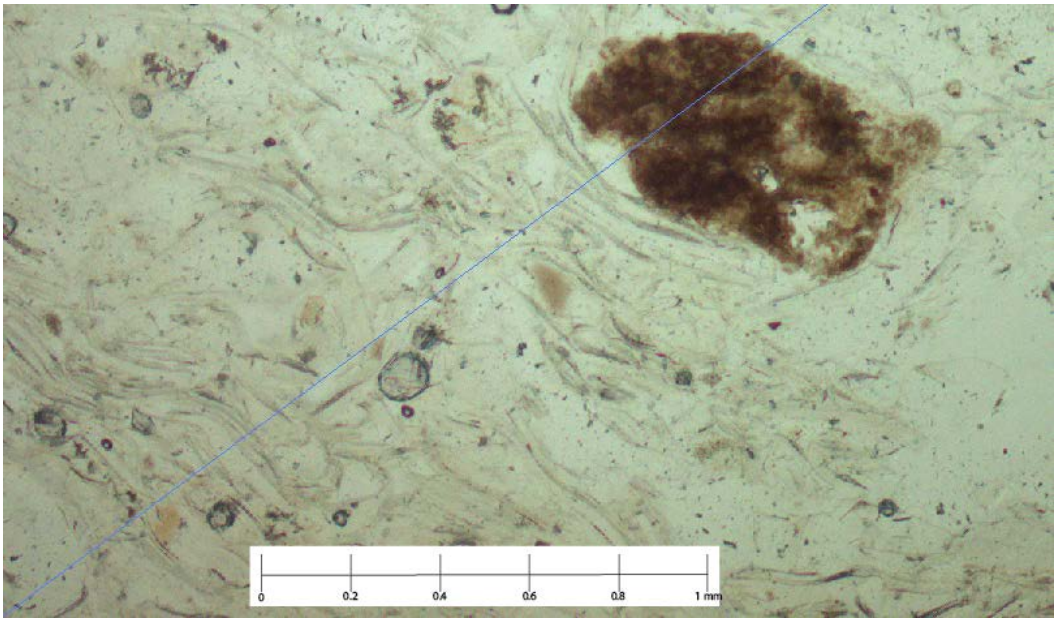

Figure 5.30. Petrographical photo under the 5x lens highlighting glass shards within the Waikino Ignimbrite.

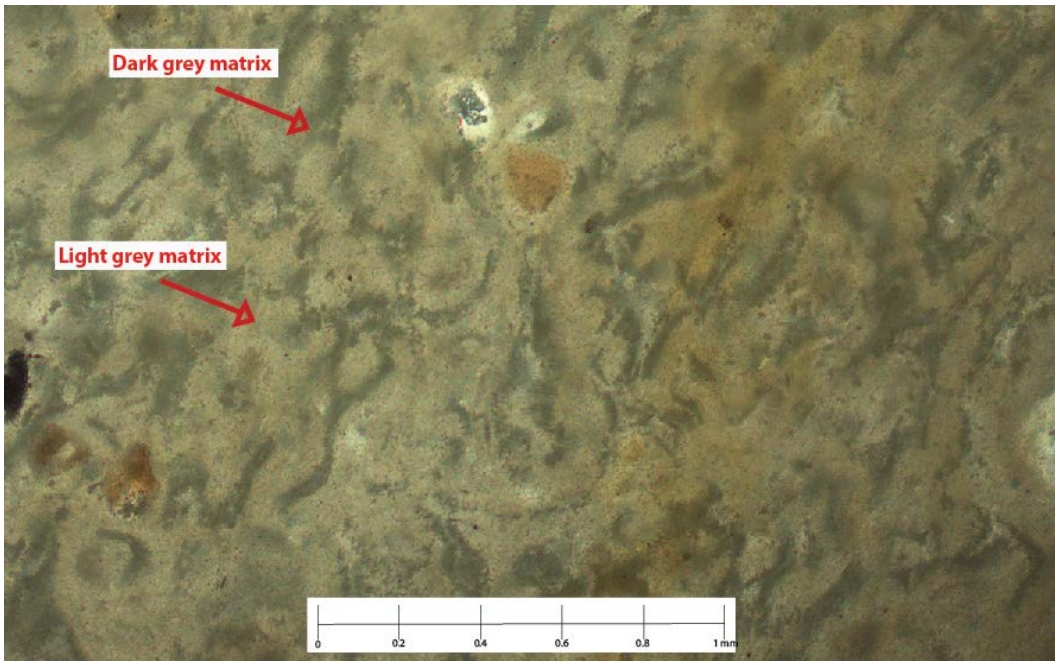

Figure 5.31. Petrographic photo under the 5x lens highlighting the different colours of matrix within the Waikino Ignimbrite.

For the Waikino Ignimbrite, as mentioned prior, it is difficult to analyse the matrix material (Figure 5.30), therefore SEM was used. Under optical microscopy, the matrix reveals dark and light grey swirls (Figure 5.31). An elemental analysis using the SEM was conducted between the two different shades of grey that were identified. Figure 5.32 shows the results of the elemental analysis

The grey image (top left, Figure 5.32) shows elemental analysis according to atomic number. This shows two distinct shades of grey in the matrix. There is also white in the grey photo indicating an iron rich, opaque mineral. The lighter grey section of the matrix is comprised of silica and potassium, and the darker grey section of the matrix is comprised of aluminium and iron. The differentiation in elemental analysis between the two matrix types would not be seen using other methods such as XRD for matrix elemental analysis.

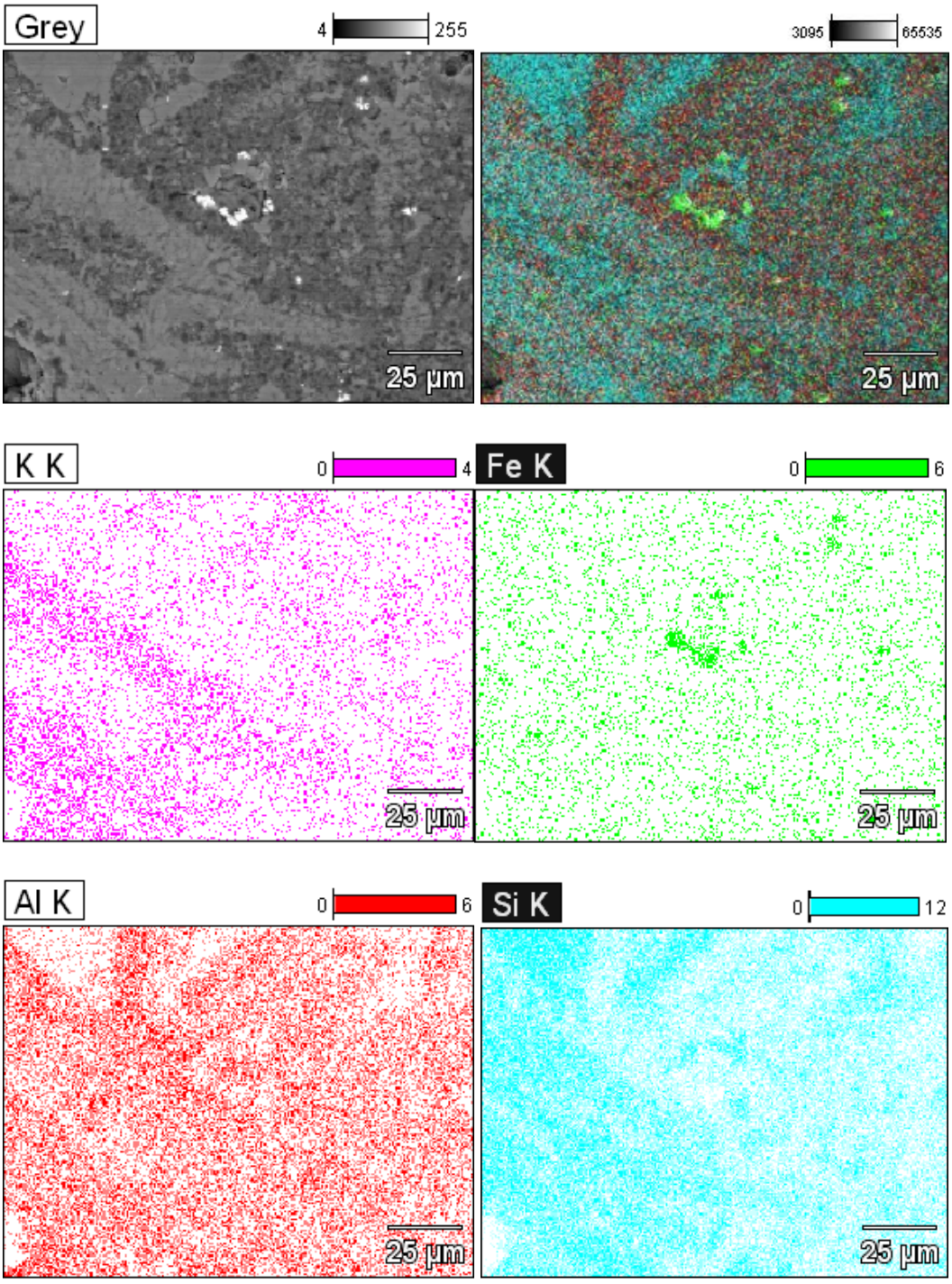

Figure 5.32. SEM EDS analysis at 15 kV was processed of the Waikino Ignimbrite matrix.

5.2.6 XRD results

The results from the XRD samples were variable due to the significant volume of glass within the matrix (Appendix VI). The Waikino Quarry sample was particularly hard to define and therefore has not been analysed. W1, W2 and W3 showed consistent results of quartz and plagioclase.

Chapter 6: Geochemistry

This chapter presents the results of the geochemical analyses that were undertaken for this study indicated in the methods chapter (Chapter 3). X-ray fluorescence spectrometry (XRF) has been used to identify the elemental composition of pumice and bulk ignimbrite samples and electron probe microanalysis (EMPA) has been used to identify the glass elemental composition.

6.1 Whole rock geochemical composition

The Owharoa and Waikino ignimbrites were both analysed using XRF spectrometry. Analysis of the Owharoa Ignimbrite included both pumice and bulk rock samples, however the Waikino Ignimbrite only included bulk rock samples as there was no distinct pumice to extract. For comparison, the XRF data for the two ignimbrites are displayed together (Figure 6.1).

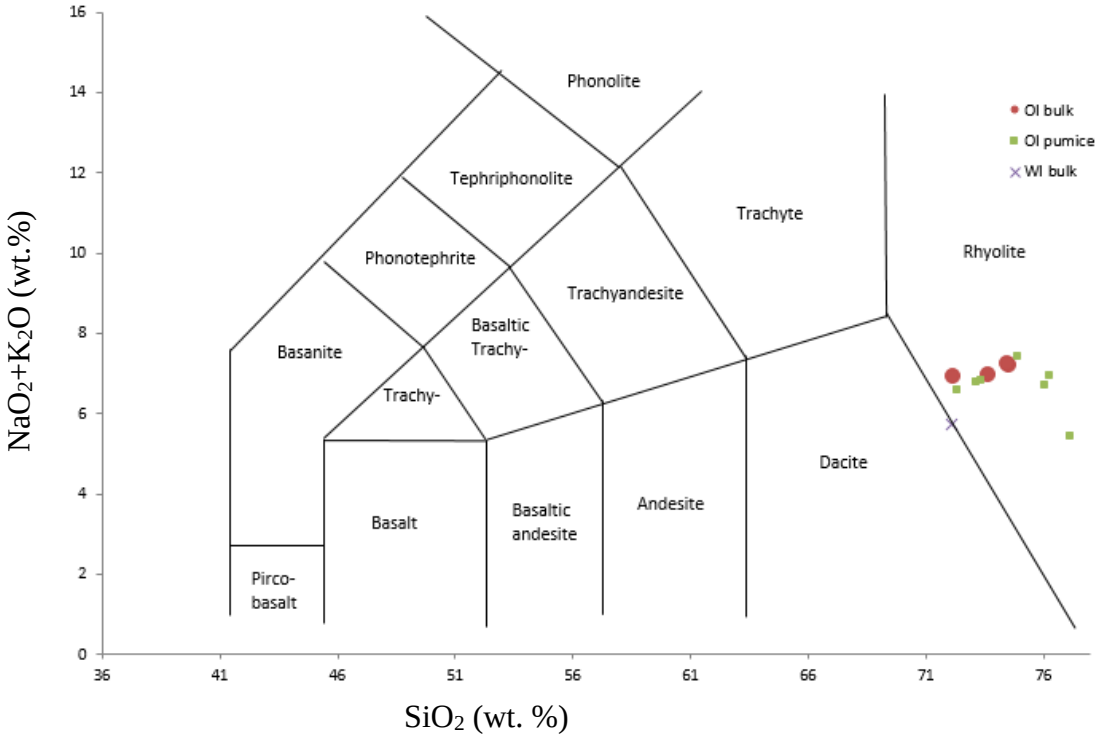

Figure 6.1. Owharoa and Waikino ignimbrite XRF results within a total alkali verses silica (TAS) diagram. The 'OI bulk' is the bulk analysis of the Owharoa Ignimbrite. 'OI pumice' is the analysis of just pumice samples from the Owharoa Ignimbrite. 'WI bulk' is a bulk sample from the Waikino Ignimbrite.

Pumice within the Owharoa Ignimbrite has a silica content of 72.5 - 77.3 wt. %, consistent with the rhyolitic mineralogy identified by Ewart and Healy (1965).

Bulk ignimbrite samples and pumice samples from the Owharoa Ignimbrite shown in Figure 6.1 have clustered together which indicates that there is not a significant difference between the two sample types and that the bulk samples have minimal contamination from lithics, or other non-juvenile components.

The Waikino Ignimbrite XRF analysis revealed the silica content for the ignimbrite to be ~72 wt. %, cusping the edge of the rhyolite and dacite boundary (Figure 6.1). The Waikino Ignimbrite sample was only able to be processed as a bulk sample and therefore may have some contamination issues, decreasing the silica content compared to the Owharoa Ignimbrite analysis. This could explain why the Waikino Ignimbrite sample is more dacitic than expected. In Chapter 5 lithics were identified within the Waikino Ignimbrite which could contribute to the contamination of the bulk sample.

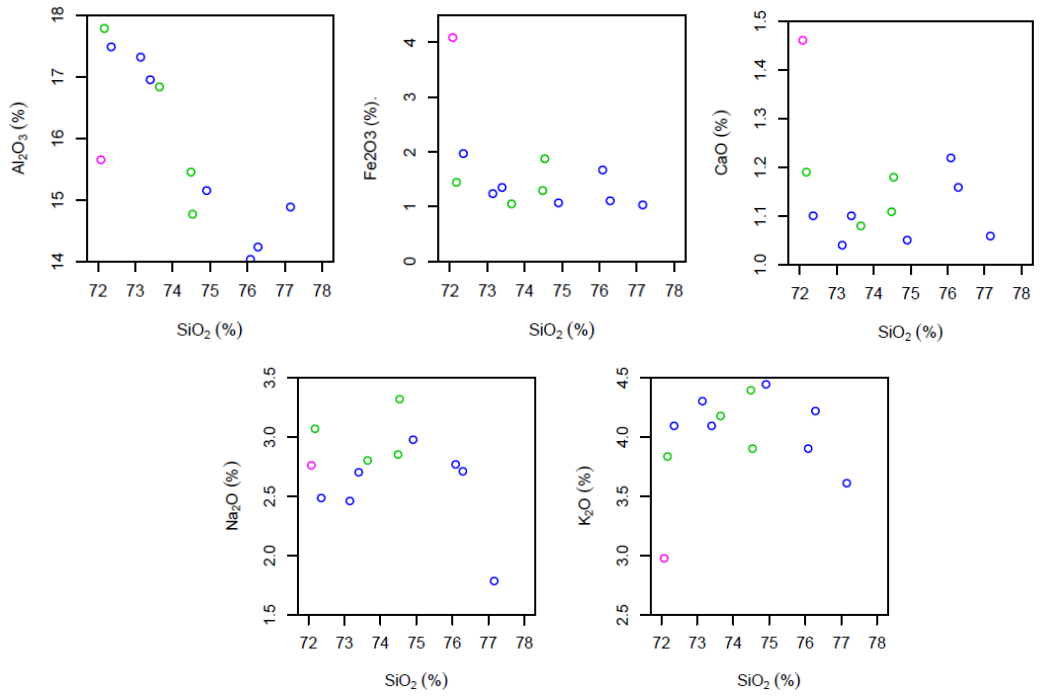

Figure 6.2: Harker plots of selected major elements against SiO_2. The Waikino Ignimbrite bulk sample is in pink, the Owharoa Ignimbrite samples are in blue (bulk) and green (pumice).

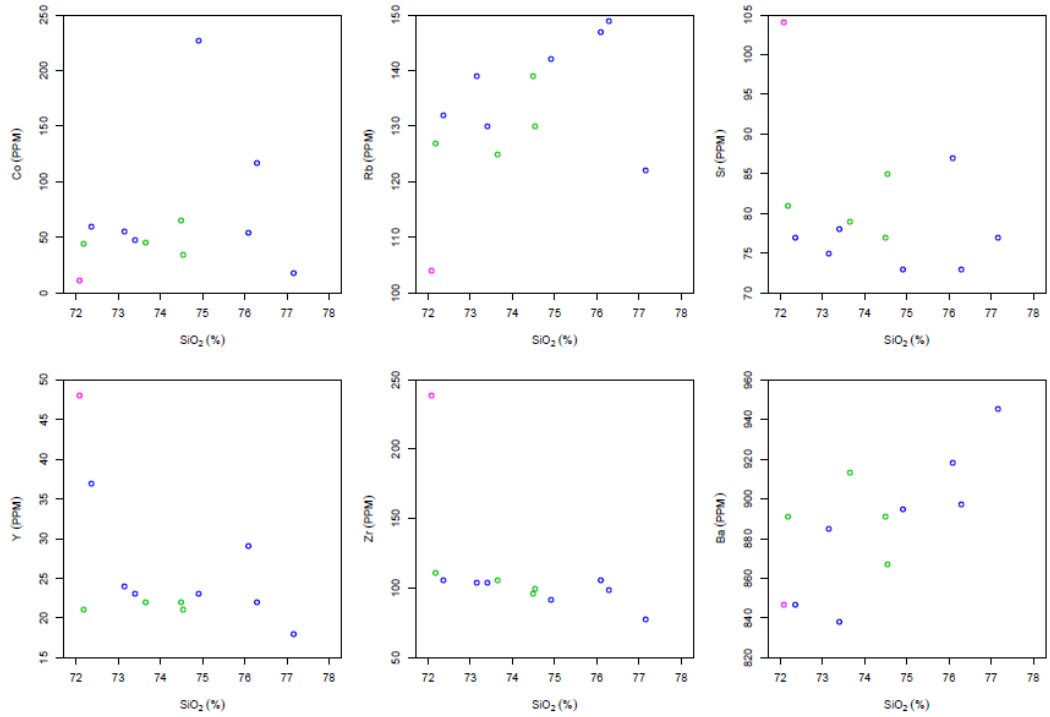

Figure 6.3: Harker plots of the selected trace elements against SiO_2 wt. %. The Waikino Ignimbrite bulk sample is in pink, the Owharoa Ignimbrite samples are in blue (bulk) and green (pumice).

Harker plots show the XRF results for the different major (Figure 6.2) and trace elements (Figure 6.3) for the Owharoa and Waikino ignimbrites. There was only one Waikino Ignimbrite result so it has been included in figures 6.2 and 6.3 along with the Owharoa Ignimbrite results. As there is only one data point for the Waikino Ignimbrite, it cannot exhibit a trend.

The bulk and pumice samples seen within the Owharoa Ignimbrite Harker plots correlate well. They plot close together, although the bulk samples occur towards the silicic end compared to the pumice.

Figure 6.2 shows that as silica increases, aluminum (Al_2O_3) decreases which is a result of aluminum precipitating into feldspars/plagioclase. Plagioclase was identified within the Owharoa Ignimbrite within Chapter 5.

Iron exhibits a minor decreasing trend with silica, indicating the precipitation of iron into either opaque minerals, such as magnetite, or mafic minerals such as biotite.

Sodium (Na_2O) shows a slight increasing then decreasing trend, which indicates the incompatibility of sodium until ~ 75 wt. % SiO_2, above which sodium

transitions into a compatible element and precipitates into a mineral. Calcium (CaO) shows the opposite trend, which indicates there is a relationship between the two elements. Sodium and calcium precipitates into plagioclase, specifically andesine, which is slightly more sodium-rich over calcium.

Potassium (K_2O) shows an increasing, then decreasing trend within the melt. This could be due to the precipitation of biotite and potassium feldspar and hornblende (trace mineral).

Figure 6.3 shows the trace element Harker plots of cobalt (Co), rubidium (Rb), strontium (Sr), yttrium (Y), zirconium (Zr) and barium (Ba) versus SiO_2 wt. %.

Cobalt (Co) shows a scattered trend (Figure 6.3), with two outliers over 100 ppm. Cobalt also covers a range of figures with no distinct trend or consistency. It may be an inconsistency with the sampling method causing the random patterns, or the cobalt may be sporadically precipitating into an accessory mineral.

Rubidium (Rb) exhibits an incompatible trend. Rubidium can substitute for potassium in hornblende and biotite, however due to the rare amounts of hornblende within the Owharoa Ignimbrite, rubidium still indicates an incompatible trend. While rubidium is increasing, potassium is decreasing.

The trace element Harker plots do not reveal any significant trends. Strontium indicates a slightly decreasing, compatible trend against silica, where strontium could be substituting into plagioclase in place of calcium in some places.

Yttrium and zirconium exhibits a minor steadily decreasing, compatible nature against silica. This is not normal, as yttrium is usually incompatible. Zirconium also shows a decreasing, compatible trend, although zirconium is normally incompatible.

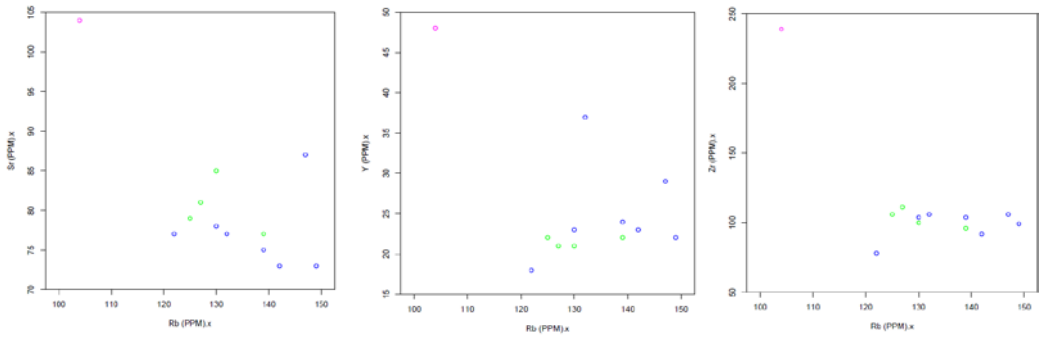

Figure 6.5. Harker plots of the XRF analysis data showing rubidium against strontium, yttrium and zirconium.

Barium shows an increasing, incompatible trend. Barium can substitute for potassium in hornblende, like rubidium, however due to the rare amounts of hornblende within the Owharoa Ignimbrite, barium still indicates an incompatible trend. The decrease of both strontium and barium could be a result of the differentiation of plagioclase. This could cause an incompatibility with strontium and barium (Cox *et al.*, 1979).

Barium shows an increasing, incompatible trend, staying within the melt rather than turning into a mineral. Barium can substitute for potassium in hornblende, like rubidium, however due to the rare amounts of hornblende within the Owharoa Ignimbrite, barium still indicates an incompatible trend.

Figure 6.5 shows the strontium, yttrium and zirconium against rubidium. Strontium appears to be decreasing with increasing rubidium, showing a compatible trend, whereas the zirconium trend is flat, and the yttrium trend is increasing with increasing rubidium, showing an incompatible trend.

Waikino Ignimbrite

The Waikino Ignimbrite shows a higher amount of titanium, iron, magnesium, calcium, strontium, yttrium and zirconium than the Owharoa Ignimbrite within the XRF results. It also has lower potassium and iron levels. However as the Waikino Ignimbrite bulk sample may have been contaminated, the XRF results are not comparable.

6.2 Glass shard compositions

6.2.1 Owharoa Ignimbrite

The analysis of glass shards was undertaken by EMPA and the results are shown in Figure 6.6.

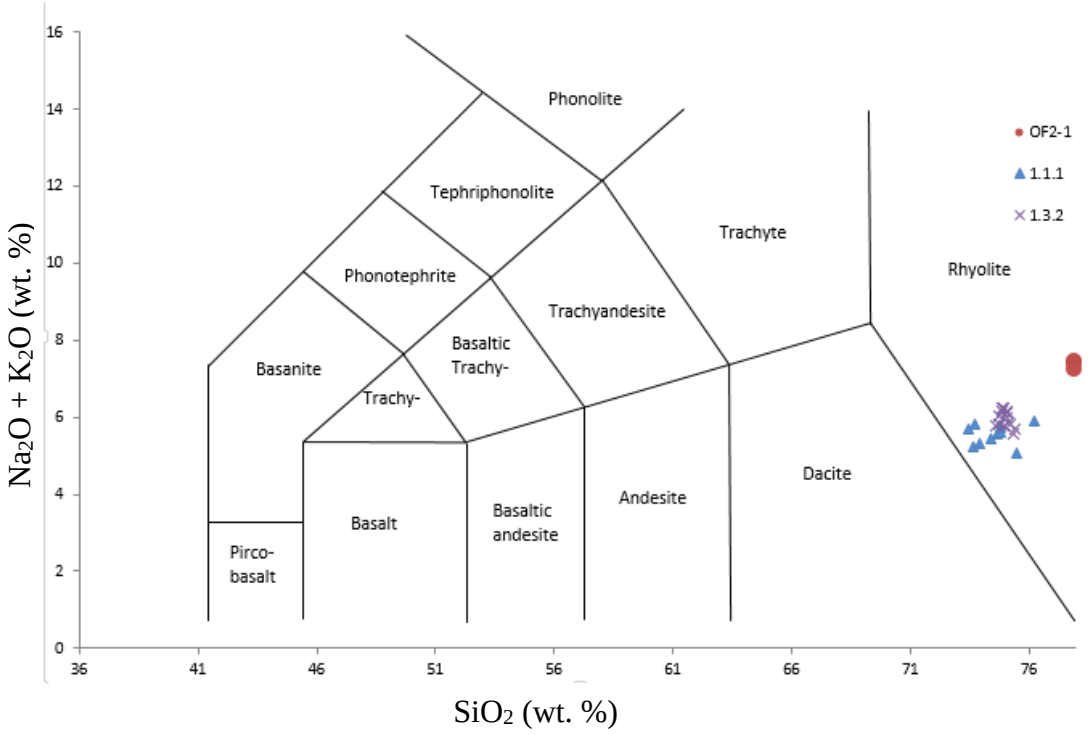

Figure 6.6. TAS diagram of the Owharoa Ignimbrite glass shard composition. The Owharoa Ignimbrite samples were matrix samples acquired from three sites within the type section (Locality 1 and 2).

The EMPA results indicate SiO_2 is generally >72 wt. % resulting in the ignimbrite being defined as a rhyolite, supporting the XRF data. The EMPA results are similar to the XRF results, however the alkali total is lower in the EMPA results. This may be due to the lack of non-juvenile contamination within the glass shards compared to the bulk ignimbrite samples.

The results from Figure 6.6 show that through the stratigraphic section at the Owharoa Falls, with samples 1.1.1, 1.3.2, and OF2-1 moving upwards through the type section. Figure 6.6 shows that the deposit becomes more silicic, vertically upwards.

Harker plots (Figure 6.7) were produced to interpret the different relationships between elements in the glass shards.

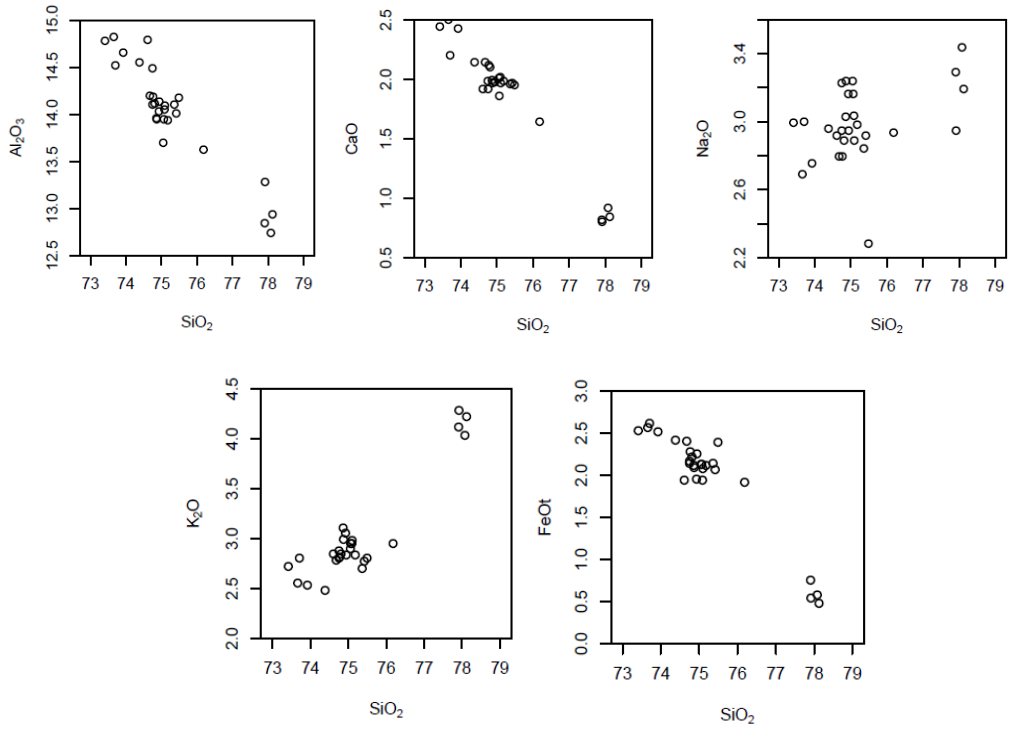

Figure 6.7. Harker plots of the electron microprobe analysis results for the Owharoa Ignimbrite. The elements within the figure are the elements that exhibited trends. All units are in wt. %.

The steady decrease of aluminium out of the melt may be due to plagioclase and biotite precipitation. Other plagioclase-forming elements also have a similar trend. Plagioclase was identified within XRD testing and aluminium may also be precipitating into this mineral. This appears consistent with XRF results.

The compatibility and steady precipitation of magnesium within the Owharoa Ignimbrite could be due to the formation of magnetite, ilmenite and biotite. This is consistent with the mineralogy in Chapter 5.

The steady decrease of calcium is a result of the compatibility of calcium and precipitation into plagioclase from the melt.

The minor, steady increase of sodium within the melt indicates that it is incompatible. This could mean that the plagioclase was forming with calcium more than sodium, resulting in a more incompatible sodium, and a compatible calcium.

Potassium exhibits an incompatible, increasing trend. Potassium precipitates into the minor mineral biotite, identified within the Owharoa Ignimbrite in Chapter 5.

Iron has a compatible trend, precipitating out of the melt into ilmenite, biotite and magnetite. This is consistent with XRF results, and shows a 2% decrease in iron against increasing silica content.

6.2.2 Waikino Ignimbrite

Figure 6.8 indicates that the SiO_2 content of the Waikino Ignimbrite glass shards is >72 wt. % resulting in the Waikino Ignimbrite being defined as a rhyolite. There is one particularly high SiO_2 content glass shard (85.7% SiO_2) which could be a result of alteration of the glass.

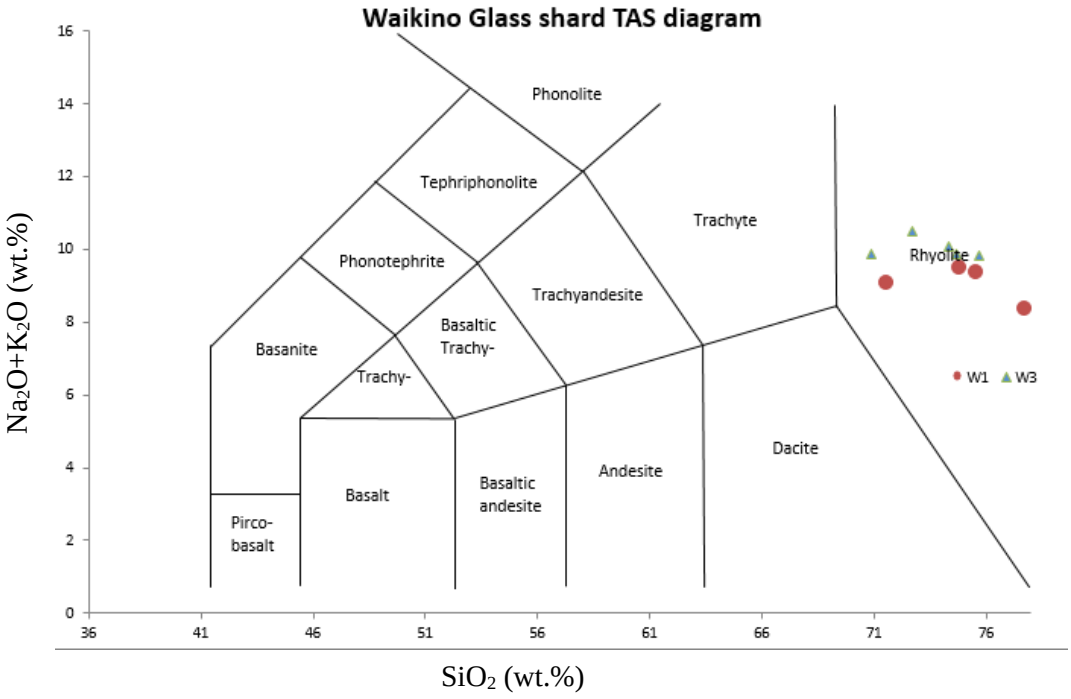

Figure 6.8. TAS diagram showing the glass shard composition of the Waikino Ignimbrite.

The Waikino Ignimbrite bulk ignimbrite composition (nearly dacite) and electron microprobe analysis results (rhyolite) are quite different. This may be due to contamination by non-juvenile material in the bulk sample compared to the glass shards.

Plagioclase and biotite crystals in the bulk rock sample tend to enrich the sodium and potassium content in the bulk rock relative to the pure glass shards. This increases the sodium and potassium percentages within the Waikino Ignimbrite glass shard EMPA analysis compared to the XRF analysis.

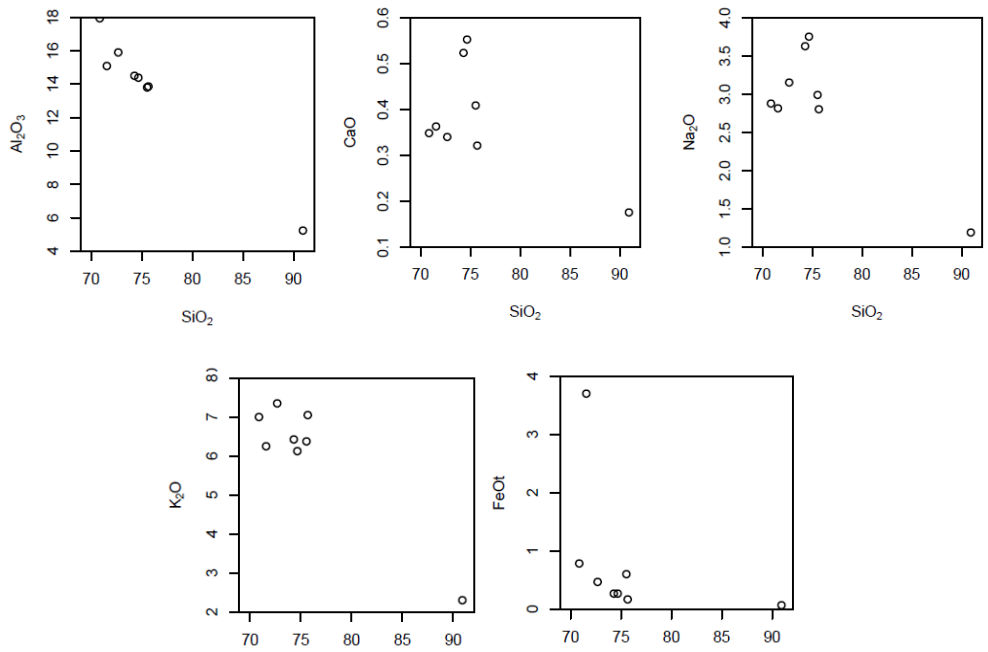

Figure 6.9. Harker plots of major elements for the Waikino Ignimbrite EMPA results on glass shards. This figure only shows elements with identifiable trends.

Figure 6.9 shows the Harker plots for the Waikino Ignimbrite using the EMP data results.

Aluminium has a decreasing compatible trend, indicating the precipitation of Al into plagioclase (anorthite) and biotite. This is consistent with the XRF analysis.

Sodium has a decreasing then increasing compatibility, changing around 75 wt. % SiO_2. This is because sodium is precipitating into plagioclase.

Potassium in the XRF data appears at 3 wt. %, and in the EMPA data it appears as a cluster around 6-7 wt. %. This is an increased amount which could indicate that the glass shards of the Waikino Ignimbrite have a higher content of potassium compared to the bulk sample of the Waikino Ignimbrite XRF analysis. There is also more iron and calcium in the bulk rock XRF sample, which lowers the potassium percentage level down in the XRF sample.

Iron has a higher percentage in XRF analysis results (~4 wt. %) compared to the EMP data results (>1 wt. %). This increase within the XRF data is most likely the result of contamination from the bulk sample. The iron within the Waikino Ignimbrite EMPA data indicates a decreasing, compatible trend which is indicative of precipitation into opaque minerals, including magnetite and ilmenite, hornblende and biotite.

6.3 Comparison between the Owharoa and Waikino ignimbrites

The Waikino Ignimbrite XRF sample is contaminated, indicated by the dacitic outcome in the TAS diagram (Figure 6.1), and in the glass results it comes out rhyolitic. Therefore, comparisons within the XRF data cannot be made between the two ignimbrites.

The Owharoa and Waikino ignimbrites share a similar percentage of sodium and aluminium. The Owharoa Ignimbrite has higher calcium and iron percentages. The Waikino Ignimbrite has a higher potassium percentage. The difference between the elemental percentages are no more than a ‘few’ percent different, indicating that these two ignimbrites are geochemically similar.

The Owharoa Ignimbrite indicates vertical zoning, identified from the type section (Figure 6.6). This zoning is an increase in silica content up through the deposit.

The Waikino Ignimbrite indicates a heterogeneous magma with areas of magma with lower silica content (and low plagioclase precipitation) and areas with higher silica content (and more minerals precipitated).

Chapter 7: Discussion

7.1 Similarities and differences between the Owharoa and Waikino Ignimbrites

The Owharoa and Waikino ignimbrites are significantly different in stratigraphic and facies characteristics but share similar mineralogical and geochemical attributes as seen in previous chapters. The differences between the physical characteristics are a result from different eruption and depositional processes. Similar mineralogical and geochemical attributes suggest that the ignimbrites share a similar, if not the same, magmatic source.

The differences between the facies characteristics of the two ignimbrites are seen in Table 7.1:

Table 7. 1. Table of the Owharoa and Waikino ignimbrites comparing facies characteristics.

Owharoa Ignimbrite	**Waikino Ignimbrite**
Pumice-rich	Pumice-poor
Four facies	Two facies
Coarse ash matrix	Fine ash matrix
3.76 ± 0.05 Ma	3.48 ± 0.19 Ma
Eutaxic	Vitriclastic
Non to densely welded	Moderately welded

The Owharoa and Waikino ignimbrites share similar crystal contents, including plagioclase, quartz, opaques, and biotite in similar percentage proportions. This indicates that the ignimbrites may share a similar magmatic source. Both ignimbrites share very similar plagioclase compositions (Figure 7.1) which is also indicative of similar magmatic compositions.

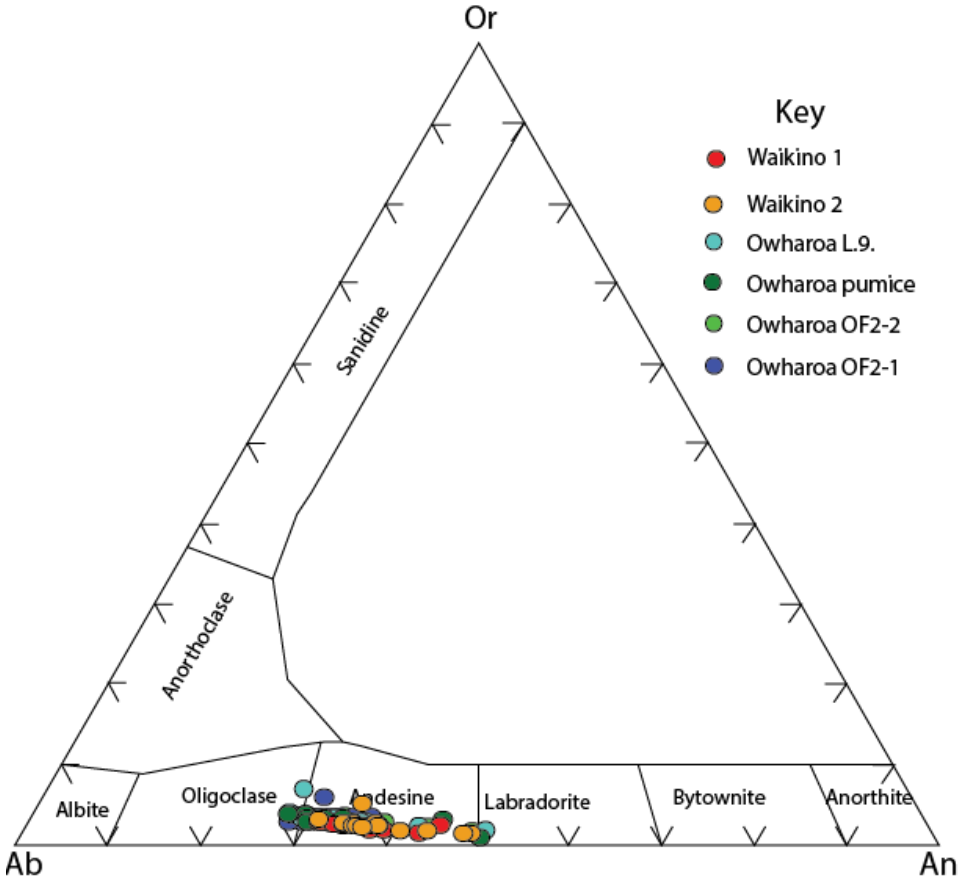

Figure 7.1. Plagioclase ternary diagram showing similar plagioclase compositions in both the Owharoa and Waikino ignimbrites. This diagram was based on glass shard EMPA data.

7.1.1 Lithic clasts and their sources

The two ignimbrites also share similar lithic contents including sandstone, ignimbrite, rhyolite, and andesite lithics. The lithic contents of the ignimbrites are indicating that both ignimbrites may have been sourced from areas of country rock of similar geology. There are several different causes to explain the lithic population, outlined below.

Scenario one: The ignimbrites could have excavated lithics from the walls of the conduit, from a stratigraphically diverse vertical country rock succession. This could indicate that the magma chamber was at or below these lithic origin sites. Greywacke lithics were identified within the Waikino Ignimbrite (Ewart and Healy, 1965), therefore the magma chamber must have been in contact with

the basement rock. This scenario is documented previously within the active TVZ where accessory lithic fragments are able to identify a complex subsurface geology (Cole *et al.,* 1998).

Scenario two: There also could have been different pyroclastic flow pulses that picked up a variety of lithic material from different locations exposed in the paleo-landscape. This could cause a variation in lithic population spatially across the landscape, however due to the minimal exposure of the Waikino Ignimbrite this cannot be confirmed. This scenario has been identified by Wright *et al*., (1980) where there accidental lithics were eroded from the substrate during passage of a pyroclastic flow.

Scenario three: Different sections of the caldera rim may have collapsed during the eruption and formed multiple vents which would have resulted in a variety of country rock lithics getting mixed into the pyroclastic flow. The ignimbrites should show vertical lithic variations within their stratigraphy, however this is not observed. To confirm the scenario, detailed lithic counts would have to be undertaken. This scenario is seen within the Crater Lake caldera in Oregon, where the vent location during the eruption changed, changing the lithic types that were being deposited (Suzuki-Kamata *et al.,* 1993).

There is no reason why these three scenarios could not have happened together, in each eruption with varying degrees of influence. The most probable scenario however is scenario one. As both the Owharoa and Waikino ignimbrites share similar lithic contents and characteristics, it is plausible that the two ignimbrites were erupted through the same geological units, picking up the similar lithics.

The ignimbrite lithics within the Owharoa and Waikino ignimbrites indicate that older ignimbrites occur beneath the subsurface. The lithics could be from the Corbett Ignimbrite, or from unknown ignimbrites deeper within or surrounding the caldera structure. The ignimbrite lithics within the Waikino Ignimbrite however could be sourced from the underlying Owharoa Ignimbrite.

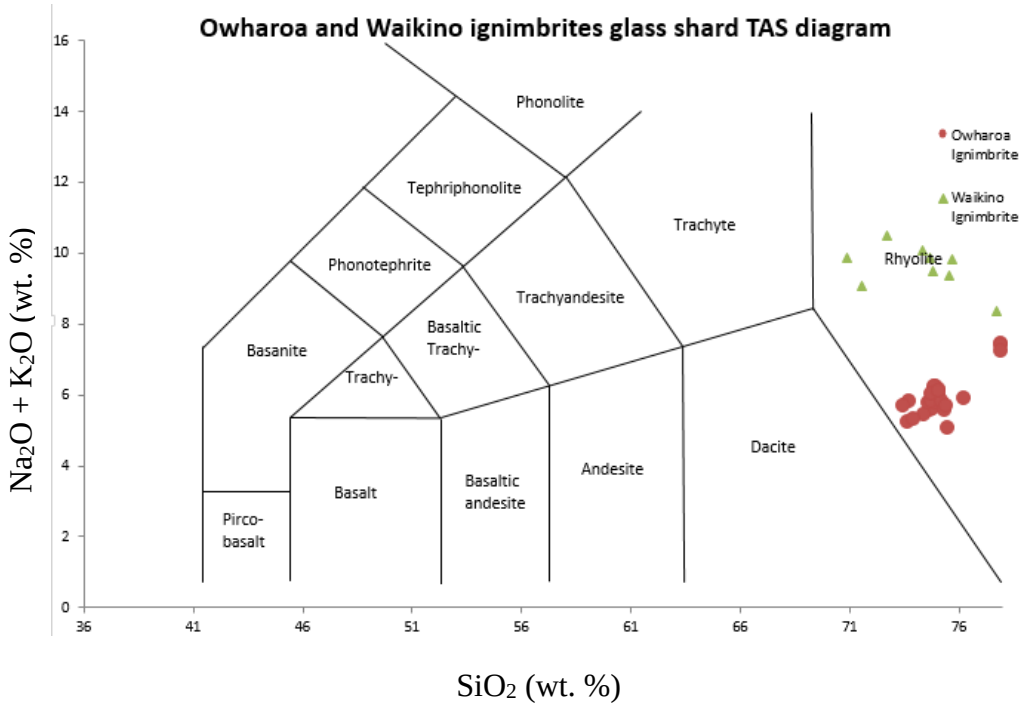

Figure 7.2. TAS diagram of the Owharoa and Waikino ignimbrites using glass shard EMPA data.

7.1.2 Effect on the modern landscape

The Owharoa Ignimbrite has its thickest deposits within the Waihi Caldera, where it is up to 80 m thick. Through the eastern section of the Karangahake Gorge, the Owharoa Ignimbrite forms large bluffs and cliffs which are hard to eroded, producing waterfalls and streams such as at locality 1 and 2.

In contrast, the Waikino Ignimbrite has limited outcrop and the deposits have created a near-flat deposit along the Waihi basin surface. Brathwaite and Christie (1996) discuss that the Waikino Ignimbrite may have been more widely spread but has been eroded away to the deposit we see today.

7.1.3 Distribution and geometry comparison

The distribution of the Owharoa and Waikino ignimbrites is consistent with the Brathwaite and Christie (1996) map (Figure 7.3) although more sites were identified in this more specific study.

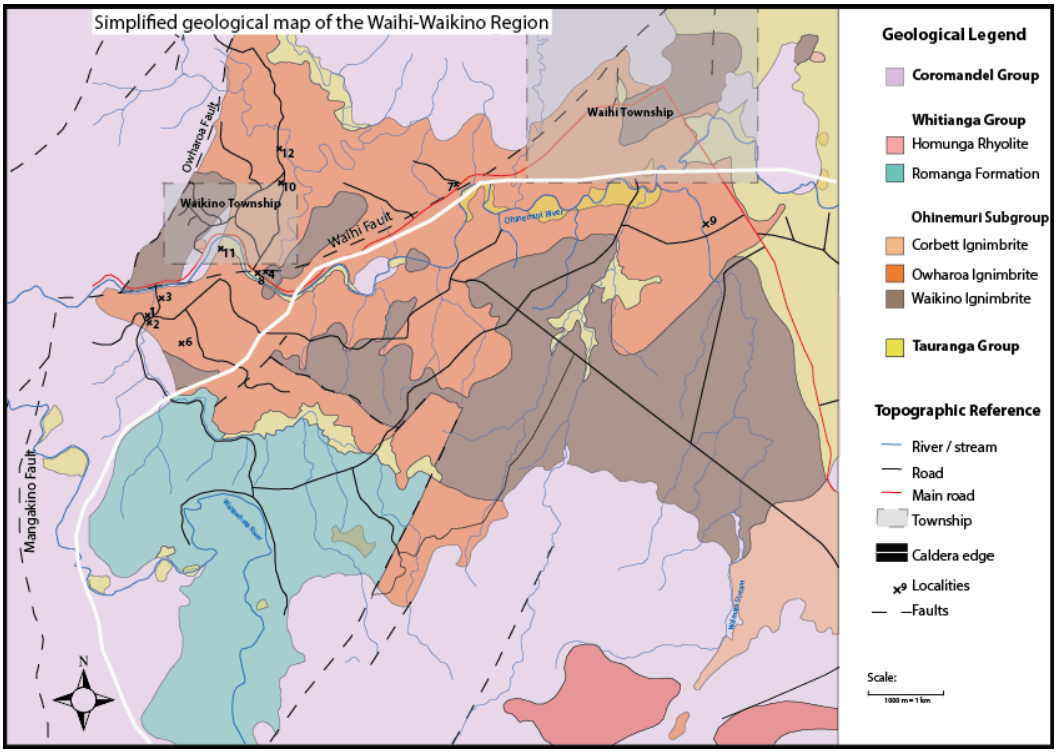

Figure 7.3. Simplified geological map of the Waihi-Waikino region (adapted from Brathwaite and Christie 1996). The map indicates localities from this study area and the caldera rim from the gravity anomalies identified (Smith et al. 2006).

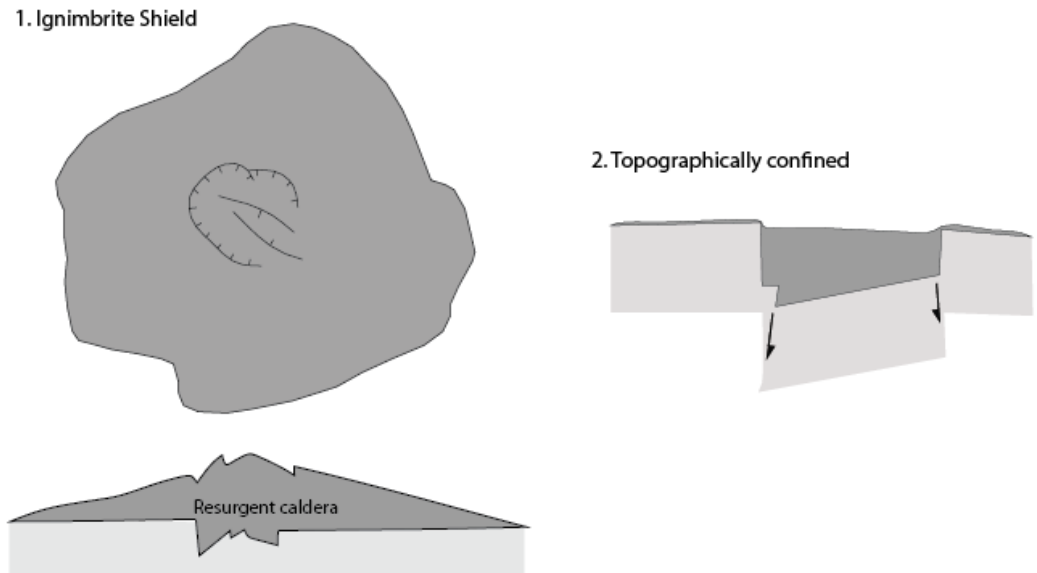

Figure 7.4. Ignimbrite shield and topographically confined ignimbrite shapes potentially identified for the Owharoa and Waikino ignimbrites. Adapted from Branney & Kokelaaar, 2002.

The deposition of the Owharoa Ignimbrite created significant volumes of ignimbrite deposit within and outside the caldera. Deposits continued through to the west through the paleo Karangahake Gorge which was dominantly an andesitic stratovolcano landscape.

If the hypothesised conventional caldera rim is extended out (white line (Figure 7.3), based on Smith *et al*., (2006) study) it would encompass nearly all of the ignimbrite deposits (excluding the 7 km northwest deposit for the Owharoa Ignimbrite identified by Brathwaite and Christie (1996) at the Awangaro Stream). This could extend out the caldera rim boundary further than previously assumed. However the deposit reported by Brathwaite and Christie (1996) that extends out to the 7 km west site shows the ignimbrite has both an intra caldera and an outflow deposit. This indicates that the Owharoa Ignimbrite could be a topographically-confined ignimbrite deposit or an ignimbrite shield (Figure 7.4). *Topographically confined ignimbrite* deposits tend to be thick (Lipman, 1984), and vary in shape depending on the shape of the caldera. *Ignimbrite shields* have a more circular geometry and are sufficiently thick to have completely buried the topographical irregularities beneath, causing a 'smoothing' of the landscape, which the Waikino Ignimbrite does, evident in the Waihi low lying hills region. Ignimbrite shields are a result of large magnitude, long duration eruptions.

The thick nature of the Waikino Ignimbrite within the caldera boundary (~75 m thick identified by drill core, from Rabone and Keal, 1985) indicates the ignimbrite could be classified as a topographically confined ignimbrite deposit or an ignimbrite shield. This deposit may have been more wide spread and since has been removed due to erosion, so this does not dismiss that the deposit could be an ignimbrite shield.

7.2 Origin of facies

7.2.1 Owharoa Ignimbrite

Five main facies were described in detail in Chapter 4 and are summarised in Table 7.2.

Table 7. 2. Table summarising the characteristics of each of the facies of the Owharoa Ignimbrite

Facies name	**Summarised description**
Facies O1 – **pumice-rich and lithic-rich facies**	Light coloured, weakly to moderately welded ignimbrite with a coarse ash matrix. Is lithic and pumice rich with rounded pumice
Facies O2 - **flattened pumice rich facies**	Creamy light grey unit, Flattened pumice/fiamme rich and lithic poor
Facies O3 - **lithic rich, pumice poor facies**	Alternating with facies O2 Moderately coarse ash matrix, lithic rich and pumice poor
Facies O4 - **dark grey, densely welded, fiamme rich facies**	Dark grey, densely welded, lithic and crystal poor, fiamme rich facies
Facies O5 - **pumice rich facies**	Grey, weakly welded, pumice rich facies. Only found at the contact with a 10 cm thickness.

Facies O1 is found dominantly in the eastern deposits of the Owharoa Ignimbrite. It represents intra-caldera deposits, but are further away from the main eruption vent. This is shown by the pumice being less welded and more rounded as a result of transportation.

Facies O2 and O3 are similar, apart from the varying pumice and lithic proportions, which alternate within the Owharoa Ignimbrite. This is indicative of pulsating pyroclastic flows with no pause between each of the depositional units, as there is no traceable contact between facies.

The alternation of pumice rich and lithic rich facies within the Owharoa Ignimbrite (seen dominantly in western sites) could be caused by several different important depositional processes as indicated by Branney and Kokelaar, (2002) and summarised below:

- Segregation mechanics with density stratification within the flow during and after deposition where the heavier lithics sink to the bottom of the

flow and the pumice rises to the top, creating the lithic rich and pumice rich facies, which repeat causing multiple flow units.

- Influx of discrete flow units that represent non-homogeneous injections of lithic- and pumice-rich material from the vent
- Different temperature pyroclastic flow pulses can create hotter deposits that would have more welding and more separation of clasts (lithics and pumice) compared to cooler non-welded deposits which would be more poorly sorted.

Facies O2 and O3 occur within the thicker parts of the deposit, closest to the proposed vent. This is why they are more densely welded.

Facies O4 also alternates with Facies O2 and O3, although it is not as frequent. This facies is the most densely welded facies and exhibits this through the presence of fiamme and a dark grey matrix. This facies also contributes to deposits within a pulsating depositional process. Facies O4 matches Facies O2, however Facies O4 may have been hotter and thicker at the time of deposition, resulting in increased welding, creating dark fiamme and a darker grey matrix.

Facies O5 occurs towards the top of the ignimbrite. Its increased pumice and lithic content indicates that the depositional flow was more concentrated in pumice and lithic material. This facies may have been present further up in the ignimbrite however it has been eroded away. The increase in pumice and lithic percentages within the pyroclastic flow may have been from the eruptive source where more material was being entrained into the flow.

Section 4.6 shows the bottom of the ignimbrite as a pumice-rich deposit, then a lithic-rich deposit. This is indicative of alternating non-welded depositional pulses. This transitioned through to the deposition of alternating facies O2, O3 and O4, which continued deposition from the pulsating pyroclastic flow. Facies O4 deposits were hotter than facies O2 and O3 deposits.

As the deposit was emplaced welding occurred, and the high degree of welding occurred to the most internal parts of the deposits. Welding occurred to the most extreme degree in facies O4 due to the increased eruption temperature of the deposit. As the deposit cooled jointing also occurred (seen at locality 1, 2 and 3).

The two main depositional processes that are associated with pyroclastic density currents (Sulpizo and Dellino, 2008) are:

- *En Masse* freezing – where the flow comes to an abrupt halt over its entire thickness; or
- Progressive aggradation – where the deposit builds up progressively due to the continuous supply of material from the current.

The Owharoa Ignimbrite could have been deposited by either of these processes. Evidence for *en masse* freezing includes the observation that the deposit is similar in facies from the east to west. Progressive aggradation is a more likely scenario, as the lithic rich and pumice rich facies could be deposited in smaller, individual flows which layer upon one another. The vertical variation of chemical composition within the Owharoa Ignimbrite (is more silicic at the top than the bottom) also supports progressive aggradation.

7.2.2 Waikino Ignimbrite

As seen in earlier chapters, there are two massive facies within the Waikino Ignimbrite, W1, a softer, massive yellow basal facies; and W2 a grey, well welded, massive facies.

W1 - Basal facies:

There are several different reasons why the basal layer of the Waikino Ignimbrite is present within this ignimbrite, which are discussed below:

- The result of a traction carpet which is typically seen in pyroclastic surges (Winter, 2010).
- The result of denser clasts in a current travelling faster than the lighter clasts, arriving first and depositing a small, coarser textured layer than W2 (Walker, 1981).
- The result of turbulent higher levels of a density stratified current which may advance faster than lower more concentrated levels, arriving earlier and depositing first (Branney and Kokelaar, 2002).
- The eruption began from one vent then transitioned to another within the caldera, producing different deposits. This layer could be the result of the initial eruption, and W2 could be the result of the second eruption area.
- W1 may be at the site due to the response to topographic angles (Branney and Kokelaar, 2002), which is common in high concentration pyroclastic deposits.

W2 – Upper well welded facies

This facies is glass rich, massive and well welded with no pumice present. It has no visible grading which is a result from either highly unsteady *en masse* deposition of a homogenous pyroclastic current or the result of steady aggradation from a consistent quasi-steady current (Branney and Kokelaar, 2002).

The interpretation of both the W1 and W2 facies within the Waikino Ignimbrite suggest several main processes that could be occurring:

1. That the deposit is the result from *en masse* deposition, with a primary coarse ash surge deposited first (W1) then the main flow body being deposited afterwards (W2), or
2. That the deposit is from quasi-steady aggradation, with either a source change or depositional flow change causing the change from W1 to W2.

There is no evidence for basal scouring or other depositional indicators between the flows, which suggests that the flows came rapidly with thick depositional units, or in a quasi-steady state.

The flow of the Waikino Ignimbrite was most likely a turbulent flow, as it is massive and well sorted (Freundt and Bursik, 2001) however it could be a grain flow as it is well sorted.

The Waikino Ignimbrite is well sorted compared to the Owharoa Ignimbrite. Depositional processes suggest that both ignimbrites were deposited rapidly, however the Owharoa Ignimbrite was deposited in rapid pulses, whereas the Waikino Ignimbrite was deposited through either a quasi-steady aggradational or *en masse* process. Both units exhibit similar thickness, although it is thought that the Waikino Ignimbrite was once thicker and more expansive in its deposit and has since been eroded away (Brathwaite and Christie, 1996).

7.3 Ignimbrite characteristics

7.3.1 Sorting

There are two different scenarios for sorting between the Owharoa and Waikino ignimbrites. The Owharoa Ignimbrite is poorly sorted and the Waikino Ignimbrite is well sorted.

Poor sorting can occur in a variety of different ways including (Branney and Kokelaar, 2002):

1. Explosive fragmentation processes (e.g. rapid shear, decompression and vesicle rupture) and turbulent mixing with limited segregation in the eruptive fountain, which results in an erupted grain size population that is very poorly sorted with abundant fine ash,
2. Production of fine ash by the erosion of friable microvesicular pumice clasts during hyper-concentrated flows in the lower parts of density currents,
3. Particle agglomeration and clustering of fine ash particles which causes fines deposition at settling velocities far greater than those of the individual constitute particles,
4. Particle interlocking in the flow boundary zone of the granular fluid within pyroclastic density currents, where particle concentrations are high,
5. From the simultaneous existence of multiple transport mechanisms in density-stratified pyroclastic density currents, or
6. From the rapidity of emplacement. Compared to most sedimentary systems, ignimbrites are exceptionally immature, taking seconds to minutes to form a deposit, resulting in a lack of sorting.

All six of these mechanisms can work together, however some processes are more dominant for the Owharoa Ignimbrite. Due to the alternating nature of the Owharoa Ignimbrite facies and the high temperature for welding it is evident that the ignimbrite was rapidly deposited via aggradation.

The Waikino Ignimbrite is a fine grained, well sorted and massive ignimbrite which creates difficulty with interpretation as there is limited features within it to indicate its processes. The Waikino Ignimbrite has no pumice and lithics are sparse (~5%), thus there are no large components to define the internal depositional structures.

The massive nature of pyroclastic density currents is a result of highly concentrated mixtures in which particle-particle interactions dominate the pyroclastic motion (Sulpizo and Dellino, 2008). The high concentration within

the Waikino Ignimbrite would be dominated by glass shards, which would be interacting during the eruption and transportation of the pyroclastic current.

The thickness of a massive deposit such as the Waikino Ignimbrite supports the concept that the Waikino Ignimbrite was a rapidly emplaced deposit, either from *en masse* deposition or aggradation in a quasi-steady state.

7.3.2 Pumice

Owharoa Ignimbrite

Within the Owharoa Ignimbrite there were five main types of pumice identified (see Chapter 5) which vary due to welding. The two extremes of the pumice variations are the rounded pumice found in the east and the flattened fiamme pumice found in the west. The rounded pumice were in moderately welded deposits and maintained the typical fibrous pumice texture, whereas the western deposits had the flattened glassy fiamme which were formed due to the intense welding, compaction and flattening of the pumice causing flame like ends. This variation is dominantly controlled by welding and temperature variations (higher welding is associated with increased temperature, resulting in flatter, glassy pumice). The lensoidal shape for the flattened pumice/fiamme is also a result of welding. The closer to the vent the deposit is, the higher the degree of welding.

Waikino Ignimbrite

The Waikino Ignimbrite has very little pumice visible and is glass shard dominated (>90%) and may have been formed from intense fragmentation. Intense fragmentation occurs when the eruption is so violent that during the course of pumice formation, the volatiles and gas expansion cause the pumice to expand and completely fragment, rather than leave intact pumice. This results in leaving large amounts of glass shards, crystals and lithics present within the ignimbrite. This has been seen before within the Kusandong Tuff, where there is no pumice within the deposit assumedly from explosive fragmentation (Sohn *et al.*, 2007). If there was any remaining pumice after the extreme fragmentation process, it would most likely float to the top of the deposit, which today has been eroded away.

Another option for the lack of pumice within the Waikino Ignimbrite is that the eruption was phreatomagmatic. If the magma was largely degassed at the time of

interaction with the water (or if the vesiculation was prematurely arrested by quenching), poorly vesicular juvenile clasts would form (McPhie *et al.*, 1993).

Another scenario for the pumice deficit in the Waikino Ignimbrite was that the eruption was cooler than the Owharoa Ignimbrite eruption. A cooler ignimbrite would have more brittle deformation, causing the pumice to snap into glass shards rather than stretch, forming an abundance of glass shards.

Cooler ignimbrites have been recorded however a review of cool verses hot ignimbrites appears to have not been undertaken. Table 7.3 highlights three different ignimbrites and their emplacement temperatures along with some characteristics.

The ignimbrites in Table 7.3 are able to be separated into two major groups – lower than approximately 400°C, and higher than 400°C. This separates the Peperino Albano Ignimbrite as a cooler ignimbrite, the Santorini deposits as hot deposits and the Taupo Ignimbrite as a varying temperature deposit (which may be due to the water influence in this deposit).

The Peperino Albano Ignimbrite exhibits some similarities to the Waikino Ignimbrite. Similarities include extreme fragmentation with the Peperino Albano Ignimbrite having 95% ash sized fragments even at proximal sites and blocky glass shards under the SEM (Porreca *et al.*, 2008). The description of the Waikino Ignimbrite is most similar to the valley ponded deposit (Table 7.3), however the Waikino Ignimbrite is more massive. The similarity between the Waikino Ignimbrite and the Peperino Albano Ignimbrite supports the extreme fragmentation eruption style, and supports a phreatomagmatic influence.

Table 7. 3. Table of the different temperatures of ignimbrites, including the Taupo Ignimbrite, ignimbrites from Santorini and from Peperino Albano.

Ignimbrite name	Temperature	Characteristics	Reference
Taupo Ignimbrite (Layer 1H)	150 – 400°C	An upper, thinner deposit which is rich in dense (lithic and crystal) components and lacks a fine ash matrix is inferred to represent coarse/dense material which formed a thin ground layer.	McClelland *et al.*, 2004
Taupo Ignimbrite (Layer 1P)	150 – 500°C	A lower, thicker deposit which is dominated by pumice and has variable contents of fine ash matrix.	McClelland *et al.*, 2004
Taupo Ignimbrite (Ignimbrite veneer (IVD) and valley ponding deposit (VPD)	130 – 150°C	Represents most of the Taupo deposit, and is inferred to be material left behind from the body and tail of the current as it spread over the landscape. It consists of two facies, landscape-mantling veneer deposits, and landscape-modifying valley-ponded ignimbrite.	McClelland *et al.*, 2004
Santorini, Greece Lower Pumice 1 Ignimbrite	400 - 527°C	A part of the Thera Pyroclastic Formation. Spatter-rich pyroclastic flow deposits on Santorini, Greece	Bardot, 2000
Santorini, Greece - Cape Riva ignimbrite	516 – 580 ≤	A part of the Thera Pyroclastic Formation. Spatter-rich pyroclastic flow deposits on Santorini, Greece	Bardot, 2000
Peperino Albano Ignimbrite – veneer facies	240 – 440°C	A relatively thin (up to a few meters in thickness), stratified, mostly parallel- to cross-bedded, lapilli- to ash-rich deposit. fines-depleted, poorly consolidated to unconsolidated layers, rich in lapilli-sized xenoliths crystals (pyroxene, biotite, leucite, hauyna, K-feldspar) and dark scoria.	Porreca *et al.*, 2008
Peperino Albano Ignimbrite – valley pond facies (VP)	160 - 440°C	Is massive and chaotic facies, homogeneous throughout the thickness of the unit. This facies has >10% block- to lapilli-size xenoliths dispersed in the grey ash matrix, made of mostly zeolitised glass-shards, crystals fragments of pyroxene, biotite, leucite, hauyna, K-feldspar and small xenolithic fragments..	Porreca *et al.*, 2008
Peperino Albano Ignimbrite - Intra crater facies	200 - 490°C	Is characterised by lobes up to 15 m thick, which drape the steep (>20°) inner slopes of the crater wall. Shows a massive structure and chaotic texture and is very similar to the VP. Comprised of >15% of bomb-sized xenoliths.	Porreca *et al.*, 2008

7.3.3 Glass shards

Glass shards are the result of bubbles cooling and breaking through the eruption process, as seen in Figure 7.5. There are different morphologies of glass shards (Chapter 5) which are a result of snapping off from different sections of the bubble (Figure 7.5). The presence of Y shaped glass shards is indicative that the ignimbrite is a welded ignimbrite, and these were found throughout the Owharoa and Waikino ignimbrites.

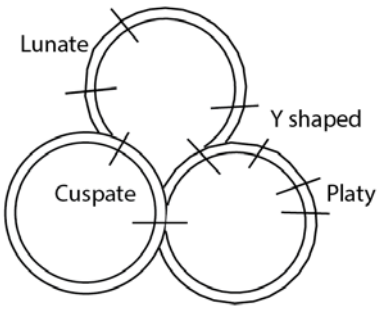

Figure 7.5. Diagram of the formation of glass shards from bubbles.

Owharoa Ignimbrite

The glass shards within the Owharoa Ignimbrite were flattened which is a result of welding. A large range of different morphologies of glass shards and at a high percentage within the ignimbrite indicate a volatile eruption, causing the shattering of pumice/bubbles to form glass shards.

Waikino Ignimbrite

The glass shards within the Waikino Ignimbrite have less diversity in morphology than the Owharoa Ignimbrite glass shards, but tend to be larger, longer and thinner in shape and under SEM the glass shards appeared blocky. The glass shards may be formed this way as the shards may have been snapped off the pumice during the formation of pumice vesicles.

7.4 Magmatic processes

Figure 7.2 shows the EMPA glass shard data for both the Owharoa and Waikino ignimbrites. For each ignimbrite the data points do not exhibit a broad spread across different compositions, however the Owharoa and Waikino ignimbrites are distinct from each other with the Waikino Ignimbrite having a higher alkali content, suggesting magma mingling did not occur in each eruption.

The Owharoa and Waikino ignimbrites (Figure 7.2) represent typical rhyolite magmas which have an estimated temperature of eruption between 700 – 900°C (Cas and Wright, 1987).

Contamination through assimilation of wall rock, magma mixing or replenishment of the magma is also plausible for varying the potassium and sodium content of the Waikino Ignimbrite compared to the Owharoa Ignimbrite. Rhyolitic magma chambers are viscous and it is harder to assimilate wall rock into the magma body. However hot magma bodies are in disequilibrium with the host country rock, causing the magma chamber to cool down and the country rock to heat, stress and assimilate (Furlong and Myers, 1985).

The Waikino Ignimbrite has a higher alkali content than the Owharoa Ignimbrite (Figure 7.2). The increased alkali content could be attributed to the larger biotites observed under optical microscopy, giving the Waikino Ignimbrite a unique magma composition compared to the Owharoa Ignimbrite. The residual Owharoa Ignimbrite magma may have regenerated but with higher alkali content sourced from either new magma or country rock.

Elemental variations within the Owharoa and Waikino ignimbrites (Chapter 6) each reflect precipitation of specific minerals out of the melt, via depletion and enrichment of different elements with respect to silica. This indicates that fractional crystallisation occurred in each magma. Elemental differences between the Owharoa and Waikino ignimbrites include higher calcium and iron percentages within the Owharoa Ignimbrite, and a higher potassium percentage within the Waikino Ignimbrite. The difference between the elemental percentages are no more than a ‘few’ percent different, indicating that these two ignimbrites are geochemically similar.

Figure 6.6 shows that through the stratigraphic column the Owharoa Ignimbrite becomes increasingly rich in silica during the eruption. This process could have occurred through compositional boundary layer convection, where crystals form at the cooler magma chamber wall, increasing the silica content, and the remaining differentiated melts rise to the top of the magma chamber (Worner, 2010). On deposition the ignimbrite would deposit the differentiated melt with lower silica contents first, then the cooler, higher silica content section second.

7.5 Eruption processes:

7.5.1 Eruption style

The Owharoa and Waikino ignimbrites are rhyolitic in composition (Figure 7.2). Both ignimbrites are significant in volume, and have a significant dispersal area when including eroded deposits (Brathwaite and Christie, 1996).

Plinian eruptions tend to be sustained, have a high, ash-rich eruption plume, high eruption rates and are typically rhyolite (Wilson, 1976). They are gas charged with a high velocity. Fragmentation during this eruption style includes bubble bursting, shearing of magma and country rock. For the Owharoa and Waikino ignimbrites the plinian eruption fits for the eruption style. Both ignimbrites are rich in ash (the Waikino Ignimbrite more so), contain lithics and have shearing of magma and burst bubbles.

The Owharoa Ignimbrite is the result of a plinian eruption as it has a rhyolitic composition along with flattened pumice, grading variations and welding variations.

The Waikino Ignimbrite has burst bubbles and shearing on a higher magnitude than the Owharoa Ignimbrite indicating that it is more explosive. The Waikino Ignimbrite may be the result of a highly explosive plinian eruption which formed through sustained, quasi-steady discharge.

Plinian eruption style is defined by the fall deposit, which was not seen beneath the Owharoa or Waikino ignimbrites. This means that the ignimbrites were formed as a consequence of the collapse of the individual eruption plumes. The Owharoa Ignimbrite may have had a fall deposit, but the pyroclastic flow deposit may have eroded it away on deposition. The fall may have been windswept and deposited in another area, which also may have occurred for the Waikino Ignimbrite.

The Waikino Ignimbrite is fine grained and has very little characteristics to aid in interpreting the deposit. Characteristically phreatomagmatic eruptions tend to be finer grained deposits with a high ash fraction (McPhie *et al.*, 1993) and have blocky, angular glass shards (Winter, 2010), which are present within the Waikino Ignimbrite. This could indicate that the Waikino Ignimbrite was the result of a phreatoplinian eruption. Water sources were present within the landscape, whether that is through aquifer interception or through lake surface water. As

mentioned earlier, the Peperino Albano Ignimbrite exhibits similar stratigraphic characteristics as the Waikino Ignimbrite and is the result of a phreatomagmatic eruption (Porreca *et al.,* 2008).

The concept that the Waikino Ignimbrite was formed through extreme fragmentation is the most plausible eruption process. To make the eruption volatile, the Waikino Ignimbrite has higher contents of volatiles, which indicate a more explosive eruption than the Owharoa Ignimbrite. The Waikino Ignimbrite's fine grained and massive characteristics support a phreatomagmatic eruption.

The Waikino Ignimbrite is similar in description to the Southern Kusandong Tuff, Korea (Sohn *et al.,* 2007). This pyroclastic deposit exhibits the virtual absence of juvenile clasts in the tuff and this has been interpreted to be due to rapid ascent, sudden decompression and full fragmentation of silicic magma into fine glass shards and crystals, which is what could have formed the Waikino Ignimbrite. The Kusandong Tuff also exhibits a very similar depositional environment (an arc setting within a basin) and crystal content to the Waikino Ignimbrite. The Waikino Ignimbrite is thicker (Brathwaite and Christie, 1996), however this may be due to the intra-caldera deposition – the Waikino Ignimbrite was deposited within the depression of a caldera against the edge of the proposed rim and outside of the rim, producing intra-caldera deposits and outflow deposits; whereas the Kusandong Tuff was deposited within a sedimentary basin environment near the middle of the basin.

7.5.2 Mechanisms of pyroclastic flow formation

There are several main causes of pyroclastic flow deposits described by Winter (2010), including vertical eruption and column collapse, lateral blasts, low pressure boiling over and dome collapse.

Vertical eruption and column collapse is also known as the 'Soufriere Type' is when the eruption column can no longer be sustained (due to loss of pressure), causing the column to collapse forming flows on the flanks. These tend to be cooler than other eruption processes. This eruption process could be the process for both the Owharoa and Waikino ignimbrites.

Low pressure boiling over produces an ash-gas fountain with no convecting plume. The boiling-over mechanism has intermediate energy between dome failure and column collapse. Flows are typically confined to pre-existing fluvial

channels high on the slopes of the volcano, or in this case, the Waihi Caldera. Depositional features include cross-bedded dunes and deposits of bedded material at breaks in slope and channel margins. Finer grained material are often observed (Douillet *et al*., 2013), which comprises the Waikino Ignimbrite.

The Owharoa and Waikino ignimbrites both have a blanket-like deposits over the landscape, and do not appear confined to fluvial channels (although it is possible the deposits within paleo-channels and within the caldera structure are thicker) and cross bedding dunes were not identified within either deposit. Finer grained material however was identified within the Waikino Ignimbrite, but this is not enough evidence to conclude the deposit is from low pressure boil over.

7.6 Post depositional processes

7.6.1 Welding

Post emplacement welding involves plastic deformation of pumice and glass shards, eliminating pore space and the original pyroclastic deposit becomes relatively dense (McPhie *et al.,* 1993). Both ignimbrites exhibit welding, shown by the flattened glass shards and hard nature of the whole deposits. This is indicative that the deposits both had to be hot enough at the time of deposition to have the heat to form the welding. The Owharoa Ignimbrite also has columnar joints as discussed in Chapter 4, as a result from welding and cooling.

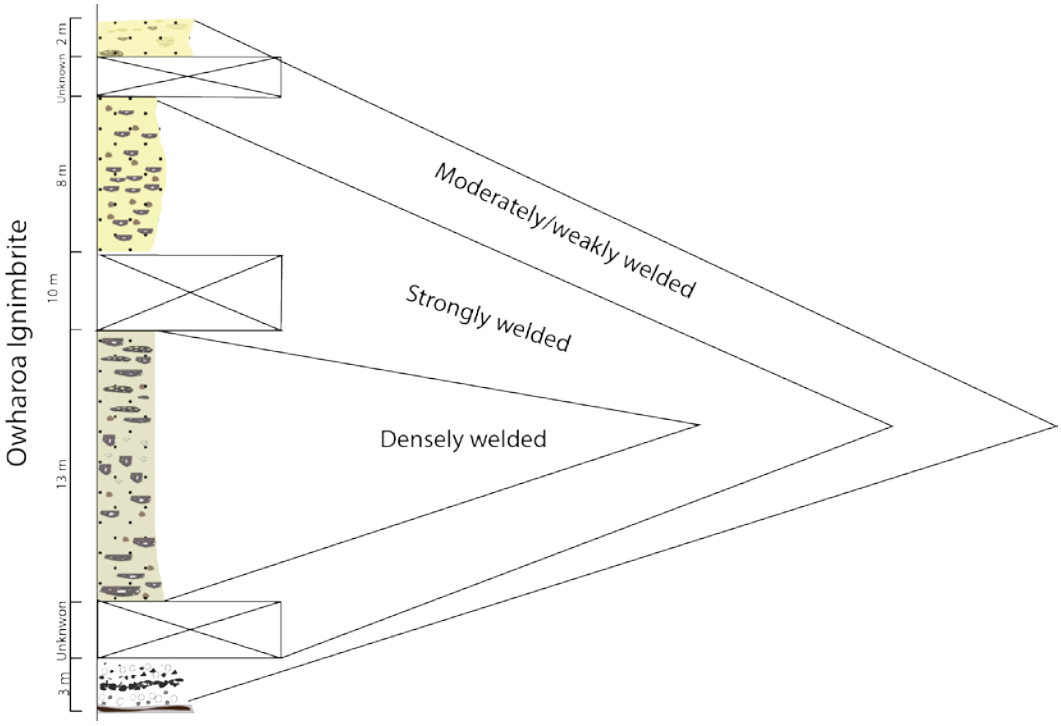

Figure 7.6. Owharoa Ignimbrite welding pattern. This is compiled from several sites across the field area. Based on the welding concept from McPhie et al., (1993). This is a simplified model to show the overall pattern, excluding the facies O2/O3/O4 alternation of alternating density changes.

The Owharoa Ignimbrite exhibits alternating welding patterns between weakly welded to moderately welded to densely welded (Figure 7.6). The welding degree is indicated by degree of flattened juvenile clasts (producing flattened pumice lenses and fiamme) and the overall colour of the ignimbrite – the darker sections of the ignimbrite (dark grey) are more densely welded, and the lighter sections (beige to white) are moderately to non-welded.

The alternating pattern between facies O2/O3/O4 is not represented within Figure 7.6 for simplicity. The alternating density changes could result from alternating depositional pulses at different temperatures.

The Waikino Ignimbrite has two facies, the lower basal facies which is non-welded, and the upper facies which is moderately welded. The moderately welded deposit appears to be one whole unit, which is consistently welded through its thickness. This is the result from either consistent quasi-steady deposition, depositing layers consistently and quickly while the deposit is hot and not leaving any scours or traction markings; or from *en masse* deposition where the deposit is deposited cools not leaving any welding patterns.

7.6.2 Vapour-phase crystallisation and devitrification

Vapour-phase crystallisation is the process of percolation of hot gasses through ignimbrites during cooling after deposition. Secondary mineralisation includes cristobalite (a polymorph of quartz) which was identified within the Owharoa Ignimbrite through XRD analysis, however this could also be attributed to devitrification. However devitrification textures were not observed in thin sections. The Waikino Ignimbrite showed no evidence of vapour-phase crystallisation.

7.7 Contact between the Owharoa Ignimbrite and the Waikino Ignimbrite.

7.7.1 Age

The Waikino Ignimbrite is 3.48 +/- 0.19 Ma, dated via U-Pb zircon dating through this study. The date corresponds well with the Owharoa Ignimbrite date (3.76 ± 0.05 Ma (Vincent, 2012)) as the dates are similar, and using the standards of error, do not overlap (Figure 7.7). This means that they are very close in age and supports the idea that they may share a similar source due to the closeness of activity.

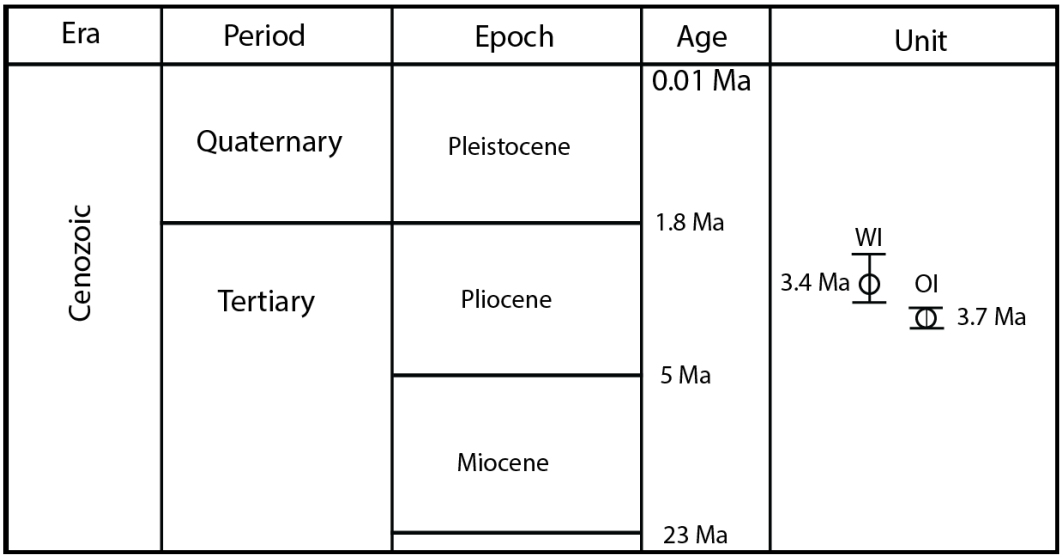

Figure 7.7. Simplified geological time scale showing the ages of the Owharoa and Waikino ignimbrites.

7.7.2 Contact

At the contact between the Owharoa Ignimbrite and the Waikino Ignimbrite the pumice in the Owharoa Ignimbrite is still flattened with a high aspect ratio. This indicates that the top of the Owharoa Ignimbrite that is seen at the site is not the true top, and that the true top has been eroded away. If this was the true top for the Owharoa Ignimbrite the pumice would be round. Therefore this means that there is geological history missing within this contact.

Rabone and Keal (1985) noted that there were lenses of fluvial andesite gravels at the contact between the Owharoa and Waikino ignimbrites in drill holes on the east side of Waihi. However at the Waikino Quarry (to the west) the contact is sharp and lacking similar material. The andesite gravels may have been deposited at the Waikino Quarry site and then eroded away before the deposition of the Waikino Ignimbrite, or the andesite gravels were never deposited here, leaving an erosional contact.

7.8 Eruption vent location

7.8.1 Owharoa Ignimbrite

The degree of welding has been used as a guide to determine the distance of deposition from the vent. The closer the deposit is to the vent, the more welded the deposit will be. Therefore, the closest deposits to the vent are the deposits seen to the west of the field area.

In context along with an eruption process, the vent location also can be justified using a 'ring fissure vent' (Figure 7.8). The Owharoa Ignimbrite proposed vent is to the western side of the caldera, where the binding fault is the Mangakino Fault, and slightly north is the second binding fault, the Waihi Fault (Figure 7.2). The eruption for the Owharoa Ignimbrite could have occurred along the Waihi Fault or at the interception of the

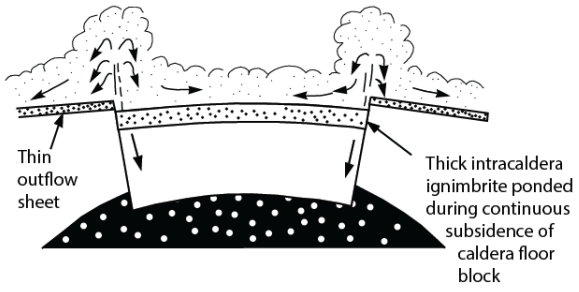

Figure 7.8. Diagram of ring fissure vents adapted from Cas and Wright, 1987.

Waihi and Mangakino Fault, creating a ring fissure vent. This does imply that there are multiple vents around the caldera, rather than just one.

7.8.2 Waikino Ignimbrite

The Waikino Ignimbrite has no paleo-flow patterns to help identify the flow direction or intensity, neither are there enough sites within this study to evaluate the different degrees of welding. Therefore the vent location is difficult to evaluate.

Due to the similar crystal and lithic content of the Waikino Ignimbrite compared to the Owharoa Ignimbrite, it is likely that the Waikino Ignimbrite is also sourced from the Waihi Caldera. Both ignimbrites contain higher percentages of plagioclase and quartz, and lower percentages of biotite and opaques.

The presence of greywacke/argillite lithics (Ewart & Healy, 1985) within the Waikino Ignimbrite infers the eruption must have erupted through basement rock. Figure 7.9 is a cross section of the Waihi Caldera from Smith *et al.*, (2006) which shows basement material with the Waipupu Formation, indicating there is source rock for basement material that could be incorporated into the Waikino Ignimbrite.

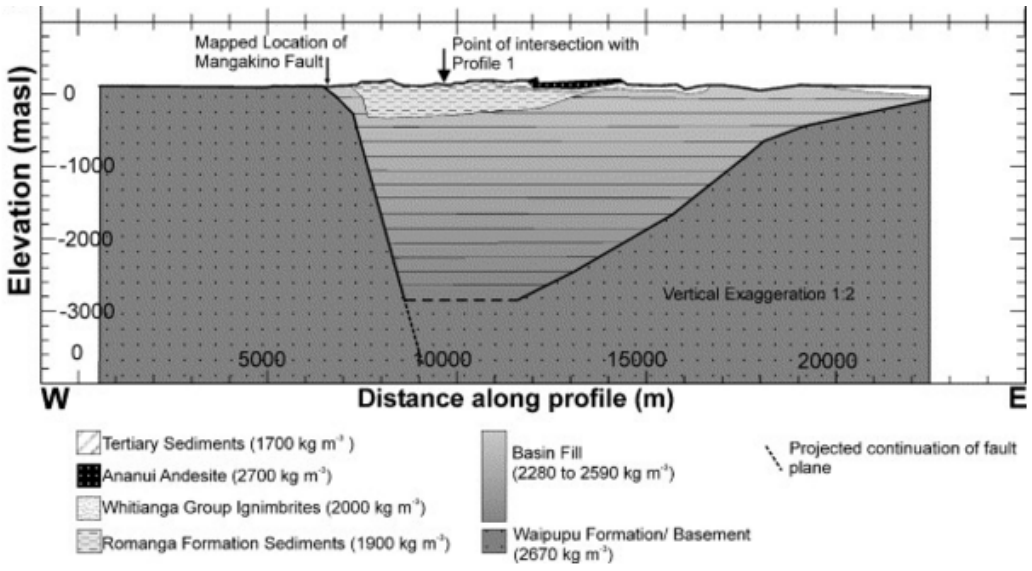

Figure 7.9. Waihi Caldera cross section from Smith et al., 2006. This cross section highlights the potential internal geological composition of the caldera.

If the Waikino Ignimbrite's eruption processes were magmatic rather than phreatomagmatic, the finer grained nature of the deposit is important. This would suggest that the vent is distal to the Owharoa Ignimbrite source vent.

The eruption vent for the Waikino Ignimbrite may have changed across the eruption source (Figure 7.13) compared to the Owharoa Ignimbrite. If it is assumed that the source is the Waihi Caldera (which has a trapdoor caldera), the magma chamber may be being accessed at different points. In Figure 7.10, at the blue arrow, the magma chamber would be more silicic, while at the orange arrow the magma would be more mafic. Therefore, the Owharoa Ignimbrite may have been erupted from the more mafic section, compared to the Waikino Ignimbrite which may have been erupted from the more silicic section. Due to the significant amount of estimation involved with this scenario, this is not the most probable situation. The side with the deepest subsidence may correspond with where the magma reservoir was shallowest, thickest, or more eruptible (Sigurdsson, 2000).

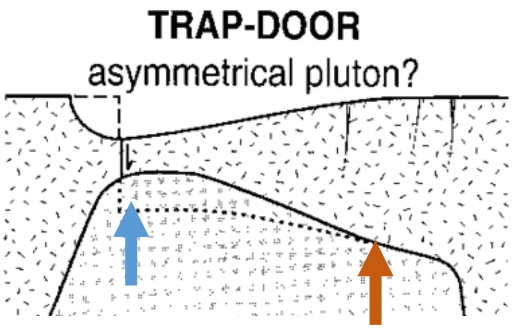

Figure 7.10: Trapdoor caldera magma chamber diagram

7.9 Waihi Caldera

As discussed in Chapter 2, the Waihi Caldera has been identified as a trapdoor caldera (Smith *et al.*, 2006, Figure 7.9) which is bounded by partial ring faults (Mangakino and Waihi faults) and by a hinged segment. It constitutes incomplete or incipient plate collapse, intermediate between plate and downsag subsidence processes (Sigurdsson, 2000). Such subsidence may be related to smaller eruptions, an asymmetrical magma chamber, or regional structural influences (Lipman, 1997).

It is possible that the reason the thickest, most densely welded deposits of the Owharoa Ignimbrite are found in the western part of the caldera, is that the deposits are closest to the vent, at the deepest part of the trapdoor caldera.

The source of the Waihi Caldera's magmatic material is currently unknown. Calderas have a source magma chamber, which tend to be granitic bodies below the surface. Granitic bodies can have lava domes around the area (which is seen in the Waihi area) which could also feed off the same magmatic source. However due to the significant difference in age of the lava dome deposits and the

dissimilarity of mineralogy compared to the Owharoa and Waikino ignimbrites it is more likely that the Waihi Caldera and the lava domes have a separate source.

The history of the Waihi Caldera is a significant part of the geological history of the Waihi area. The Romanga Formation, the lacustrine siltstone, mudstone and tuffaceous sandstone formed within the Waihi Caldera structure comprises a significant infilling of the caldera (Figure 7.10). Using the age of the Romanga Formation, the potential life span of the caldera lake can be estimated. Ages using palynological samples range from Opoitian-Mangapanian age (~5 – 3 Ma), but most indicate mid to late Pliocene in age for most of the formation (Brathwaite & Christie, 1996). According to Brathwaite & Christie (1996) the Romanga Formation appears to span about 1.5 Ma, which is longer than the 0.1 – 1 Ma life spans estimated for permanent lakes in the Taupo Volcanic Zone (Smith *et al.*, 2006). This could significantly expand the expected life spans for calderas if this is correct.

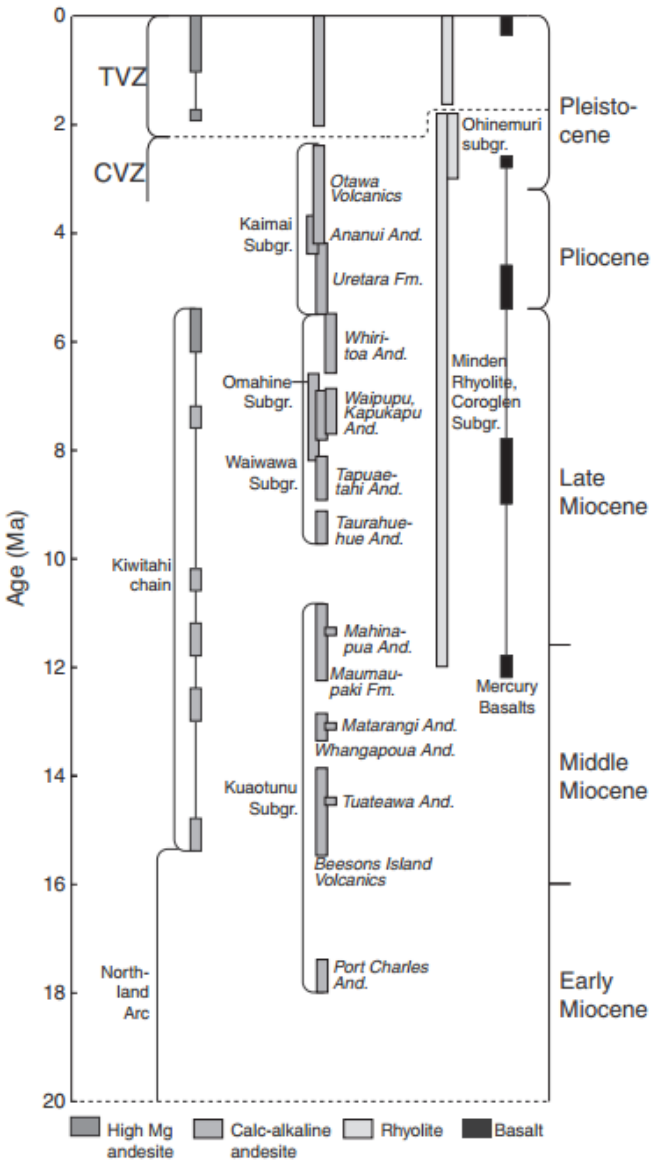

Figure 7.11. Volcanic stratigraphy of the Coromandel Volcanic Zone, from Booden et al., 2012, based on Skinner 1986, Adams et al., 1994, Brathwaite & Christie 1996, Nicholson et al., 2004, Briggs et al. 2005

7.10 Geological history

This section discusses the revised geological history surrounding the Waihi Caldera within Waihi. The area described within the history covers the field area seen in Figure 7.2. Descriptions of units are from Brathwaite & Christie (1996). A basic overview of the geological history is in Figure 7.11.

Figure 7.12 shows the geological history of the Waihi-Waikino region in a three dimensional aspect. These diagrams focus on the western side of the caldera and the Karangahake Gorge, where the majority of the deposits for the Owharoa and Waikino ignimbrite units are distributed.

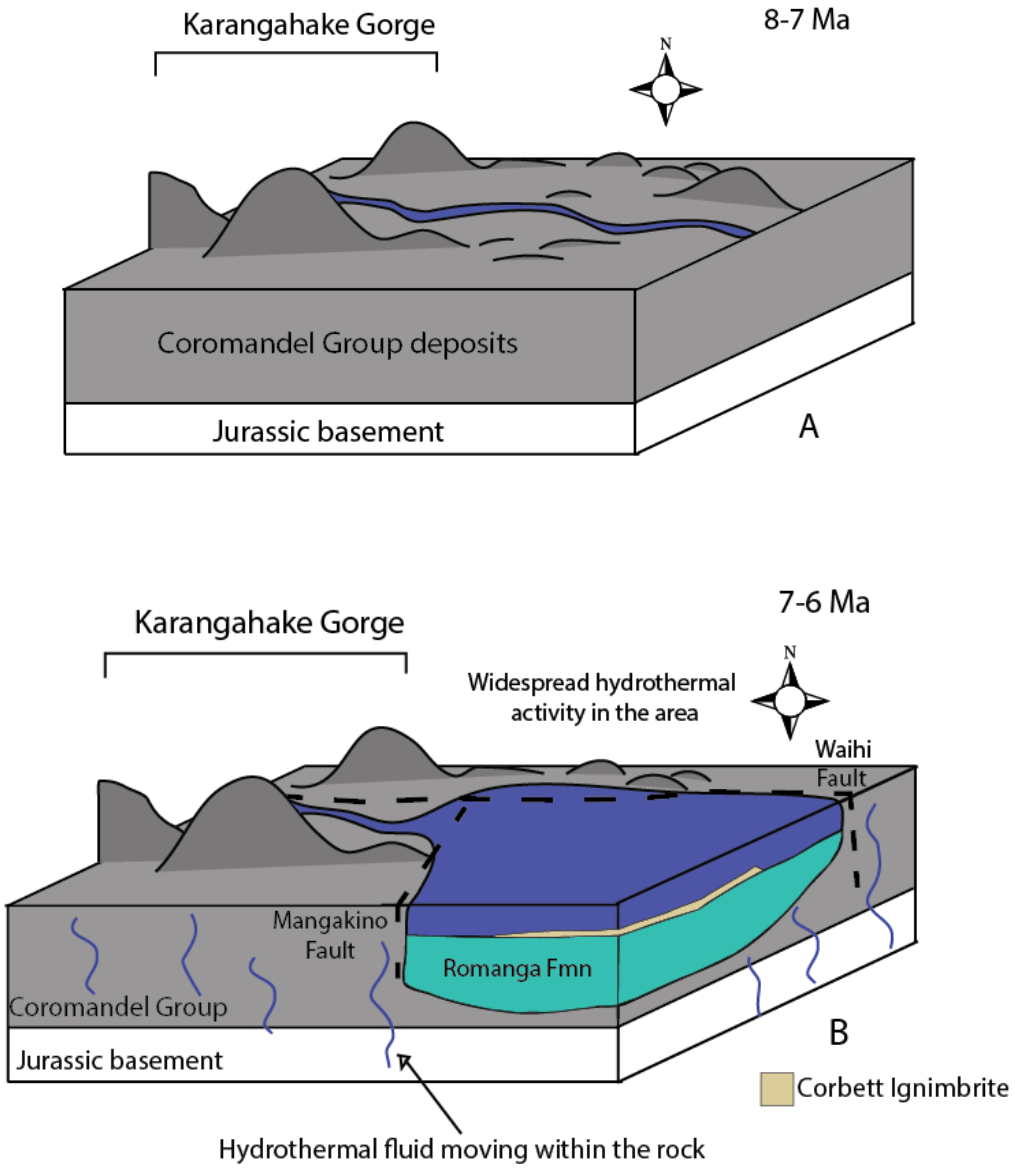

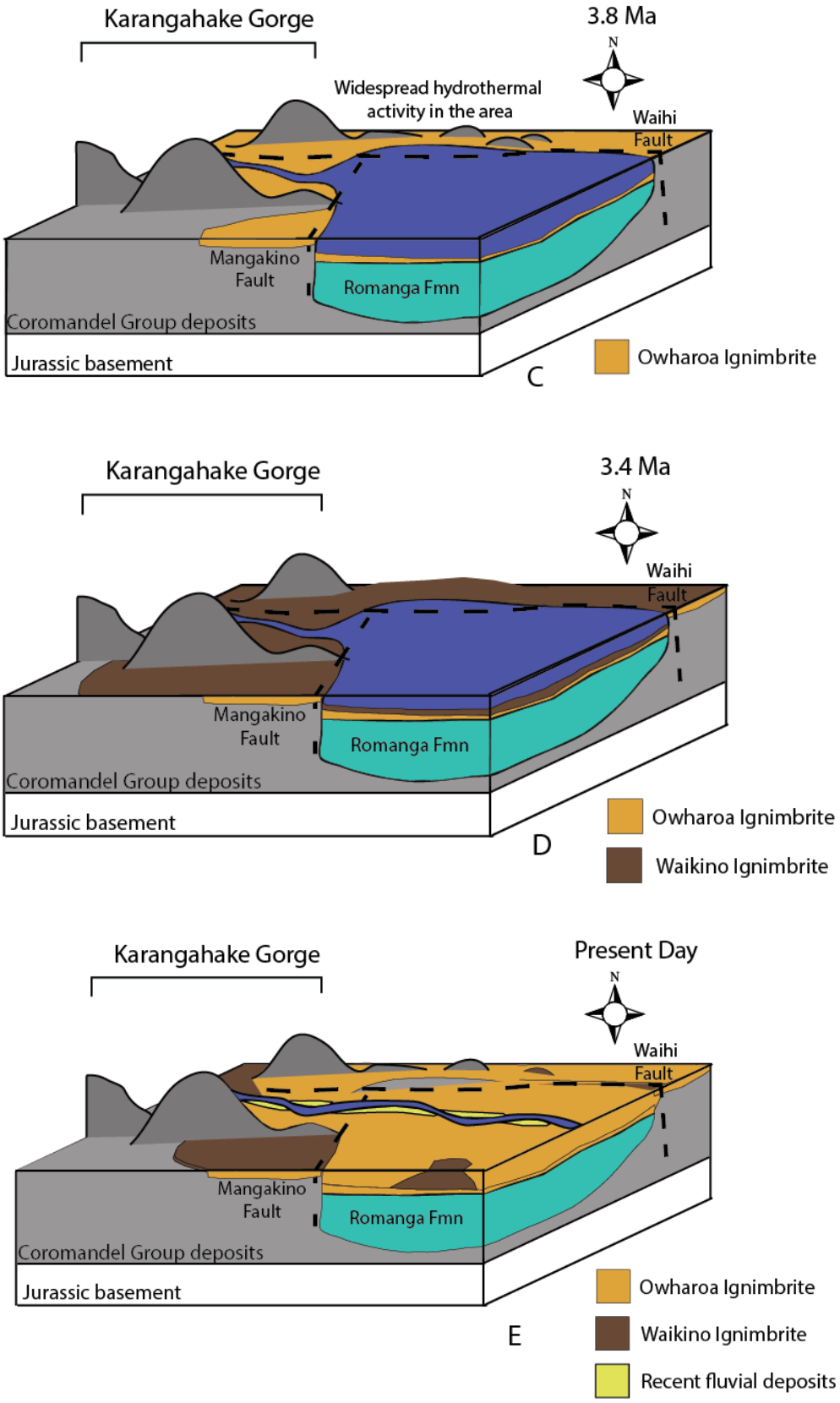

Figure 7.12. Time scale sketches (A through to E) of the geological history of the Waihi-Waikino region, focusing on the caldera formation and deposition of the Ohinemuri Subgroup Ignimbrites.

7.10.1 Basement

Greywacke basement is assumed to extend south beneath the Waihi area where it was originally estimated from seismic and gravity data to lie at depths of 0.2 – 3 km below the surface (Hochstein & Nixon, 1979).

Greywacke basement would have been laid down during the late Jurassic period. This basement material correlates with the younger part of the Torlesse terrane.

7.10.2 Coromandel Group

The Coromandel Group (Figure 7.12 A) comprises different andesite-dacite-rhyolite lava flows. These deposits include that of the Waipupu Formation (7.9-6.3 Ma) which was deposited on top of the Jurassic greywacke and argillite material forming andesitic hillscapes, which have been stratovolcanoes. The Coromandel Group also encompasses the Mangakara Dacite (6.9 ± 0.5 Ma), Waitekauri Dacite, Uretara Formation, and the Ananui Andesite (which overlies and intrudes into the Uretara Formation and locally intrude the Romanga Formation).

The Waimata Rhyolite is comprised of a dome complex of fine grained felsitic, plagioclase-hypersthene rhyolite with minor obsidian which intrudes into the Uretara Formation. This created localised lava domes in the Waihi region.

Origin of the Caldera

Andesitic landforms dominated the landscape with rhyolitic intrusions and flows covering the surface from the Coromandel Group. The Waihi Caldera's lifespan according to Brathwaite & Christie (1996) spans about 1.5 Ma (using the Romanga Formation as a reference). This means it would have formed approximately 5 Ma and was active to ~3 Ma, after the Waikino Ignimbrite was deposited (Figure 7.12 B)

The Waihi and Mangakino faults that constrain the Waihi Caldera can be assumed to have become active in the Waihi area when the caldera became active. The Waihi Fault (Figure 7.2) is mainly inferred, and follows a distinct topographic low. This fault marks a major boundary between the late Miocene Waiwawa subgroup to the north and the Pliocene Kaimai subgroup to the south. This boundary supports the concept that the Waihi Fault was active during the Pliocene. The Mangakino Fault is north striking as seen in Figure 7.2. This fault juxtaposes the Waipupu Formation against the Uretara Formation. The faults are thought to have

been active before the hydrothermal activity within the Waihi area or occurring at the same time – meaning that the caldera bounding faults were active around 7-6 Ma. This fault activation may have initiated the caldera formation, creating the start of the caldera life span. To initiate the caldera formation there would also have to be a large magma body beneath the surface.

Romanga Formation

The Romanga Formation is the lacustrine siltstone, mudstone and tuffaceous sandstone presumed to occur within the Waihi Caldera (Figure 7.12 B). Its age ranges (using palynological samples) from Opoitian-Mangapanian age (~5 – 3 Ma), but most indicate mid to late Pliocene in age for most of the formation (Brathwaite & Christie, 1996).

White (1995) describes the Romanga Formation based on drill cores, which included:

- *Upper boulder, cobble and pebble conglomerate unit with subordinate intercalated sandstone, up to 100 m thick.*
- *A basal, locally carbonaceous tuffaceous sandstone, siltstone and mudstone up to 12 m thick.*

The Romanga Formation is evidence for a lake. Whether this lake is a caldera lake or another kind of lake is arguable. The Romanga Formation however is confined to the proposed caldera, supporting that the Romanga Formation is the result of a caldera lake. The lake deposits indicate ranges in energies, from high energy deposit conglomerates from river environments to sandstone, siltstone and mudstone deposits which are indicative of a deepening, decreasing energy environments. This shows an evolution over time of the caldera lake.

The Romanga Formation maximum age is approximately ~4-3.8 Ma, which is based on present day deposits. Younger deposits may have been eroded away. After this deposit the Owharoa Ignimbrite was deposited (as there is no record of the Romanga Formation above the Owharoa and Waikino ignimbrites). However the andesite pebbles within the contact of the Owharoa and Waikino ignimbrites are not attributed to a formation, and therefore could still be a part of the Romanga Formation.

7.10.3 Whitianga Group and the Ohinemuri Subgroup

Corbett Ignimbrite

The Corbett Ignimbrite is described as a plagioclase-hornblende-hypersthene±augite pumice-lapilli and lithic-crystal rich ignimbrite which overlies lake sediments of the Romanga Formation and underlies the Owharoa and Waikino ignimbrites (Brathwaite & Christie, 1996). It has been assumed to be deposited within the Late Pliocene. The Corbett Ignimbrite was the first ignimbrite to be deposited within the Waihi-Waikino region which has been identified at the surface (Figure 7.12 B).

There is no clear description of a contact between the Corbett and the Owharoa Ignimbrite, and no contacts were identified in the field. A potential contact was identified in drill core (Rabone & Keal, 1985) however the lower ignimbrite was not conclusively defined as the Corbett Ignimbrite (Rabone & Keal, 1985). This lower geological unit below the contact is described as a pumice lapilli tuff (which could be the Corbett Ignimbrite) overlain by 3 m of andesite boulder alluvium and 2 m of the Owharoa Ignimbrite. This would indicated that between the eruptions of the Corbett and Owharoa ignimbrites there was a high energy depositional environment, depositing 3 m of boulder alluvium.

Owharoa Ignimbrite

The Owharoa Ignimbrite was erupted from a plinian eruption from the deepest sector of the Waihi Caldera (western side) 3.76 ± 0.05 Ma (Vincent, 2012), possibly related to the Mangakino Fault (as this fault is directly to the west of the potential eruption source). This eruption resulted in a pyroclastic flow which deposited material, alternating between lithic rich and pumice rich pulses, with ranging temperatures, that caused welding variations and ranges of different pumice. This is seen within Figure 7.12 C.

Sedimentary erosion and deposition

The contact between the Owharoa and Waikino ignimbrites includes evidence of erosional and depositional environments at different localities.

The erosional environment at locality 4 indicates that this section of the Owharoa Ignimbrite was exposed and suggests either:

- That the lake was not up this high during this time exposing the surface of the ignimbrite

- The lake may have been filled so that only rivers were present which then eroded the Owharoa ignimbrite

The depositional environment between the Owharoa and Waikino ignimbrites is recorded as lenses of fluvial andesite gravels in drill holes on the east side of Waihi (Rabone & Keal, 1985). This is indicative of a moderate energy depositional environment – such as a river. Rivers present at this contact site indicates that the caldera lake may have been shrinking, leaving a more fluvial environment rather than lacustrine.

Eruption of Waikino Ignimbrite

The Waikino Ignimbrite was deposited 3.48 +/- 0.19 Ma via an extremely violent eruption. This eruption was either a phreatoplinian or a magmatic plinian eruption, which created a quasi-steady aggradational/*en masse* depositional unit forming the Waikino Ignimbrite. W1 was deposited first as an earlier deposit and W2 was deposited after and proceeded to weld, creating a hard ignimbrite that is seen in the field. This is seen in Figure 7.12 D.

In Chapter 6 it is discussed that the Waikino Ignimbrite may have had magma mixing occurring. This can help account for the difference between the silica content(s) of the ignimbrite. This magma mixing could have begun after the deposition of the Owharoa Ignimbrite, and a new source could be feeding the main magma chamber.

7.10.4 Pebble conglomerate

The next deposit on top of the Waikino Ignimbrite is the pebble conglomerate located at Samson Road. This deposit is attributed to the Ruahihi Formation and is the result of a high energy, fluvial depositional environment. This shows a transition from the caldera as a lacustrine environment, to a fluvial environment with high energy. This could have been the result of the paleo Ohinemuri River, which could have provided the environment for the deposition of the pebble conglomerate.

7.10.5 Younger sediments

The Gordon Formation is a sequence of terrestrial fan deposits which mark the contact between the Kaimai Range and Hauraki Plains (Houghton & Cuthbertson, 1989) deposited during the mid to Late Pleistocene.

The Ruahihi Formation is described as modern fluvial sediments of streams from the eastern Kaimai Range and the Tauranga Basin. The Gordon and Ruahihi Formations were both deposited near present fluvial channels (including along the Ohinemuri River). These are the most recent deposits in the Waihi-Waikino region and have been deposited on both the Owharoa and Waikino ignimbrites. There is no description of the contact that is shared between the volcanic and sedimentary deposits.

These younger fluvial sediments are grouped together as ‘Fluvial sediments’ in Figure 7.12 E and represent the landscape that we see today in the Waihi-Waikino area.

Chapter 8: Conclusions

The Owharoa and Waikino ignimbrites are similar in petrography and geochemistry but are significantly different in stratigraphy and physical characteristics.

The Owharoa Ignimbrite has five main facies controlled by welding and lithic and pumice contents. The Waikino Ignimbrite has two facies, W1, a basal surge deposit and W2 a massive glass rich deposit. The Owharoa Ignimbrite is dated at 3.76 ± 0.05 Ma (Vincent, 2012) which underlies the younger Waikino Ignimbrite which is dated at 3.48 +/- 0.19 Ma. The Waikino Ignimbrite date was closer than expected to the Owharoa Ignimbrite date, but indicates a close volcanic relationship between the two units.

Petrographically the Owharoa and Waikino ignimbrites share a similar mineralogical relationship (plagioclase, quartz, biotite, opaque minerals and the occasional hornblende). The Owharoa Ignimbrite's pumice was analysed in detail but as there is no pumice in the Waikino Ignimbrite there is no comparison able to be made. Lithic analysis was used to interpret the eruption source and correlating the two ignimbrites, which indicated that both ignimbrites most likely came from the Waihi Caldera.

The geochemical analysis of the Owharoa and Waikino ignimbrites showed further correlation. Both units were rhyolitic with similar lithic contents, and shared similar geochemistry (with a few minor differences). This supported the concept of the Owharoa and Waikino ignimbrites sharing the same magmatic source.

The Waihi Caldera provides the most probable source for the eruptions of the Owharoa and Waikino Ignimbrites. There are several reasons for this conclusion, including:

- Proximity to deposits – both the Owharoa and Waikino ignimbrites have thick deposits (> 75 m) within the caldera boundaries.
- Lithic contents are similar between both ignimbrites and have a similarity to the stratigraphy of the caldera including andesite, ignimbrites, rhyolites and basement lithics.
- Geochemically similar magma (although the Waikino Ignimbrite does have higher alkali content).

This study has indicated that the Waihi Caldera is polygenetic (as expected), producing at least the Owharoa and Waikino ignimbrites. The Owharoa and Waikino ignimbrites highlight contrasting deposits, from a typical lithic and pumice rich ignimbrite to a fine grained, pumice depleted ignimbrite. The contrast of the ignimbrites indicates that different eruption processes occurred from the same caldera.

The interpretation of the Owharoa and Waikino ignimbrites allows for more accurate constraints on the deposits within the Waihi region. The Waikino Ignimbrite date constricts the Waihi region volcanism to being older than previously estimated, but also constrains the Waihi Caldera – a structure in the Waihi area with little knowledge on its life. This is important as it highlights important features (such as the Waihi Caldera's long time span) which could be applicable to the currently active TVZ with active calderas throughout the region.

References

Adams, C.J; Graham, I.J; Seward, D; Skinner, D.N. (1994). Geochronological and geochemical evolution of late Cenozoic volcanism in the Coromandel Peninsula, New Zealand. *New Zealand Journal of Geology and Geophysics, 37* p 359-379.

Bardot, L. (2000). Emplacement temperature determinations of proximal pyroclastic deposits on Santorini, Greece, and their implications. *Bulletin of Volcanology 61,* p 450 - 467

Bell, J.M; Fraser, C. (1912). The geology of the Waihi-Tairua Subdivision. *New Zealand Geological Survey* bulletin 15.

Black, L.P; Kamoc, S.L; Allen, C.M; Davis, D.W; Aleinikoff, J.N; Valley, J.W; Mundil, R; Campbell, I.H; Korscha, R.J; Williams, I.S; Foudoulis, C. (2004). Improved $^{206}Pb/^{238}U$ microprobe geochronology by the ministering of a trace-element-related matrix effect; SHRIMP, ID-TIMS, ELA-ICP-MS and oxygen isotope documentation for a series of zircon standards. *Chemical Geology 205,* p 115-140.

Black, P.M; Skinner, D.N.B. (1979). The major oxide geochemistry of upper Tertiary Coromandel Group (andesites and dacites), northern Hauraki Volcanic Region, New Zealand. *Australia and New Zealand Association for the Advancement of Science Congress, abstracts, 1* p 211-228.

Booden, M.A; Smith, I.E.M; Jeffrey, L; Mauk, P.M.B. (2012). Geochemical and isotopic development of the Coromandel Volcanic Zone, northern New Zealand, since 18 Ma. *Journal of Volcanology and Geothermal Research* p 15-32.

Brathwaite, R.L; Torckler L.K; Jones, P.K. (2006). The Martha Hill epithermal deposit, Waihi–geology and mining history. *Australian Institute of Mineral and Metal Monogram.*

Brathwaite, R.L., & Christie, A.B. (1996). Geology of the Waihi area 1: 50 000. *Institute of Geological & Nuclear Sciences Geological Map*, *21*(1).

Brathwaite, R.L; McKay, D.F. (1989). Geology and exploration of the Martha Hill gold-silver deposit, Waihi. *Mineral Deposits of New Zealand, Monograph.*

Branney, M.J. Kokelaar, P. (2002). *Pyroclastic density currents and the sedimentation of ignimbrites*. The Geological Society. London.

Briggs, R.M. Houghton, B.F. McWilliams, M. & Wilson, C.J.N. (2005). $^{40}Ar/^{39}Ar$ ages of silicic volcanic rocks in the Tauranga-Kaimai area, New Zealand: Dating the transition between volcanism in the Coromandel Arc and the Taupo Volcanic Zone. *New Zealand Journal of Geology and Geophysics*, 48:3, p 459-469.

Bromley, CJ; Brathwaite, RL. (1991). Waihi Basin structure in light of recent geophysical surveys. Proceedings of the 25th Annual Conference 1991, *New Zealand branch of the Australasian Institute of Mining and Metallurgy* p 225-238.

Brothers, R. (1986). Upper Tertiary and Quaternary volcanism and subduction zone regression, North Island, New Zealand. *Journal of the Royal Society of New Zealand*, 16. Pages 275-298.

Bull, K. McPhie, J. (2007). Fiamme textures in volcanic successions: Flaming issues of definition and interpretation. *Journal of Volcanology and Geothermal research 164*, p 205-216.

Carter, L; Shane, P; Alloway, B; Hall, I; Harris, S; Westgate, J. (2003). Demise of one volcanic zone and birth of another—A 12 m.y. marine record of major rhyolitic eruptions from New Zealand. *Geology* 31; no. 6; p. 493–496

Cas, R.A.F.; Wright, J.V. (1987). *Volcanic Successions Modern and Ancient.* Allen & Unwin Publishing, London.

Cole, J.W.; Briggs, R.M.; Smith, I.E.M. (2015). Progression. *In*: Graham, I.J. (chief editor) "A Continent on the Move: New Zealand Geoscience Revealed, Second Edition". *Geoscience Society of New Zealand with GNS Science, Wellington, GSNZ Miscellaneous Publication 141,* p. 156-159.

Cole, J.W.; Brown, S.J.A.; Burt, R.M.; Beresford, S.W.; Wilson, C.J.N. (1998). Lithic types in ignimbrites as a guide to the evolution of a caldera complex, Taupo volcanic centre, New Zealand. *Journal of Volcanology and Geothermal Research 80* p 217–237

Cole, J.W. (1990). Structural control and origin of volcanism in the Taupo volcanic zone, New Zealand. *Bulletin of volcanology, 52*(6), 445-459.

Cook, E.T. (2016). *Felsic volcanism in the eastern Waihi area; process origins of the Corbett and Ratarua ignimbrites and the Hikurangi Rhyolite*. Unpublished M.Sc(Research) thesis, University of Waikato.

Couper, P.G. Lawton, D.C. (1978). Final report on exploration licence 33-051, Unpublished open-file company report. *Ministry of Economic Development report* MR350.

Cox, K.J.; Bell, J.D.; Pankhurst, R.J. (1979). *The Interpretation of igneous rocks*. George Allen & Unwin, London.

Davey, F.J; Henrys, S.A.; Lodolo, E. (1994). Asymmetric rifting in a continental back-arc environment, North Island, New Zealand. *Journal of volcanology and geothermal research 68,* p 209-238.

De Ronde, C; Hannington, M. D; Stoffers, P; Wright I. C; Ditchburn, R.G; Reyes A. G; Baker E. T; Massoth G. J; Lupton J. E; Walker, S.L; Greene, R.R; Soong, C.W.R; Ishibashi, J; Lebon, G.T; Bray, C.J; Resing, J.A. (2005). Evolution of a Submarine Magmatic-Hydrothermal System: Brothers Volcano, Southern Kermadec Arc, New Zealand. *Economic Geology*, 100 p 1097-1133.

Douillet, G. A.; Tsang-Hin-Sun, È.; Kueppers, U.; Letort, J.; Pacheco, D. A.; Goldstein, F; Dingwell, D. B. (2013). Sedimentology and geomorphology of the deposits from the August 2006 pyroclastic density currents at Tungurahua volcano, Ecuador. *Bulletin of Volcanology, 75*(11), p 1-21.

Edbrooke, S.W. (compiler). (2001). Geology of the Auckland area: scale 1:250,000. Lower Hutt: *Institute of Geological & Nuclear Sciences Limited*. Institute of Geological & Nuclear Sciences 1:250,000 geological map 3. 74 p

Ewart, A.; Healy, J. (1965). Ignimbrites of the Waihi District. In: B.N. Thompson, L.O. Kermode and A. Ewart *(ed.), New Zealand volcanology, Central Volcanic region.* Department of Scientific and Industrial Research information series 50, p 139-146

Fedo, C. M.; Sircombe, K. N; Rainbird, R. H. (2003). Detrital zircon analysis of the sedimentary record. *Reviews in Mineralogy & Geochemistry*, vol. 53, no. p. 277-303.

Gifkins, CC; Allen, RL; McPhie, J. (2005). Apparent welding textures in altered pumice-rich rocks. *Journal of Volcanology and Geothermal Research* 142 p 29– 47.

Google Maps. (2016). Map of the Waihi-Waikino region, North Island, New Zealand. Accessed 6th January 2016.

Hatherton, T. (1969). The geophysical significance of calc-alkaline andesites of New Zealand. *New Zealand Journal of Geophysics*, 12. p 436-459.

Haworth, AV. (1993). *Volcanic geology and hydrothermal alteration of the lower Waitekauri valley, Waihi, New Zealand*. Unpublished M.Sc. thesis, University of Waikato.

Henderson, J.; Bartrum, J.A. (1913). The geology of the Aroha subdivision, Hauraki, Auckland. Wellington: Government Printer. New Zealand *Geological Survey bulletin 16*.

Hoskin, PWO; Wysoczanski RJ; Briggs RM. (1998). U-Pb age determination of "Lenticulite" (Owharoa Ignimbrite) at Waikino, Waihi area, Coromandel Peninsula, and implications (abstract*). Geological Society of New Zealand Miscellaneous Publication* 101A: 123.

Hunt, P. (1991). The volcanic geology of the Whiritoa Hill area. Unpublished M.Sc. Thesis, University of Waikato.

Hunt, T.M; Syms, M.C. (1977). Sheet 3 – Auckland. Magnetic map of New Zealand 1:250,000. Wellington, Department of Scientific and Industrial Research.

Jackson, S.E; Pearson, N.J; Griffin, W.L; Belousova, E.A. (2004). The application of laser ablation-inductively coupled plasma-mass spectrometry to in situ U-Pb zircon geochronology. *Chemical Geology* 211, p 47-69.

Janoušek, V.; Farrow, C. M; Erban, V. (2006). Interpretation of whole-rock geochemical data in igneous geochemistry: introducing Geochemical Data Toolkit (GCDkit). *Journal of Petrology 47(6*), p 1255-1259. doi:10.1093/petrology/egl013

Janoušek, V.; Farrow, C.; M., Erban, V.; Trubač, J. (2011). Brand new geochemical data toolkit (GCDkit 3.0) – is it worth upgrading and browsing documentation? (Yes!). G*eologicke výzkumy na Morave a ve Slezsku, 18*, p 26-30.

King, P.R. (2000). Tectonic reconstructions of New Zealand: 40 Ma to the present: *New Zealand Journal of Geology and Geophysics*, v. 43, p. 611–638

Kohn, B.P. (1973). *Some aspects of New Zealand Quaternary pyroclastic rocks*. Unpublished Ph.D. thesis. Victoria University of Wellington

Lipman, P.W. (1997). Subsidence of ash-flow calderas: relation to caldera size and magma-chamber geometry. *Bulletin of Volcanology*, 59, pages 198-218.

Lipman, P.W. (1984). The roots of ash flow calderas in Western North America: windows into the tops of granitic batholiths. *Journal of Geophysical Research.* B89, p 8801-8841.

Malengreau, B; Skinner, D; Bromley, C; Black, P. (2000). Geophysical characterisation of large silicic volcanic structures in the Coromandel Peninsula, New Zealand. *New Zealand Journal of Geology and Geophysics*, 43 p 171-186

Marshall, P. (1935). Acid rocks of the Taupo-Rotorua volcanic district. *Trans. Roy. Soc. NZ, 64*, p 323-366.

McClelland, E; Wilson C. J. N.; Bardot, L. (2004) Palaeotemperature determinations for the 1.8-ka Taupo ignimbrite, New Zealand, and implications for the emplacement history of a high-velocity pyroclastic flow. *Bulletin of Volcanology 66,* p 492–513

McPhie, J.; Doyle, M.; Allen, R. (1993). *Volcanic Textures: a guide to the interpretation of textures in volcanic rocks.* Hobart: Centre for Ore Deposit and Exploration Studies, University of Tasmania.

Morgan, P.G. (1910). The igneous rocks of the Waihi Goldfield. *Transactions of the New Zealand Institute 43*, p 272.

Morgan, P.G. (1924). The geology and mines of the Waihi District, Hauraki Goldfield, New Zealand. *New Zealand Geological Survey bulletin* 26.

Nicholson, K.N; Black, P.M; Hoskin, P.W.O; Smith, I.E.M. (2004). Silicic volcanism and back-arc extension related to migration of the Late Cainozoic Australian-Pacific plate boundary. *Journal of Volcanology and Geothermal Research* 131, p 295-306.

Porreca, M; Mattei, M; MacNiocaill, C; Giordano, G; McClelland, E; Funiciello, R. (2008). Paleomagnetic evidence for low-temperature emplacement of

the phreatomagmatic Peperino Albano ignimbrite (Colli Albani volcano, Central Italy). *Bulletin of Volcanology 70*, p 877–893

Rabone, S. D. C. (1971). *Igneous geology of the western Waitekauri Valley, Ohinemuri.* Unpublished MSc thesis, University of Auckland.

Rabone, S.D.C. (1975). Petrography and hydrothermal alteration of Tertiary andesite-rhyolite volcanics in the Waitekauri Valley, Ohinemuri. *New Zealand Journal of Geology and Geophysics* 18 p 239-258.

Rabone, S.D.C. Keal, P. (1985). Progress report: PL 31-758 Waihi, June to December 1984: Amoco Minerals Ltd. Unpublished open-file mining company report. *Institute of Geological and Nuclear Sciences* MR810

Richards, R. E. (2009). U-Pb geochronology of detrital zircon from Eocene - Oligocene sediments in the Te Anau Basin (New Zealand) and inferred provenance. MSc Thesis, University of Waikato.

Sigurdsson, H; Houghton, B.F. (2000). *Encyclopedia of volcanoes*. San Diego: Academic Press.

Skinner, D. N. (1993).*Geology of the Coromandel Harbour area*. Institute of Geological & Nuclear Sciences.

Skinner, D.N. (1986). Neogene Volcanism of the Hauraki Volcanic Region. In *Late Cenozoic Volcanism in New Zealand*. The Royal Society of New Zealand, Bulletin 23, p 21-47msith

Smith, N. Cassidy, J. Locke, C. Mauk, J. Christie, A. (2006). The role of regional-scale faults in controlling a trapdoor caldera, Coromandel Peninsula, New Zealand. *Journal of Volcanology and Geothermal Research*, 149, pages 312-328.

Solari, L.A; Gomez-Tuena, A; Bernal, J.P; Perez-Arvizu, O; Tanner, M. (2010). U-Pb zircon Geochronology with an Integrated LA-ICP-MS microanalytical Workstation: Achievements in Precision and Accuracy. *Geo Standards and Geoanalytical Research, 34* p 5-18

Stagpoole, V.M.; Christie, A.B.; Henrys, S.A.; Woodward, D.J. (2001). Aeromagnetic map of the Coromandel region: total force anomalies. *Institute of Geological and Nuclear Sciences* geophysical map 14. Lower Hutt, New Zealand.

Stevens, M.T. (2010). *Miocene and Pliocene Silicic Coromandel Volcanic Zone Tephras from ODP Site 1124-C: Petrogenetic Applications and Temporal Evolution.* Completed MSc (Hons) at Victoria University of Wellington.

Sulpizo, R.; Dellino, P. (2008). Chapter 2: Sedimentology, depositional mechanisms and pulsating behavior of pyroclastic density currents. From Gottsmann & Marti (ed.) *Caldera volcanism analysis, modelling and response.* Elsevier.

Suzuki-Kamata, K; Kamata, H; Bacon, C.R. (1993). Evolution of the caldera-forming eruption at Crater Lake, Oregon, indicated by component analysis of lithic fragments. *Journal of Geophysical Research, 98,* p 14059–14074.

Thrasher, G.P. (1986). Basement structure and sediment thickness beneath the continental shelf of the Hauraki Gulf and offshore Coromandel region, New Zealand. *New Zealand Journal of Geology and Geophysics, 29*, p 41-50.

Vermeesch, P. (2012). On the visualization of detrital age distributions. *Chemical Geology 312* p 190-194.

Vincent, K.A. (2012). *U-Pb Dating of Silicic Volcanic Rocks of the Eastern Coromandel Peninsula*. Completed M.Sc. thesis. University of Waikato.

White, P.D. (1995). *Final Report, PL 31-1340, Waitete*. New Zealand Petroleum and Minerals, Ministry of Business, Innovation and Employment, Wellington, unpusblished open-file mineral report MR3353.

Walker, G.P.L. (1981). Charactertistics of two phreatoplininan ashes, and their water flushed origin. *Journal of Volcanology and Geothermal Research, 9*, p 395-407.

Watson, G. S. (1956). A test for randomness of directions. *Geophysical Supplements to the Monthly Notices of the Royal Astronomical Society*, *7*(4), p 160-161.

Wilson, L. (1976). Explosive Volcanic Eruptions—III. Plinian Eruption Columns. *Geophys. J. Int. 45* p 543-556.

Wilson, C.J.N; Charlier, B.I.A; Fagan, C.J; Spinks, KD; Gravley, DM; Simmons, SF; Browne, PRL. (2008). U-Pb dating of zircon in hydrothermally altered rocks as a correlation tool: Application to the Mangakino geothermal field, New Zealand. *Journal of Volcanology and Geothermal Research 176*, p 191-198

Wilson, C.J.N., Houghton, B.F., McWillams, M.O., Lanphere, M.A., Weaver, S.D., Briggs, R.M. (1995). Volcanic and structural evolution of Taupo Volcanic Zone, New Zealand: a review. *Journal of Volcanology and Geothermal Research 68*, p 1- 28.

Winter, J.D. (2010). *Principles of igneous and metamorphic petrology*. Pearson Education.

Woodward, D.J. (1971). Sheet 3 Auckland, gravity map of New Zealand, Bouguer Anomalies. *Department of Scientific and Industrial Research*. Wellington N.Z

Worner, G. (2010). Process of magma evolution and magmatic suites. From: Encyclopedia of Life Support Systems. Developed under the Auspices of the UNESCO, Eolss Publishers, Paris, France.

Wright, J.V., Smith, A.L., Self, S. (1980). A working terminology of pyroclastic deposits. *Journal of Volcanology and Geothermal Research. 8*, p 315–336.

Appendix

Appendix I: Location and sample and testing catalogue

Rock name*	Site no.	Site name	GPS coordinates	Location description	Sample nos.	University of Waikato no.	Thin section number	Other testing methods
OI	1	Lower Owharoa Falls	37°25'11.50"S 175°45'49.19"E	At the Owharoa Falls base, closest to the river. On the Hauraki Rail Trail.	1.1	W150-400	1.1, 1.1.1, 1.1.11	P.C.#, XRD, XRF, EMPA
					1.2	W150-401	1.2.1	XRF
					1.3	W150-402	1.3.1	2x XRD, XRF, EMPA
					1.4	W150-403	1.4.1, 1.4.2, 1.4.3	P.C.#
					1.5	W150-404	1.5.1, 1.5.2	
					1.6	W150-405	1.6.1, 1.9.3	P.C.#, SEM
OI	2	Upper Owharoa Falls	37°25'15.28"S 175°45'48.68"E	Two waterfall terraces up from the Owharoa Falls – access from the bridge above the falls.	2.1	W150-406	2.1, 2.1.1, 2.1.2	P.C.#, EMPA
					2.2		OF2.1, OF2.2	(P)
					2.3	W150-407	2.2.1	SEM, EMPA
					2.4	W150-408	2.3.1	
					2.5	W150-409	2.4	
					2.6	W150-410	2.5.1, 2.5.2	
					2.7	W150-411	2.6.1	XRF
					2.8	W150-412	2.7.1, 2.7.2	P.C.#
					2.9	W150-413	2.8.1	
						W150-414	2.9.1	
OI	3	Owharoa Quarry (Across road from Owharoa Falls)	37°25'10.64"S 175°45'53.84"E	Other side of the road of the Owharoa Falls	3.1	W150-415	3.1	
OI, WI	4	Old Waikino Quarry	37°24'55.41"S 175°46'51.90"E	Along the rail way tracks east from the Waikino Station café, next to the bridge.	4.1 (OI)	W150-416	4.1.1, 4.1.2	
					4.2 (OI)	W150-417		
					4.3 (WI)	W150-418	4.2	U-Pb zircon dating, SEM, XRD (Wai Q), XRF
					4.4 (WI)	W150-419		

PC	5	Old Karangahake Quarry		Along the Hauraki Rail trail, west of the Owharoa Falls for ~1.5 km.	-			
OI	6	Farm cutting parallel to Owharoa Falls and Hollis Road	37°25'43.01"S 175°46'25.03"E	Drive way next to the bridge that goes over the Owharoa upper falls. Farm track on the farm.	-			
OI	7	Samson Road and State highway Intersection	37°24'10.55"S 175°48'43.56"E	On the corner of Samson Road and the State highway	A M4 SC Pumice section MSC	W150-421 W150-422 W150-423 W150-424 W150-425	7.6.1 7.7.1 7.5.1, 7.5.2 7.1 7.4.1, 7.4.2	 XRF
WI	8	Waikino section parallel to highway and river	-37.416345, 175.782307	In between the Waikino Station Café and the Waikino Quarry	8.1	W150-440	8.1, 8.2, 8X W1, W2, W3	WAI2 - P.C.#, SEM XRD, W3 and WAI1 EMPA, all 3 (P)
OI	9a	McHardy Farm, site a, large outcrop	37°24’31.73”S 175°50’48.64”E	Eastern side of Crean Road property – rock face left of the house in first paddock	9A1 9A	W150-426 W150-427		 XRF
OI	9b	McHardy Farm, large outcrop north of 9a	37°24’32.39”S 175°50’45.56”E	Eastern side of Crean Road property – rock face left of the house in second paddock	9B	W150-428		XRF
OI	9c	McHardy Farm, stream to the south	37°24’26.54”S 175°51’5.68”E	Eastern side of Crean Road property – left side of property, stream running down boundary	9X1 9X2 9X4	W150-441 W150-442 W150-443	9.1.1 – 9.1.8 9.2.1, 9.2.2 9.3.3-9.3.4, McH1, McH2, P (pumice sample)	9.1.7 - P.C.# XRD, XRF, SEM (P)
OI	10	Old Waitekauri	-37.409639,	On the northern corner of Waiktekauri Road	10.1	W150-429	10.1.6	

		Road	175.772376	and Old Waitekauri Road				
OI	11	Opposite Waikino Tavern	-37.414202, 175.771731	Opposite the Waikino Tavern, across the walkway bridge – samples and description were taken from the open rock face.	11.1 11A 11B 11C 11D 11E 11F	W150-430 W150-431 W150-432 W150-433 W150-434 W150-435 W150-436	 11.1.1 11.2.2, 11.3.1 11.5.1 	SEM, XRF (P) XRD, XRF
OI	12	Corner of Waitekauri Road and Campbell Road	-37.401241, 175.784253	A site on the corner, on the northern side of the intersection between the Waitekauri and Campbell Road.	12.1 12.2	W150-437 W150-438	12-1-1 12-2-1, 12.2.2	XRF XRD

*OI – Owharoa Ignimbrite, WI – Waikino Ignimbrite, PC – Pebble conglomerate, # - Point counting, (P) – polished thin section, SEM – Scanning electron microscopy analysis (including EDS), EMPA – electron microprobe analysis

Appendix II: Age data for the Waikino Ignimbrite

Instrument settings for LA-ICPMS

ICP-MS

Model	Elan 6100 DRCII ICP-MS (Perkin Elmer Sciex)
Gas flows	
Plasma (Ar)	15 L.min
Auxiliary (Ar)	1.2 L.min
Carrier (He)	1.0 L.min
Nebuliser	0.6 to 0.7 optimised range
Shield torch	Used for most analyses
Vacuum pressure	1 x 10-5 Torr
Software	Elan 3.4

LASER

Model	RESOlution SE series excimer laser
Wavelength	193 nm
Repetition rate	5 Hz
Pre-ablation laser warm-up	Laser fired continuously
Spot size	30 μm (60 for NIST)
Incident pulse energy	c. 0.04 mJ
Energy density on sample (fluence)	c. 6 J.cm2
Software	Geostar v8.50

DATA ACQUISITION PARAMETERS

Data acquisition protocol	Time resolved analyses
Scanning mode	Peak hopping, 1 point per peak
Detector mode	Pulse counting, dead time correction applied
Isotopes determined	206Pb, 207Pb, 208Pb, 204Pb, 232Th, 235U, 238U, 29Si, 91Zr
Dwell time per isotope	50, 50, 50, 50, 30, 50, 50, 15, 15 ms respectively
Quadrapole settling time	c. 2 ms
Data acquisition	85 s (40 s background, 45 s ablation)
Software	Elan v 3.4

Results from the LA-ICPMS

Spot no.	Final Age 206Pb/238U (My)	Final Age 206Pb/238U Int 2 S.E. (My)
Waikino - 5	3.31	0.29
Waikino - 6	3.9	1.6
Waikino - 7	3.6	1.3
Waikino - 9	3.43	0.75
Waikino - 12	3.5	1.3
Waikino - 13	3.37	0.58
Waikino - 15	3.6	1.1
Waikino - 16	2.55	0.77
Waikino - 19	2.6	0.98
Waikino - 21	3.62	0.4
Waikino - 24	3	0.75
Waikino - 25	3.2	0.6
Waikino - 26	4.26	0.79
Waikino - 27	3.17	0.51
Waikino - 28	3.9	1
Waikino - 34	3.6	1.1
Waikino - 42	4.12	0.84
Waikino - 43	3.79	0.89
Waikino - 56	4.4	1.3
Waikino - 60	4.35	0.6
Waikino - 61	4.3	1.3
Final age	**3.48**	**0.19**

Appendix III: Point counting analysis for the Owharoa and Waikino ignimbrites

Table for the different componentry percentages of the Owharoa and Waikino ignimbrites

	Percentage (%) per thin section						
Waikato number	**W150-400**	**W150-403**	**W150-405**	**W150-406**	**W150-412**	**W150-441**	**W150-440**
Ignimbrite	**Owharoa**						**Waikino**
Sample # - Component (%) ˇ	**1.1.1**	**1.4.2**	**1.6.1**	**2.1.2**	**2.7.1**	**9.1.7**	**Wai 2**
Pumice	46.36	26.7	37.8	41.37	38.2	45.125	0[1]
Lithics	5.77	0.76	5.88	0.99	4.99	9.625	2.18
Matrix (unresolvable)	28.35	35.09	26.3	27.01	36.79	19.375	88.3[2]
Glass shards	15.72	30.48	24.9	25.12	14.97	20.5	**
Oxyhydroxides							3.03
Free crystals							
Plagioclase	1.99	5.46	3.1	4.68	1.95	3.5	2.46
Quartz	0.59	1.82	1.5	0.29	1.27	1.5	0.94
Biotite	0.39	0.38	0.09	0.09	0.39	0.25	0.094
Hornblende	0	0.095	0.09	0	0.19	0	0
Opaques	0.09	0.32	0.18	0.09	0.58	0.125	0.66

[1]*visual field estimates suggest <2%*

[2]*include glass shards and unresolvable fine grained material*

Appendix IV: SEM analysis list

UoW no.	Mount number	Sample	Locality
W150-405	1	Owharoa Ignimbrite pumice chip	2
W150-418	2	Waikino Ignimbrite chip	4
W150-405	3	Owharoa Ignimbrite chip	2
W150-430	4	Owharoa Ignimbrite chip	11
W150-430	5	Owharoa Ignimbrite chip	11
W150-443	6	Owharoa Ignimbrite chip	9
W150-440	7	Waikino Ignimbrite chip	8
W150-440	8	Waikino Ignimbrite chip	8
	Thin section analysis		
W150-405	-	Owharoa Ignimbrite thin section sample	1
W150-440	-	Waikino Ignimbrite thin section sample	8

Appendix V: Scanning Electron Microscopy results

Appendix V.1: SEM backscatter elemental analysis

Elemental analysis of the Owharoa Ignimbrite matrix:

Data Type: Counts Mag: 3500 Acc. Voltage: 15.0 kV

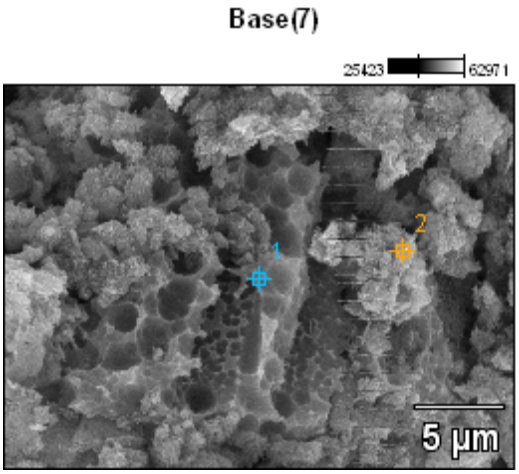

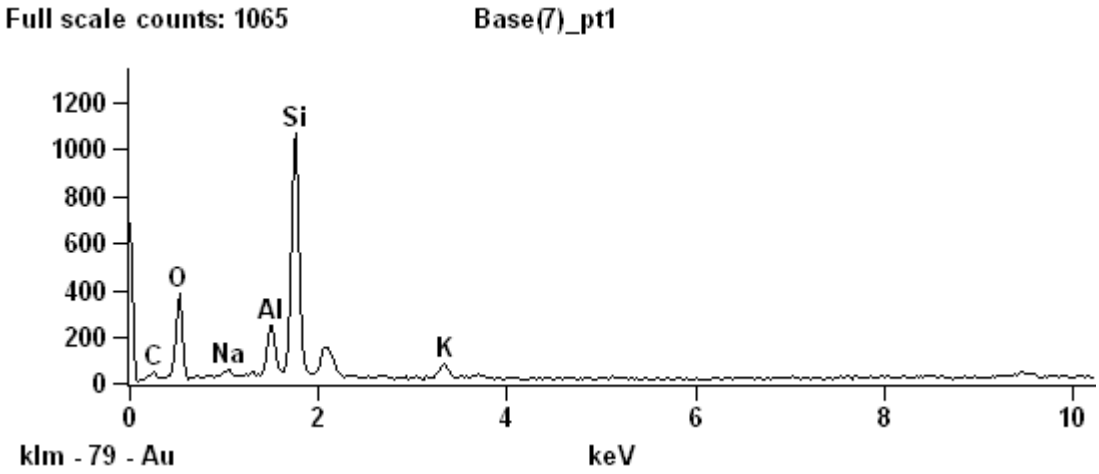

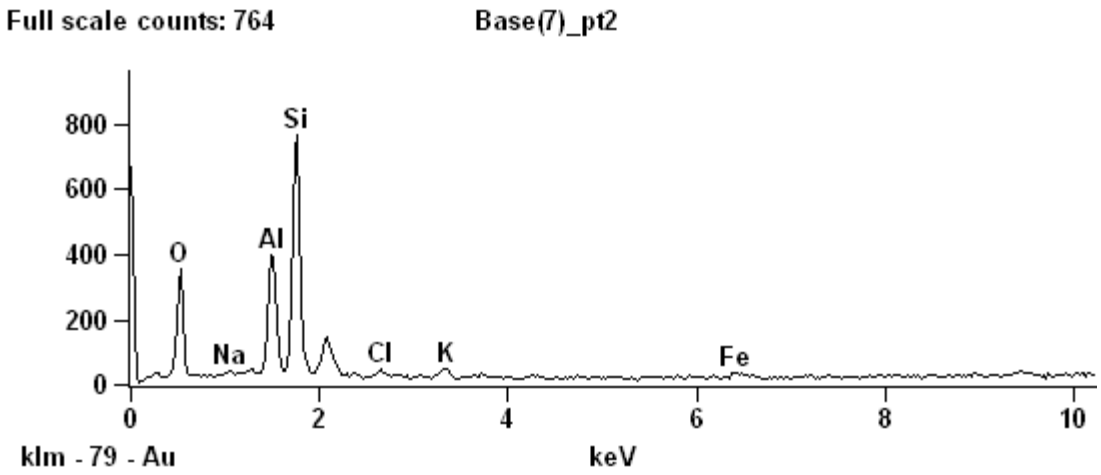

Base (7) analysis

Weight %

	C-K	O-K	Na-K	Al-K	Si-K	Cl-K	K-K	Fe-K
Base(7)_pt1	7.97	43.46	1.42	6.37	37.28		3.50	
Base(7)_pt2		42.45	1.02	14.10	34.34	1.58	2.63	3.87

Weight % Error (+/- 1 Sigma)

	C-K	O-K	Na-K	Al-K	Si-K	Cl-K	K-K	Fe-K
Base(7)_pt1	+/-1.33	+/-0.72	+/-0.17	+/-0.18	+/-0.49		+/-0.22	
Base(7)_pt2		+/-1.08	+/-0.19	+/-0.25	+/-0.59	+/-0.21	+/-0.23	+/-1.10

Atom %

	C-K	O-K	Na-K	Al-K	Si-K	Cl-K	K-K	Fe-K
Base(7)_pt1	13.02	53.32	1.21	4.63	26.06		1.76	
Base(7)_pt2		57.37	0.96	11.30	26.44	0.97	1.46	1.50

Atom % Error (+/- 1 Sigma)

	C-K	O-K	Na-K	Al-K	Si-K	Cl-K	K-K	Fe-K
Base(7)_pt1	+/-2.17	+/-0.88	+/-0.15	+/-0.13	+/-0.35		+/-0.11	
Base(7)_pt2		+/-1.45	+/-0.18	+/-0.20	+/-0.45	+/-0.13	+/-0.13	+/-0.43

Waikino Ignimbrite matrix

Data Type: Counts Mag: 3500 Acc. Voltage: 15.0 kV

Waikino Ignimbrite matrix(9)

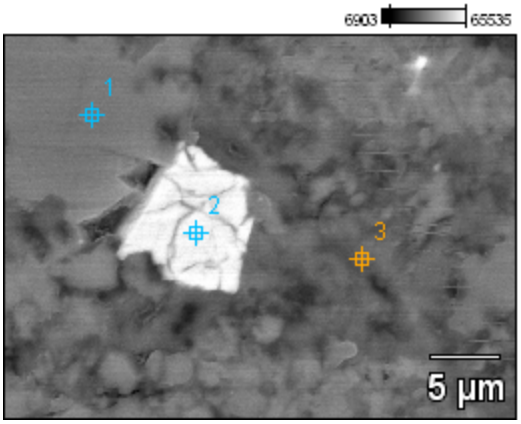

Full scale counts: 2462 Waikino Ignimbrite matrix(9)_pt1

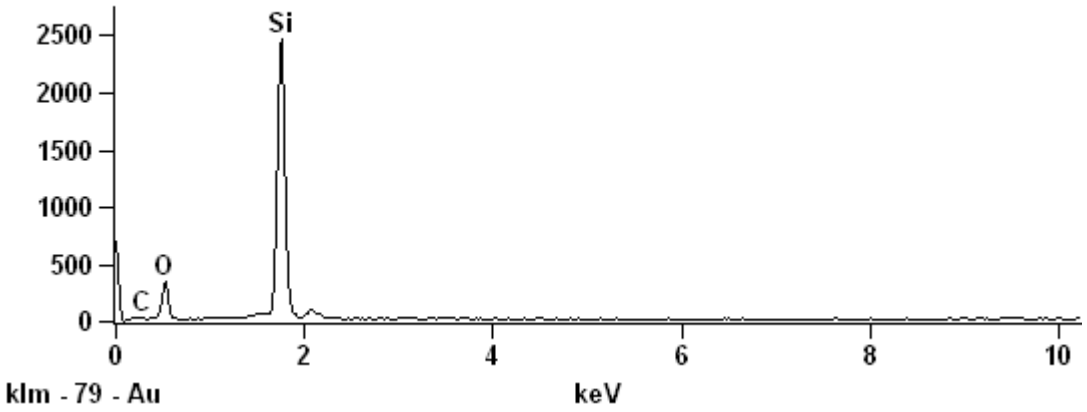

Full scale counts: 768 Waikino Ignimbrite matrix(9)_pt2

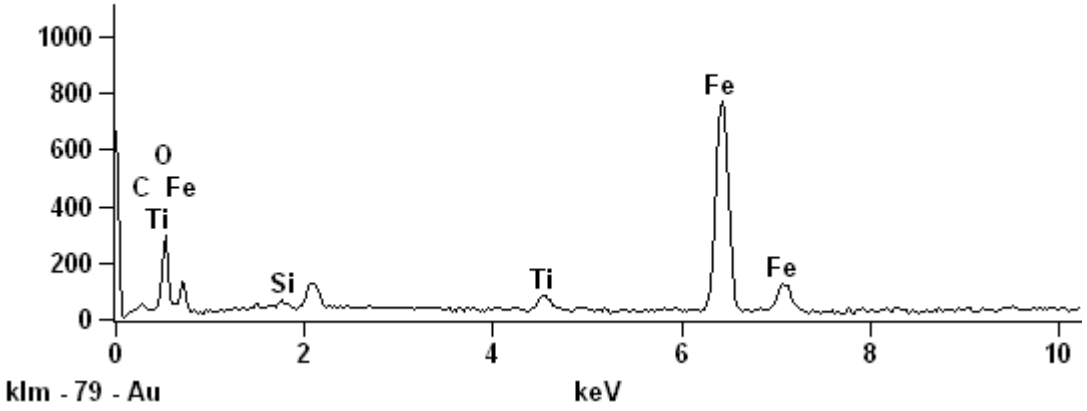

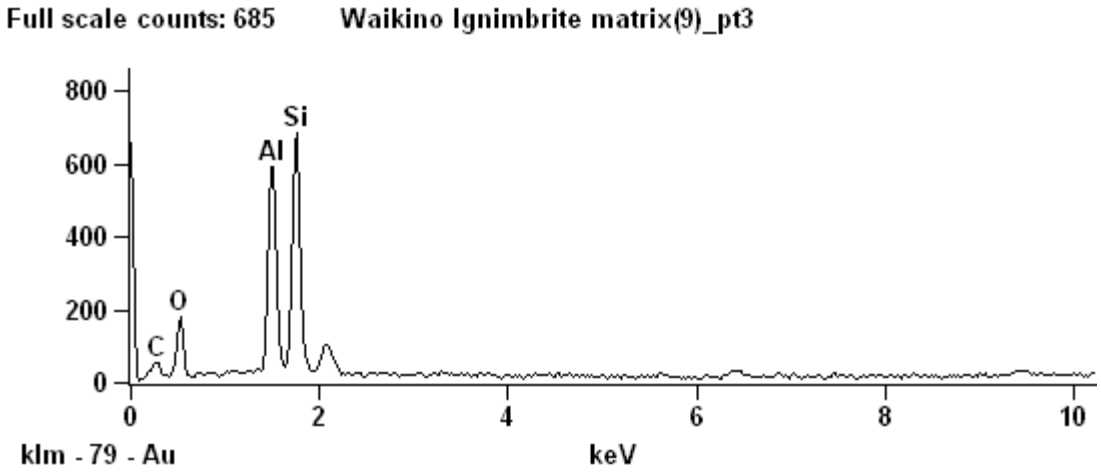
Full scale counts: 685
Waikino Ignimbrite matrix(9)_pt3
800
600
400
200
0
Si
Al
O
C
0
2
4
6
8
10
klm - 79 - Au
keV

(9) Weight %

	C-K	O-K	Al-K	Si-K	Ti-K	Fe-K
Waikino Ignimbrite matrix(9)_pt1	6.89	32.74		60.37		
Waikino Ignimbrite matrix(9)_pt2	1.87	8.19		0.71	2.51	86.72
Waikino Ignimbrite matrix(9)_pt3	24.82	27.50	18.72	28.96		

Weight % Error (+/- 1 Sigma)

	C-K	O-K	Al-K	Si-K	Ti-K	Fe-K
Waikino Ignimbrite matrix(9)_pt1	+/-1.35	+/-0.77		+/-0.45		
Waikino Ignimbrite matrix(9)_pt2	+/-0.32	+/-0.29		+/-0.12	+/-0.29	+/-1.50
Waikino Ignimbrite matrix(9)_pt3	+/-2.16	+/-1.06	+/-0.37	+/-0.55		

Atom %

	C-K	O-K	Al-K	Si-K	Ti-K	Fe-K
Waikino Ignimbrite matrix(9)_pt1	12.02	42.91		45.07		
Waikino Ignimbrite matrix(9)_pt2	6.78	22.27		1.10	2.28	67.57
Waikino Ignimbrite matrix(9)_pt3	37.50	31.19	12.59	18.71		

Atom % Error (+/- 1 Sigma)

	C-K	O-K	Al-K	Si-K	Ti-K	Fe-K
Waikino Ignimbrite matrix(9)_pt1	+/-2.36	+/-1.00		+/-0.33		
Waikino Ignimbrite matrix(9)_pt2	+/-1.16	+/-0.79		+/-0.19	+/-0.26	+/-1.17
Waikino Ignimbrite matrix(9)_pt3	+/-3.27	+/-1.21	+/-0.25	+/-0.35		

Appendix VI: XRD analysis and results

XRD analysis list

Waikato number	Ignimbrite	Sample type	Sample number
W150-440	Waikino	Bulk	W1
W150-440	Waikino	Bulk	W2
W150-440	Waikino	Bulk	W3
W150-419	Waikino	Bulk	Wai Q
W150-400	Owharoa	Bulk	OI 1.1
W150-402	Owharoa	Bulk	OI 1.3 A
W150-402	Owharoa	Bulk	OI 1.3 B
W150-443	Owharoa	Bulk	OI X4
W150-436	Owharoa	Matrix	11F
W150-438	Owharoa	Bulk	12.2

Owharoa Ignimbrite

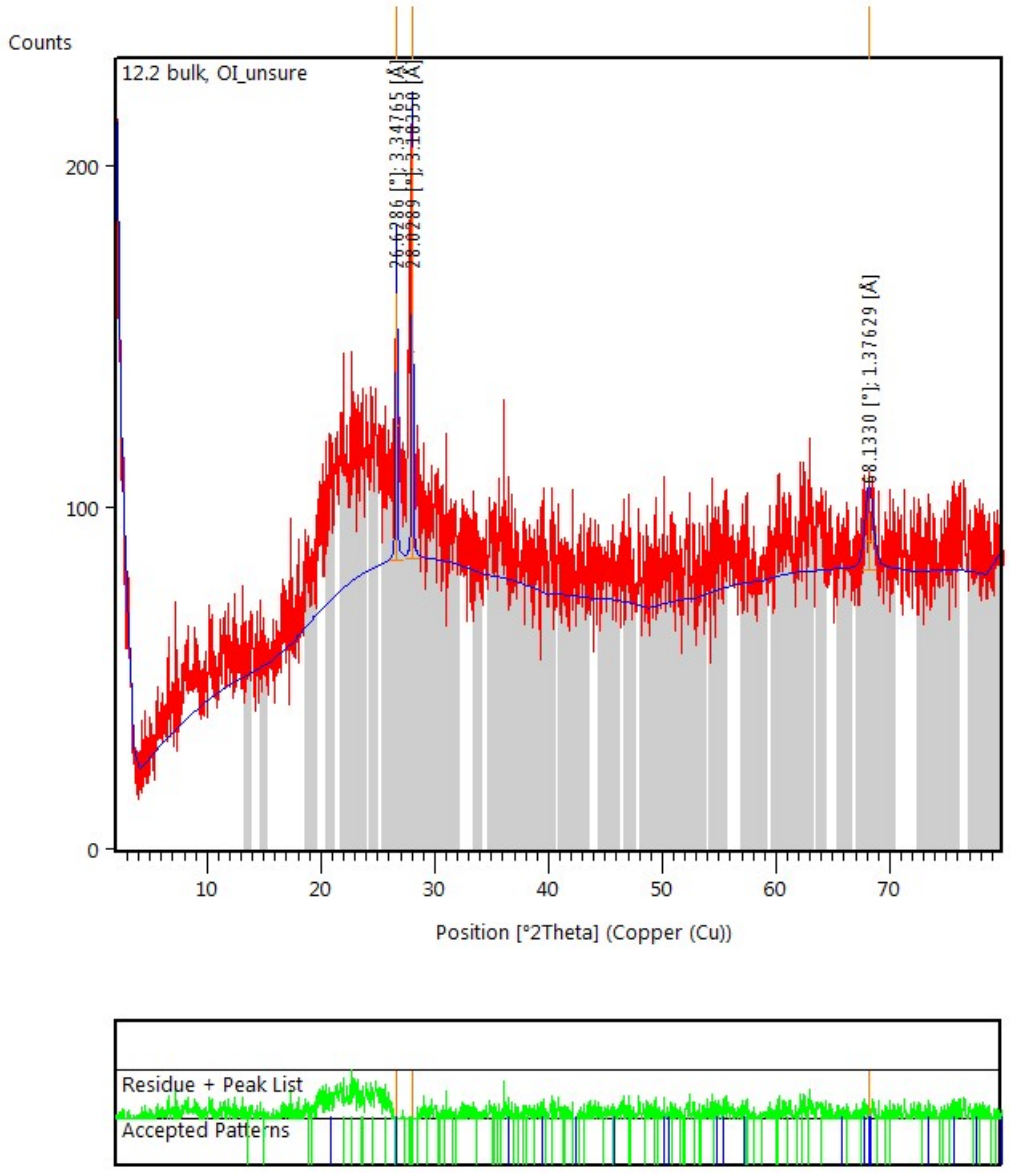

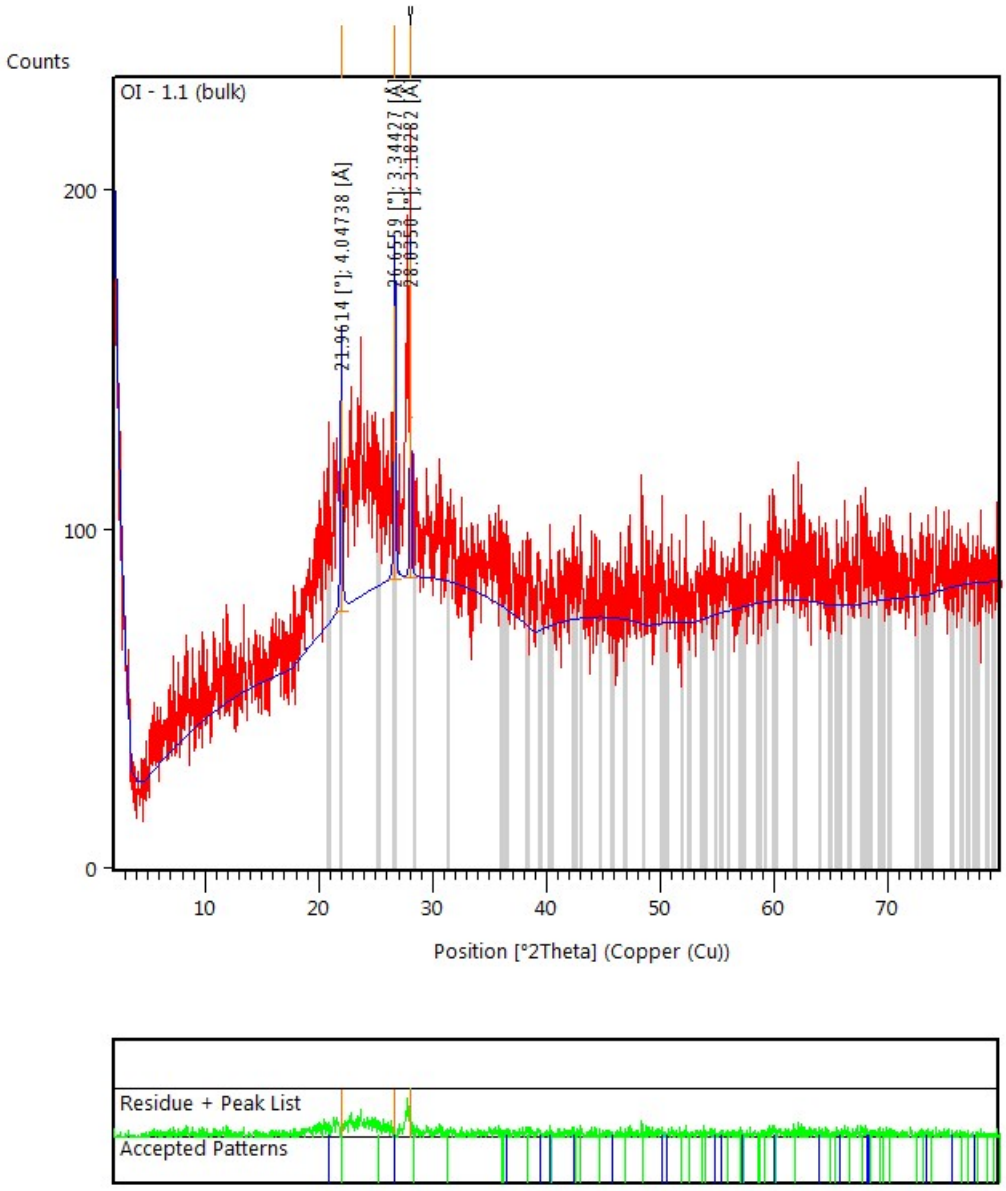
Counts
OI - 1.1 (bulk)
200
100
0
21.9614 [°]; 4.04738 [Å]
26.6559 [°]; 3.34427 [Å]
28.0358 [°]; 3.18282 [Å]
10
20
30
40
50
60
70
Position [°2Theta] (Copper (Cu))
Residue + Peak List
Accepted Patterns

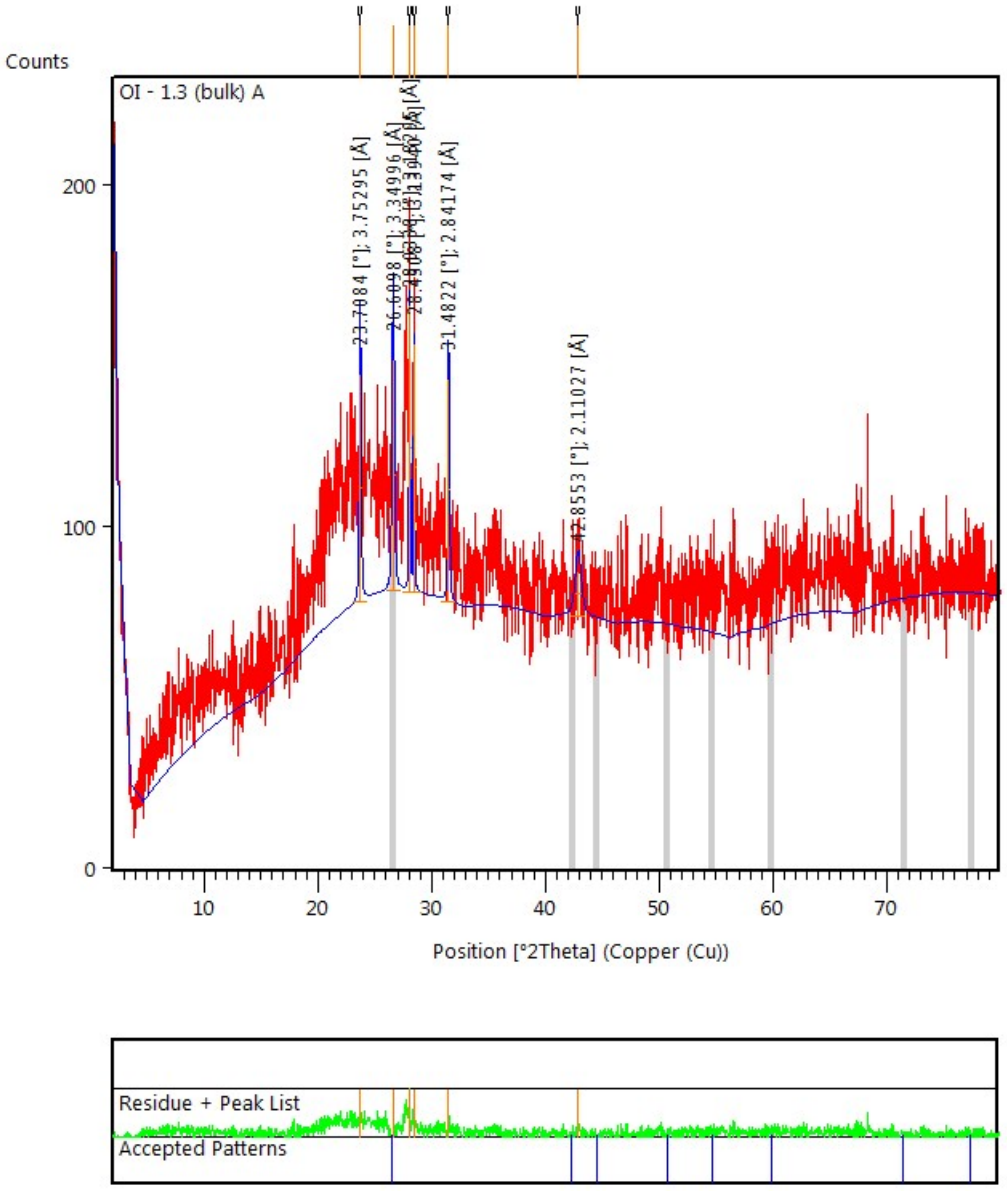
Counts
OI - 1.3 (bulk) A
200
100
0
23.7884 [°]; 3.75295 [Å]
26.6098 [°]; 3.34996 [Å]
31.4822 [°]; 2.84174 [Å]
42.8553 [°]; 2.11027 [Å]
10
20
30
40
50
60
70
Position [°2Theta] (Copper (Cu))
Residue + Peak List
Accepted Patterns

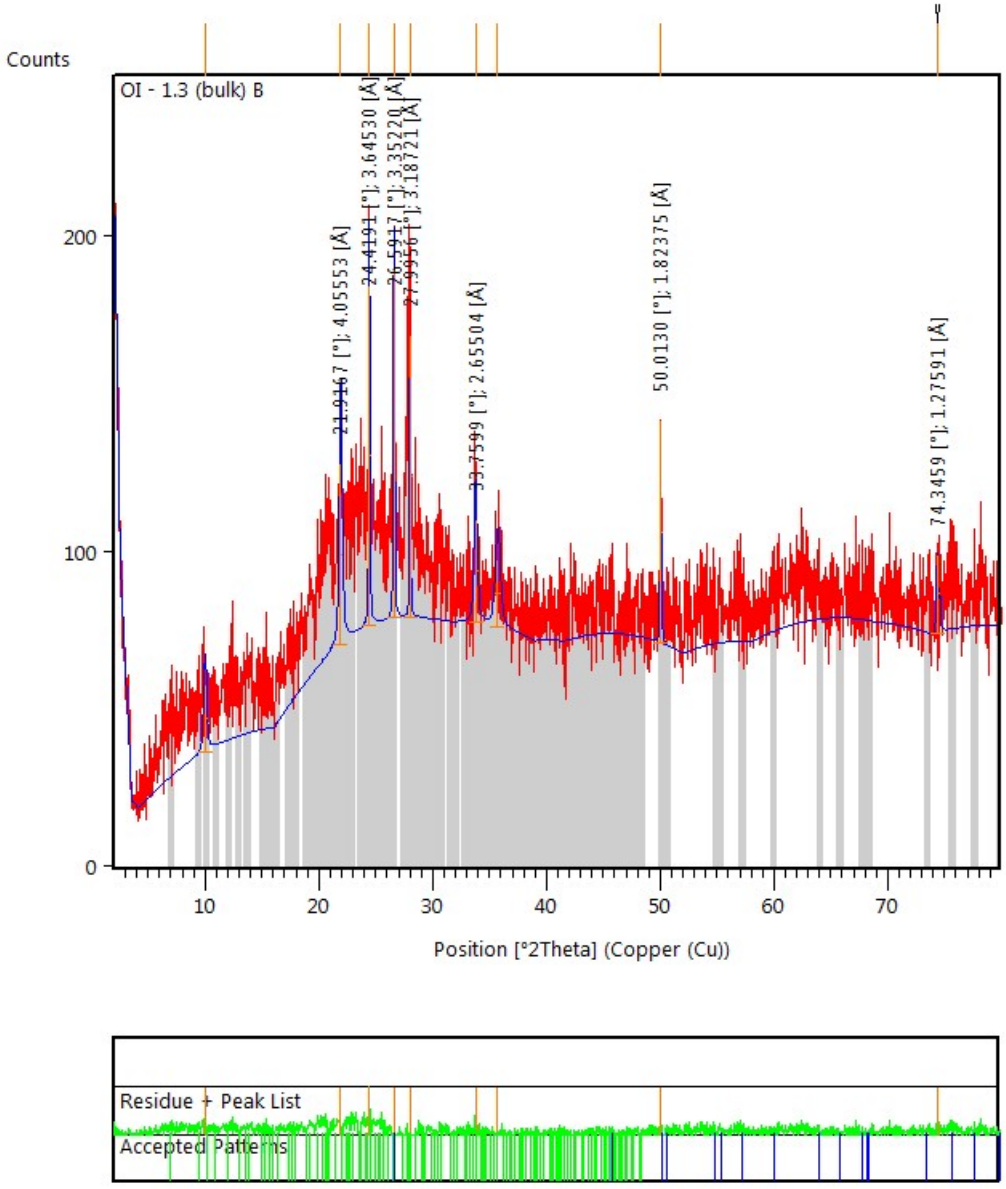
Counts
OI - 1.3 (bulk) B
200
100
0
21.9167 [°]; 4.05553 [Å]
24.4191 [°]; 3.64530 [Å]
26.5917 [°]; 3.35220 [Å]
27.9956 [°]; 3.18721 [Å]
33.7599 [°]; 2.65504 [Å]
50.0130 [°]; 1.82375 [Å]
74.3459 [°]; 1.27591 [Å]
10
20
30
40
50
60
70
Position [°2Theta] (Copper (Cu))
Residue + Peak List
Accepted Patterns

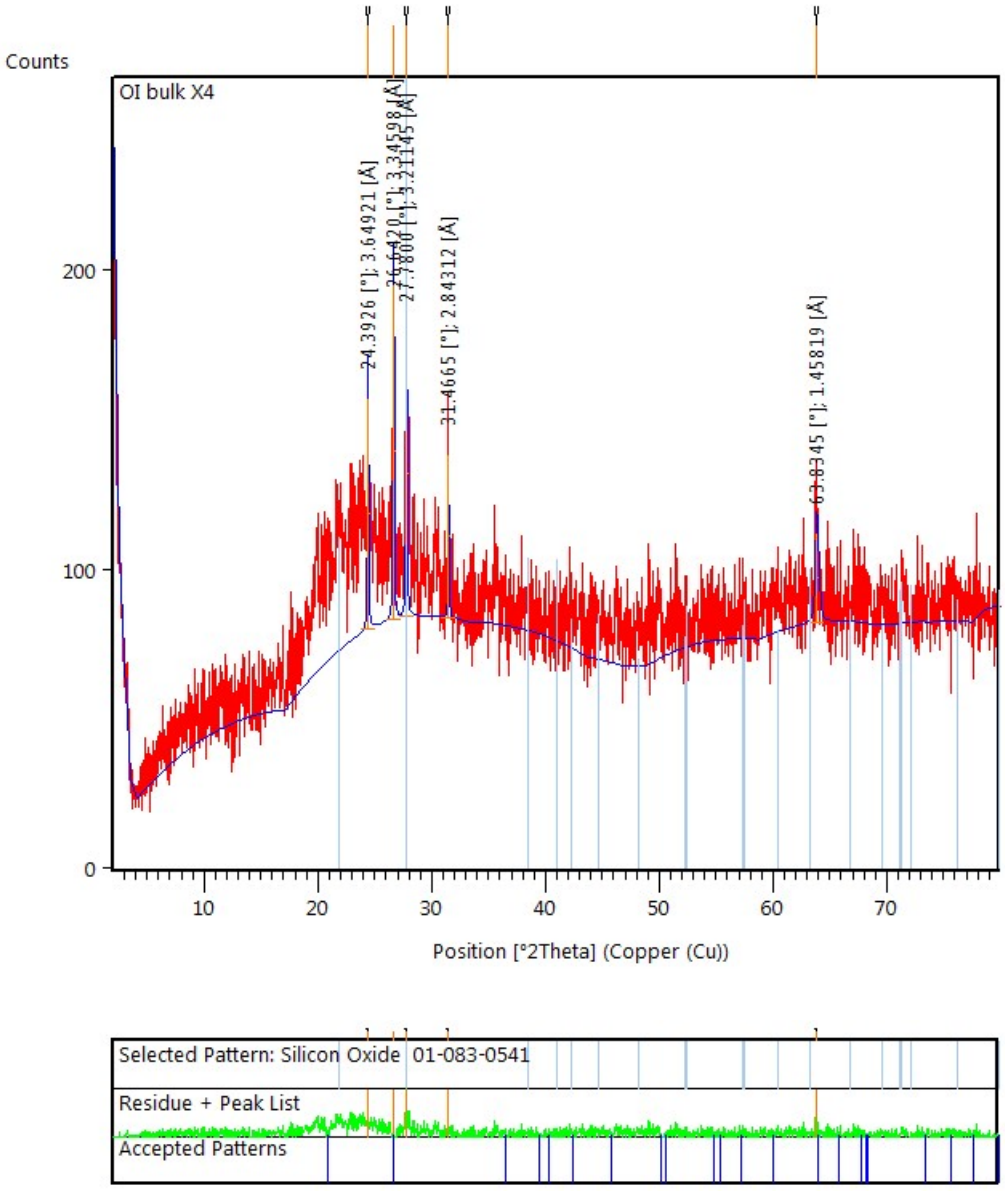
Counts
OI bulk X4
24.3926 [°]; 3.64921 [Å]
31.4665 [°]; 2.84312 [Å]
63.0345 [°]; 1.45819 [Å]
200
100
0
10
20
30
40
50
60
70
Position [°2Theta] (Copper (Cu))
Selected Pattern: Silicon Oxide 01-083-0541
Residue + Peak List
Accepted Patterns

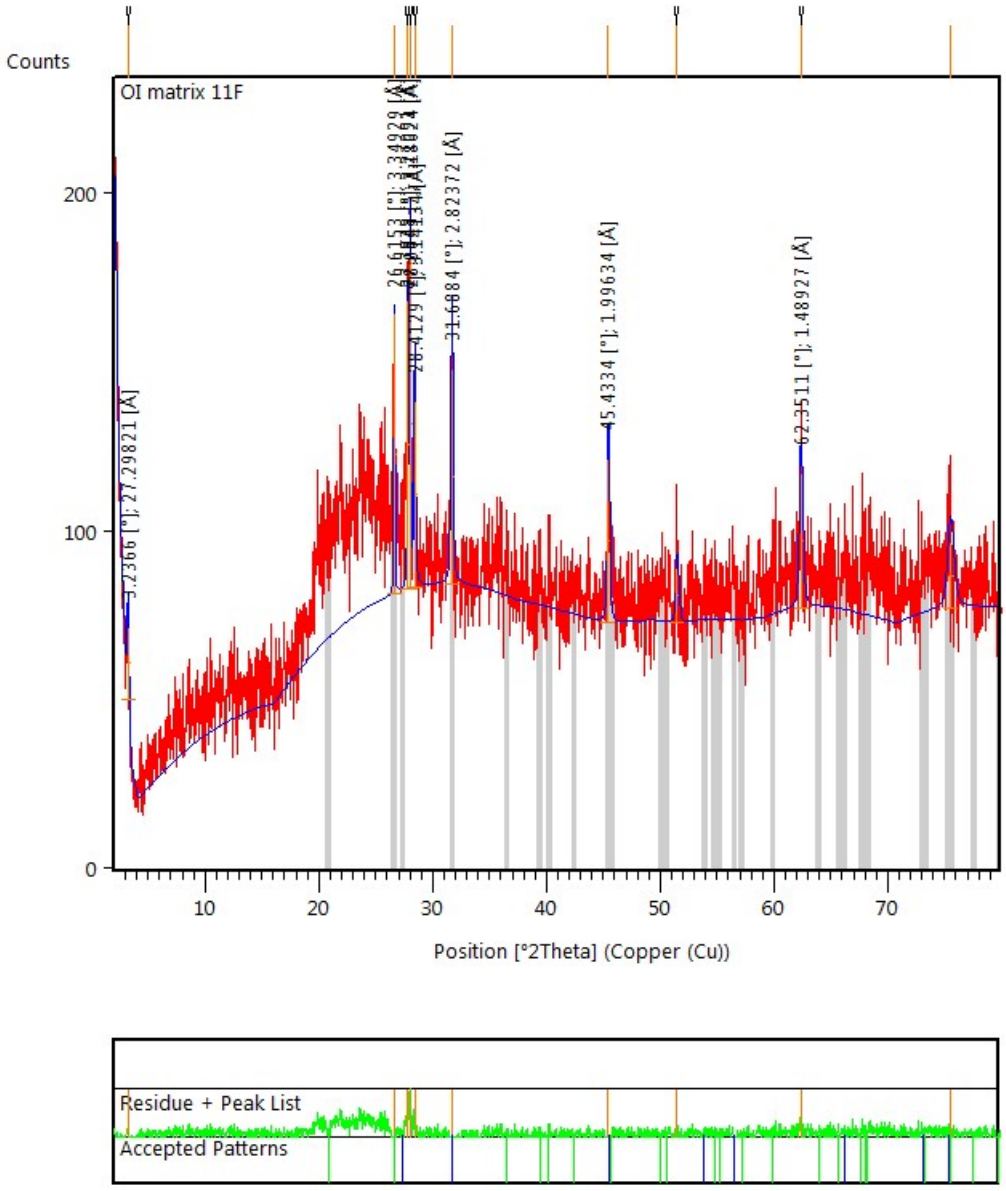
Counts
OI matrix 11F
200
100
0
5.2366 [°]; 27.29821 [Å]
31.6084 [°]; 2.82372 [Å]
45.4334 [°]; 1.99634 [Å]
62.3511 [°]; 1.48927 [Å]
10
20
30
40
50
60
70
Position [°2Theta] (Copper (Cu))
Residue + Peak List
Accepted Patterns

Waikino Ignimbrite

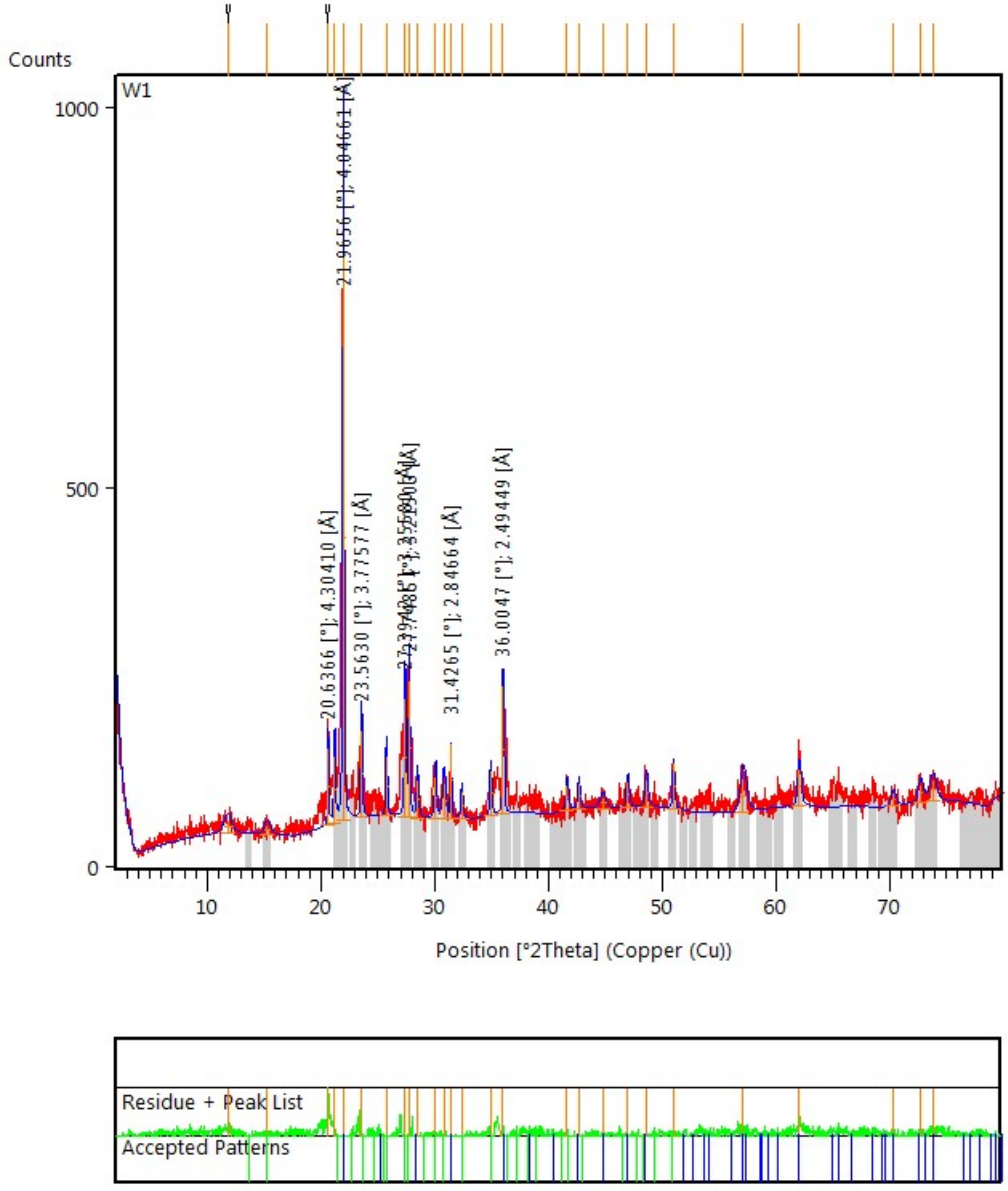

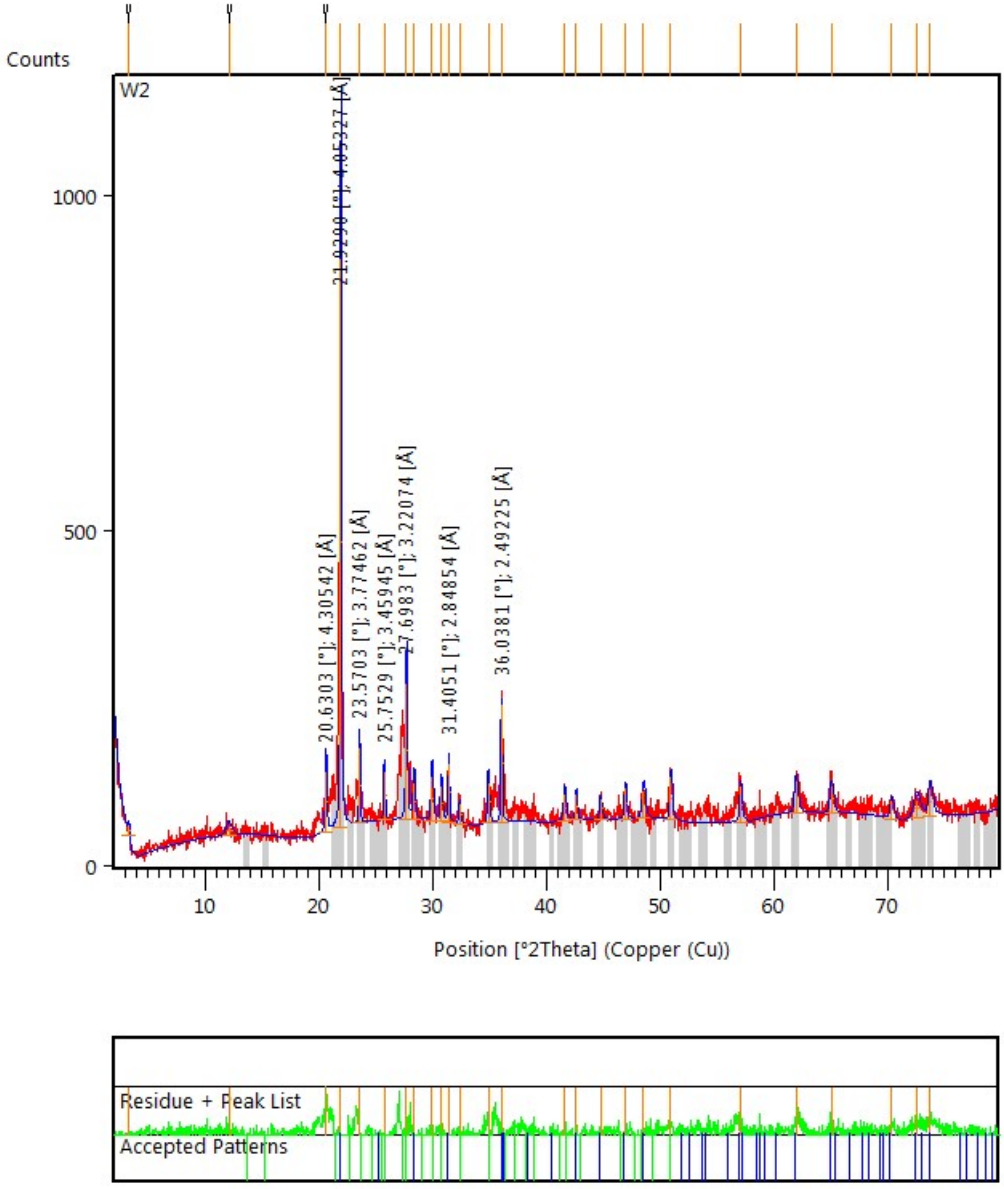
Counts
W2
1000
500
0
21.9290 [°]; 4.05327 [Å]
20.6303 [°]; 4.30542 [Å]
23.5703 [°]; 3.77462 [Å]
25.7529 [°]; 3.45945 [Å]
27.6983 [°]; 3.22074 [Å]
31.4051 [°]; 2.84854 [Å]
36.0381 [°]; 2.49225 [Å]
10
20
30
40
50
60
70
Position [°2Theta] (Copper (Cu))
Residue + Peak List
Accepted Patterns

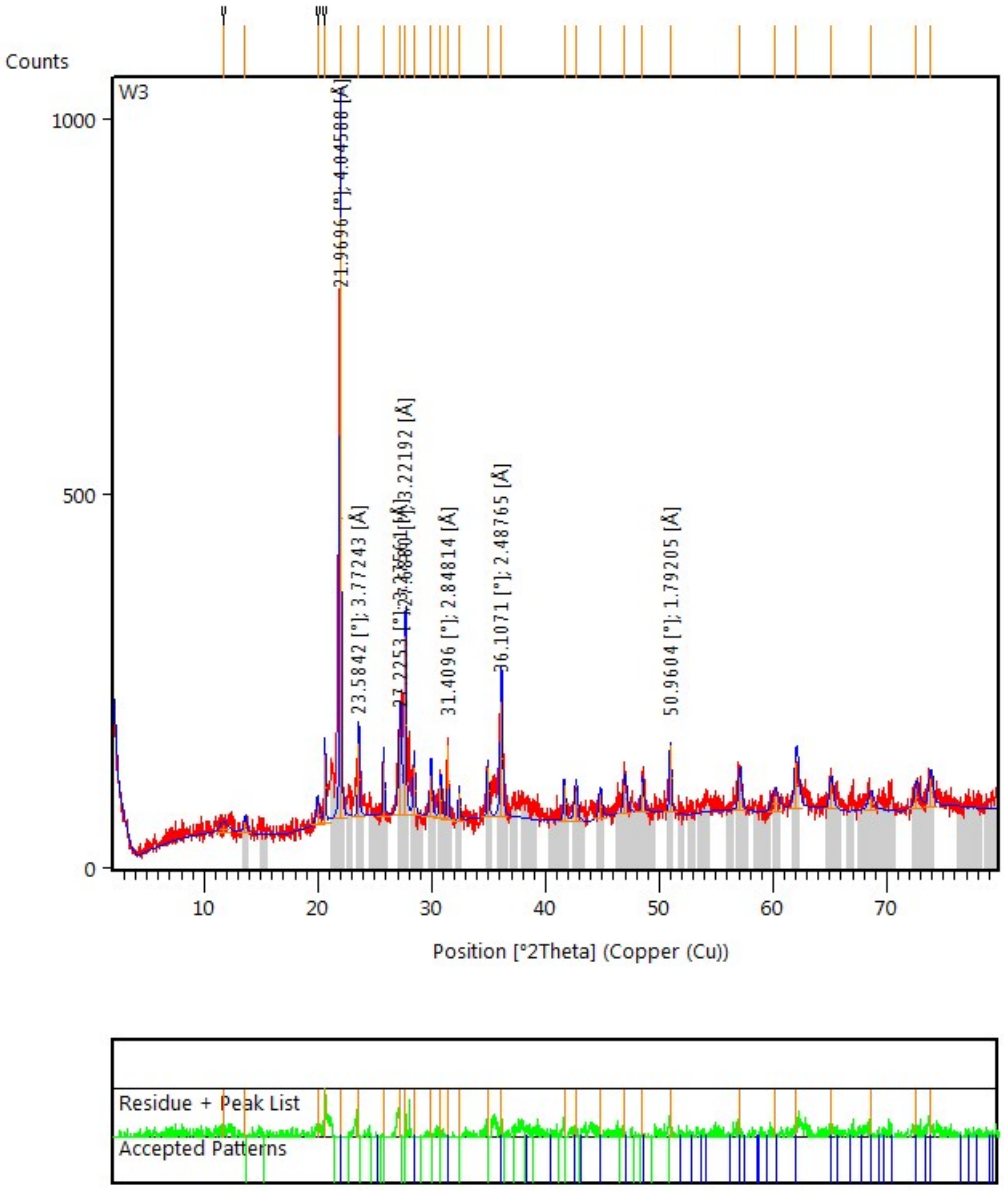
Counts
W3
1000
500
0
21.9696 [°]; 4.04508 [Å]
23.5842 [°]; 3.77243 [Å]
27.2253 [°]; 3.27601 [Å]
27.6860 [°]; 3.22192 [Å]
31.4096 [°]; 2.84814 [Å]
36.1071 [°]; 2.48765 [Å]
50.9604 [°]; 1.79205 [Å]
10
20
30
40
50
60
70
Position [°2Theta] (Copper (Cu))
Residue + Peak List
Accepted Patterns

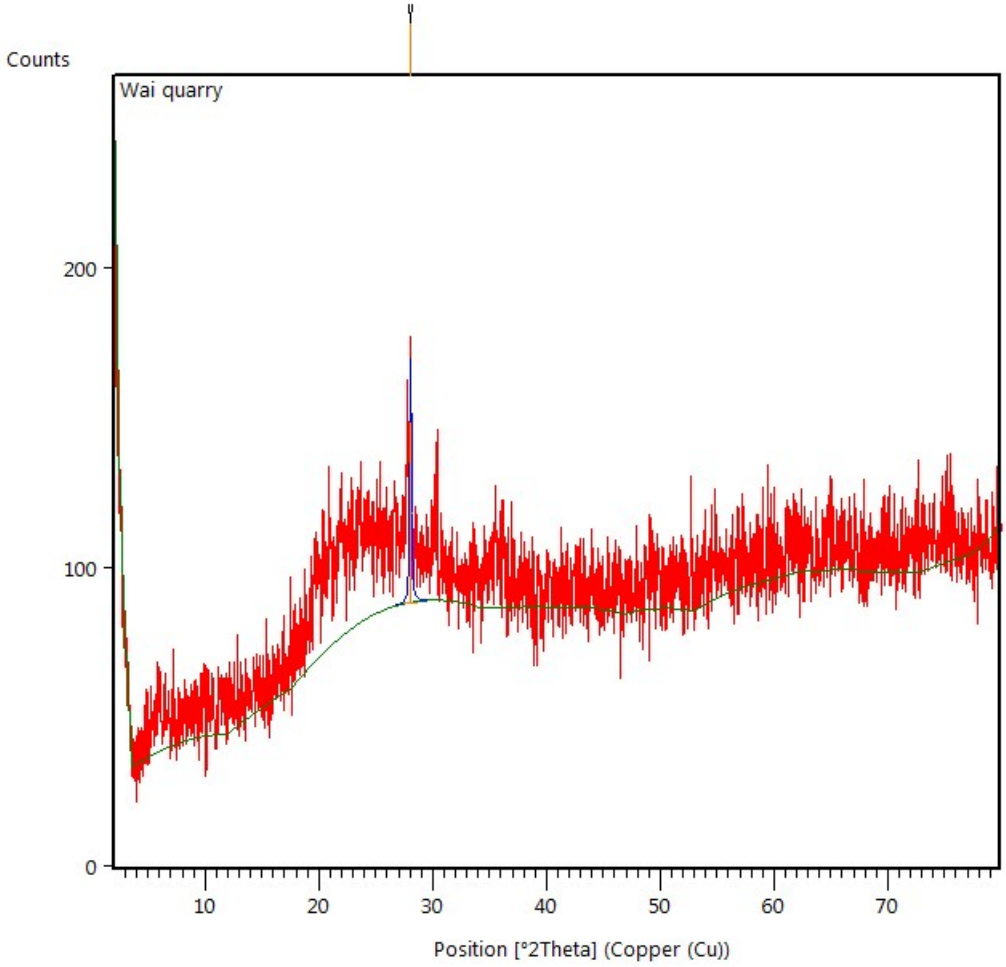
Counts
Wai quarry
200
100
0
10
20
30
40
50
60
70
Position [°2Theta] (Copper (Cu))

Appendix VII: XRF analysis list and results

UoW no.	Ignimbrite	Sample type	Sample number/locality
W150- 430	Owharoa	Pumice	11
W150-436	Owharoa	Pumice	11F
W150-401	Owharoa	Pumice	1 (1.2)
W150-428	Owharoa	Pumice	9
W150-411	Owharoa	Pumice	2.6
W150-443	Owharoa	Pumice	X.4
W150-437	Owharoa	Pumice	12.1
W150-443	Owharoa	Bulk	9-3-4
W150-427	Owharoa	Bulk	9-A
W150-400	Owharoa	Bulk	1-1
W150-402	Owharoa	Bulk	1-3
W150-425	Owharoa	Bulk	Samson Rd
W150-418	Waikino	Bulk	WQ

XRF results (normalised) for the Owharoa and Waikino ignimbrites												
UoW no.	**W150-436**	**W150-401**	**W150-437**	**W150-411**	**W150-443**	**W150-427**	**W150-430**	**W150-428**	**W150-400**	**W150-402**	**W150-425**	**W150-418**
Sample Name	**11F**	**1-2 OI**	**12-1**	**2-6 OI**	**9-3-4**	**9-A**	**L11**	**L9**	**OI 1-1**	**OI 1-3**	**Samson RD**	**WQ**
Sample type	**Pumice**	**Pumice**	**Pumice**	**Pumice**	**Bulk**	**Bulk**	**Pumice**	**Pumice**	**Bulk**	**Bulk**	**Bulk**	**Bulk**
Major Elements												
SiO2 (%)	73.15	73.65	76.09	74.54	72.18	77.16	76.29	73.40	74.49	74.91	72.36	72.08
TiO2 (%)	0.12	0.12	0.13	0.12	0.14	0.09	0.11	0.13	0.12	0.11	0.12	0.26
Al2O3 (%)	17.32	16.84	14.04	14.77	17.78	14.89	14.24	16.96	15.46	15.16	17.49	15.65
Fe2O3 (%)#	1.24	1.05	1.67	1.88	1.44	1.03	1.11	1.35	1.29	1.08	1.98	4.08
MnO (%)	0.03	0.02	0.05	0.02	0.07	0.02	0.02	0.02	0.04	0.03	0.02	0.10
MgO (%)	0.34	0.25	0.11	0.27	0.29	0.35	0.11	0.25	0.26	0.25	0.34	0.64
CaO (%)	1.04	1.08	1.22	1.18	1.19	1.06	1.16	1.10	1.11	1.05	1.10	1.46
Na2O (%)	2.46	2.80	2.77	3.32	3.07	1.79	2.71	2.70	2.85	2.98	2.49	2.76
K2O (%)	4.30	4.18	3.90	3.90	3.84	3.61	4.22	4.09	4.39	4.44	4.09	2.98
P2O5 (%)	0.00	0.00	0.03	0.00	0.01	0.00	0.02	0.00	0.00	0.00	0.00	0.00
LOI (%)*	5.43	4.68	5.11	4.09	5.59	6.72	4.37	5.03	4.30	3.99	5.12	5.76
Sum (%)*	99.61	99.71	98.58	99.72	99.71	99.35	100.13	99.74	99.73	99.70	99.73	99.52

Trace Elements													
F (PPM)	485	446	397	531	513	287	425	467	442	434	535	610
S (PPM)	0	0	0	0	89	3198	0	0	0	0	32	123
Cl (PPM)	1912	996	563	955	793	1536	794	852	902	1031	656	2282
Sc (PPM)	6	6	6	5	7	6	4	5	5	6	6	13
V (PPM)	4	2	5	4	7	5	4	6	5	3	4	12
Cr (PPM)	0	0	0	0	0	0	0	0	0	0	0	0
Co (PPM)	55	46	54	35	44	18	117	48	65	227	60	11
Ni (PPM)	7	7	6	3	4	5	9	5	6	11	5	3
Cu (PPM)	8	6	6	6	6	7	5	7	6	6	8	4
Zn (PPM)	31	28	37	31	52	26	28	42	28	21	50	87
Ga (PPM)	18	16	17	15	17	13	16	15	15	14	16	17
As (PPM)	7	10	8	7	7	5	13	6	8	8	7	8
Rb (PPM)	139	125	147	130	127	122	149	130	139	142	132	104
Sr (PPM)	75	79	87	85	81	77	73	78	77	73	77	104
Y (PPM)	24	22	29	21	21	18	22	23	22	23	37	48
Zr (PPM)	104	106	106	100	111	78	99	104	96	92	106	239
Nb (PPM)	7	8	7	7	7	6	6	7	7	7	7	9
Mo (PPM)	1	1	4	1	1	1	4	1	1	1	1	2
Sn (PPM)	5	6	6	4	4	5	4	5	5	6	6	5
Sb (PPM)	3	3	4	2	2	3	2	2	2	3	2	2
Cs (PPM)	8	6	8	5	9	7	8	5	7	8	6	3

Ba (PPM)	885	913	918	867	891	945	897	838	891	895	847	847
La (PPM)	28	20	34	27	26	16	24	22	19	20	52	34
Ce (PPM)	58	53	63	56	70	42	62	57	61	55	65	72
Nd (PPM)	23	20	25	23	26	17	25	27	22	22	34	34
Tl (PPM)	0	0	1	0	0	0	1	0	0	0	0	0
Pb (PPM)	17	18	21	18	21	16	18	21	16	14	19	26
Th (PPM)	16	16	16	14	15	14	15	15	14	14	15	13
U (PPM)	4	4	4	3	4	4	4	4	3	3	3	3

* Numbers are given in raw form. Remaining data is normalised. Trace data is raw data. # Fe203 is for all Fe.

Appendix VIII: Electron Microprobe analysis

Normalised Glass analysis

Normalised data for the Owharoa Ignimbrite for the glass shard samples under the electron microprobe								
UoW no.	**-**	**-**	**W150-400**	**W150-400**	**W150-400**	**W150-400**	**W150-400**	**W150-400**
Sample no.	**standard-01**	**Standard-02**	**1.1.1-04**	**1.1.1-07**	**1.1.1-08**	**1.1.1-09**	**1.1.1-10**	**1.1.1-11**
	wt%	**wt%**	**wt%**	**wt%**	**wt%**	**wt%**	**wt%**	**wt%**
SiO_2	77.836	77.721	74.811	74.678	74.773	74.384	73.707	73.661
TiO_2	0.065	0.083	0.366	0.360	0.411	0.394	0.397	0.444
Al_2O_3	12.159	12.214	14.117	14.202	14.191	14.554	14.524	14.823
FeO	1.128	1.084	2.221	2.402	2.278	2.413	2.618	2.567
MnO	0.049	0.000	0.073	0.035	0.051	0.039	0.044	0.053
MgO	0.009	0.028	0.442	0.433	0.440	0.486	0.495	0.570
CaO	0.454	0.459	2.100	2.147	2.120	2.142	2.201	2.499
Na_2O	3.222	3.437	2.888	2.797	2.794	2.962	2.999	2.694
K_2O	5.007	4.911	2.850	2.789	2.813	2.486	2.803	2.552
Cl	0.093	0.079	0.168	0.204	0.169	0.181	0.274	0.178
Total *	97.988	98.449	95.705	95.532	95.493	95.432	95.159	91.764

* Numbers are given in raw form. Remaining data is normalised

UoW no.	W150-400	W150-400	W150-400	W150-400	W150-402	W150-402	W150-402	W150-402
Sample no.	1.1.1-12	1.1.1-13	1.1.1-14	1.1.1-15	1.3.2-01	1.3.2-02	1.3.2-03	1.3.2-04
	wt%	wt%	wt%	wt%	wt%	wt%	wt%	wt%
SiO_2	76.187	73.923	73.417	75.494	74.610	74.947	75.092	53.081
TiO_2	0.272	0.421	0.424	0.346	0.341	0.322	0.345	0.019
Al_2O_3	13.627	14.662	14.777	14.176	14.791	14.136	14.058	29.673
FeO	1.917	2.519	2.525	2.386	1.946	2.257	1.939	0.575
MnO	0.042	0.083	0.034	0.017	0.051	0.030	0.068	0.000
MgO	0.277	0.523	0.539	0.418	0.414	0.382	0.353	0.038
CaO	1.643	2.427	2.440	1.955	1.915	1.979	2.015	12.575
Na_2O	2.937	2.758	2.994	2.281	2.919	2.951	3.034	3.852
K_2O	2.956	2.537	2.717	2.800	2.850	2.834	2.948	0.183
Cl	0.183	0.191	0.171	0.162	0.211	0.210	0.192	0.008
Total *	95.515	94.12	95.696	93.843	95.956	96.642	97.079	100.679

* Numbers are given in raw form. Remaining data is normalised

UoW no.	W150-402	W150-402	W150-402	W150-402	W150-402	W150-402	W150-402	W150-402
Sample no.	1.3.2-05	1.3.2-06	1.3.2-07	1.3.2-08	1.3.2-09	1.3.2-10	1.3.2-11	1.3.2-12
	wt%	wt%	wt%	wt%	wt%	wt%	wt%	wt%
SiO_2	75.102	74.865	74.755	74.931	75.185	75.058	74.875	74.753
TiO_2	0.338	0.327	0.333	0.320	0.346	0.329	0.320	0.347
Al_2O_3	14.098	13.963	14.488	14.034	13.942	13.701	13.945	14.109
FeO	2.083	2.113	2.139	1.956	2.118	2.135	2.091	2.171
MnO	0.035	0.036	0.024	0.044	0.052	0.091	0.074	0.070
MgO	0.358	0.402	0.361	0.377	0.408	0.391	0.333	0.384
CaO	1.965	1.990	1.921	1.978	1.981	2.006	1.972	1.987
Na_2O	2.891	3.033	2.950	3.161	2.984	3.241	3.242	3.226
K_2O	2.979	3.104	2.879	3.056	2.838	2.903	2.994	2.807
Cl	0.194	0.215	0.192	0.187	0.188	0.187	0.200	0.189
Total *	96.382	93.287	93.003	96.318	96.064	96.343	97.002	97.103

* Numbers are given in raw form. Remaining data is normalised

UoW no. / Sample no.	W150-402 1.3.2-13	W150-402 1.3.2-14	W150-402 1.3.2-15
	wt%	wt%	wt%
SiO_2	75.36761	75.06942	75.42156
TiO_2	0.315093	0.315851	0.312961
Al_2O_3	14.10952	13.95114	14.01522
FeO	2.139099	2.123223	2.066172
MnO	0.041596	0.078447	0.010467
MgO	0.376448	0.364365	0.359016
CaO	1.959194	1.860014	1.969876
Na_2O	2.843119	3.163675	2.91818
K_2O	2.703771	2.956204	2.76955
Cl	0.187184	0.151733	0.203058
Total *	96.162	96.881	95.539

* Numbers are given in raw form. Remaining data is normalised

Normalised data for the Waikino Ignimbrite for the glass shard samples under the electron microprobe											
UoW no.	**W150-440**	**W150-440**	**W150-440**	**W150-440**	**W150-440**	**W150-440**	**W150-440**	**W150-440**	**W150-440**	**W150-440**	**W150-440**
Glass samples	**W3-Glass-shards-1**	**W3-Glass-shards-2**	**W3-Glass-shards-3**	**W3-Glass-shards-4**	**W3-Glass-shards-5**	**W3-Glass-shards-6**	**WAI1-Glass-shards-1**	**WAI1-Glass-shards-2**	**WAI1-Glass-shards-2**	**WAI1 - Glass shards 3**	**WAI1-Glass-shards-4**
	wt%	**wt%**	**wt%**	**wt%**	**wt%**	**wt%**	**Wt%**	**wt%**	**wt%**	**wt%**	**wt%**
SiO_2	90.923	72.690	70.875	74.676	74.313	75.693	77.706	85.772	74.816	71.580	75.550
TiO_2	0.050	0.046	0.065	0.038	0.263	0.046	0.077	0.066	0.023	0.042	0.136
Al_2O_3	5.253	15.903	17.932	14.394	14.496	13.852	12.265	8.110	15.037	15.117	13.813
FeO	0.082	0.479	0.792	0.275	0.279	0.183	1.076	0.334	0.189	3.707	0.602
MnO	0.000	0.000	0.018	0.021	0.005	0.005	0.000	0.015	0.000	0.024	0.013
MgO	0.000	0.021	0.031	0.008	0.000	0.000	0.016	0.013	0.009	0.016	0.025
CaO	0.176	0.340	0.348	0.553	0.524	0.322	0.443	0.250	0.391	0.364	0.409
Na_2O	1.198	3.150	2.881	3.746	3.631	2.805	3.330	2.016	3.319	2.821	2.991
K_2O	2.303	7.356	6.997	6.120	6.439	7.043	5.021	3.344	6.195	6.251	6.383
Cl	0.019	0.021	0.079	0.217	0.064	0.066	0.084	0.102	0.025	0.101	0.099
Total*	99.318	96.573	94.168	96.228	95.060	94.630	99.520	96.359	99.385	92.883	96.344

* Numbers are given in raw form. Remaining data is normalised

Raw plagioclase analysis

Raw plagioclase data for the Owharoa and Waikino ignimbrites from electron microprobe analysis										
UoW no.	**-**	**-**	**W150-440**	**W150-440**	**W150-440**	**W150-440**	**W150-440**	**W150-440**	**W150-440**	**W150-440**
Sample no.	**Plagioclase-01**	**Plagioclase-02**	**WAI1-Plagioclase-a**	**WAI1-Plagioclase-a-rim**	**WAI1-Plagioclase-b**	**WAI1-Plagioclase-b-rim**	**WAI1-Plagioclase-c-centre**	**WAI1-Plagioclase-c-middle**	**WAI1-Plagioclase-c-rim**	**WAI1-plagioclase-f-centre**
SiO_2	50.605	50.776	60.014	60.299	0.104	11.417	60.072	59.859	59.439	57.605
TiO_2	0.023	0.044	0	0	42.225	35.033	0	0	0	0
Al_2O_3	31.287	31.318	25.707	25.766	0.085	0.261	25.407	26.144	26.001	26.843
FeO	0.593	0.434	0.262	0.302	66.287	48.396	0.219	0.226	0.246	0.369
MgO	0.117	0.14	0	0.013	1.063	0.82	0	0	0.005	0.006
CaO	14.045	13.994	6.931	6.922	0	0	6.922	7.165	7.48	8.468
Na_2O	3.449	3.251	6.27	6.012	0.038	0.02	6.368	6.288	6.309	6.079
K_2O	0.119	0.102	0.412	0.385	0.006	0.015	0.411	0.398	0.36	0.318
Total	100.238	100.059	99.596	99.699	109.808	95.962	99.399	100.08	99.84	99.688

UoW no.	W150-440	W150-440	W150-440	W150-440	W150-440	W150-440	W150-440	W150-406	W150-406	W150-406
Sample no.	WAI1-plagioclase-g-centre	WAI1-plagioclase-h-rim	WAI1-plagioclase-i-centre	WAI1-plagioclase-i-middle	WAI1-plagioclase-i-rim	WAI1-Plagioclase-k-center	WAI1-Plagioclase-k-middle	OF2-1-Plagioclase-1	OF2-1-Plagioclase-2core	OF2-1-Plagioclase-2rim
SiO_2	60.184	59.125	59.861	59.883	60.676	59.048	59.069	62.034	60.441	56.414
TiO_2	0.004	0.001	0	0.009	0.007	0.009	0.007	0	0	0.031
Al_2O_3	25.063	25.74	25.784	25.096	24.695	24.526	25.505	24.364	25.23	24.694
FeO	0.286	0.268	0.311	0.21	0.215	0.291	0.195	0.244	0.217	2.34
MgO	0.011	0.018	0.018	0.014	0	0.014	0.005	0	0	0.404
CaO	6.587	7.286	7.29	6.463	6.024	5.999	7.012	5.512	6.443	4.112
Na_2O	6.393	6.286	4.73	6.666	6.969	6.874	6.471	6.813	6.441	4.858
K_2O	0.465	0.445	0.406	0.478	0.519	0.493	0.378	0.49	0.52	0.688
Total	98.993	99.169	98.4	98.819	99.105	97.254	98.642	99.457	99.292	93.541

UoW no.	W150-406 OF2-1-	W150-406 OF2-1-	W150-406 OF2-1-	W150-406 OF2-1-	W150-406 OF2-1-	W150-406 OF2-1-	W150-406 OF2-1-	W150-406 OF2-1-	W150-406 OF2-1-	W150-406 OF2-1-
Sample no.	Plagioclase-4core	Plagioclase-4middle	Plagioclase-4rim	Plagioclase-5-core	Plagioclase-5-rim	Plagioclase-7-core	Plagioclase-7-rim	Plagioclase-8-core	Plagioclase-8-rim	Plagioclase-9-core
SiO_2	60.626	60.366	59.752	59.447	59.788	61.652	64.532	61.877	57.864	76.277
TiO_2	0	0.005	0.01	0	0	0	0.002	0	0	0.078
Al_2O_3	26.32	25.37	24.509	25.665	25.75	25.899	27.038	24.536	25.789	12.722
FeO	0.181	0.107	0.185	0.183	0.168	0.103	0.246	0.201	0.275	1.122
MgO	0	0	0.013	0	0	0	0.005	0.01	0	0.079
CaO	6.126	6.597	6.225	6.727	6.867	6.306	6.339	5.328	7.284	0.761
Na_2O	8.512	6.752	5.77	7.025	6.139	6.792	8.336	6.928	6.959	1.043
K_2O	0.55	0.471	0.521	0.464	0.44	0.54	0.542	0.6	0.528	1.829
Total	**102.315**	**99.668**	**96.985**	**99.511**	**99.152**	**101.292**	**107.04**	**99.48**	**98.699**	**93.911**

UoW no	W150-406 OF2-1-	W150-406 OF2-1-	W150-406 OF2-1-	W150-406 OF2-1-	W150-440 W3-	W150-440 W3-	W150-440 W3-	W150-440 W3-	W150-440 W3-	W150-440 W3-
Sample no.	Plagioclase -11-rim	Plagioclase -11-core	Plagioclase -12-core	Plagioclase -12-rim	Plagioclase -1-center	Plagioclase -1-mid	Plagioclase -1-rim	Plagioclase -2-middle	Plagioclase -3- centre	Plagioclase -3-rim
SiO_2	61.357	60.106	60.801	61.88	59.768	59.304	59.048	59.558	55.774	56.731
TiO_2	0	0	0	0	0	0	0	0.006	0	0
Al_2O_3	24.692	24.891	24.608	26.661	25.48	25.397	25.195	25.295	27.817	28.108
FeO	0.168	0.159	0.203	0.268	0.208	0.212	0.259	0.239	0.31	0.335
MgO	0.003	0	0.018	0.005	0.004	0.006	0.005	0.007	0.009	0.008
CaO	5.872	6.231	5.936	6.757	6.986	7.126	7.072	6.839	9.633	9.614
Na_2O	6.703	6.876	7.026	7.626	6.69	6.778	6.605	6.724	5.634	5.483
K_2O	0.563	0.521	0.559	0.57	0.401	0.39	0.402	0.427	0.236	0.247
Total	99.358	98.784	99.151	103.767	99.537	99.213	98.586	99.095	99.413	100.526

UoW no	W150-440	W150-440	W150-440	W150-440	W150-440	W150-440	W150-440	W150-440	W150-440	W150-443
Sample no.	W3-Plagioclase-4-centre	W3-Plagioclase-5-center	W3-Plagioclase-5-rim	W3-Plagioclase-5-bottom	W3-Plagioclase-5-top	W3-Plagioclase-6-center	W3-Plagioclase-6-rim	W3-Plagioclase-8	W3-Plagioclase-9-end	McH1-Plagioclase-1
SiO_2	55.944	57.673	60.419	60.078	58.95	59.899	58.988	57.118	58.725	61.194
TiO_2	0.005	0	0.009	0.005	0	0.011	0	0	0.001	0.005
Al_2O_3	24.257	26.13	24.648	25.129	25.536	25.019	25.526	26.929	25.641	23.824
FeO	0.248	0.23	0.143	0.23	0.243	0.288	0.266	0.228	0.283	0.183
MgO	0.022	0.019	0	0.01	0.004	0	0	0.006	0	0.007
CaO	6.301	8.055	6.087	6.633	7.166	6.605	7.15	8.624	7.343	5.388
Na_2O	5.938	6.28	7.047	6.809	6.208	6.755	6.427	5.966	6.597	7.503
K_2O	0.758	0.309	0.518	0.443	0.417	0.417	0.404	0.301	0.386	0.659
Total	93.473	98.696	98.871	99.337	98.524	98.994	98.761	99.172	98.976	98.763

UoW no	W150-443 McH1-Plagioclase-2b	W150-443 McH1-Plagioclase-2c	W150-443 McH1-Plagioclase-3-rim	W150-443 McH1-Plagioclase-3-centre	W150-443 McH1-Plagioclase-4-centre	W150-443 McH1-Plagioclase-4-rim	W150-443 McH1-Plagioclase-5-centre	W150-443 McH1-Plagioclase-5-mid	W150-443 McH1-Plagioclase-5-rim	W150-443 McH1-Plagioclase-7-centre
Sample no.										
SiO_2	60.431	60.259	59.507	59.224	60.049	59.624	58.909	58.77	58.507	58.56
TiO_2	0	0	0.005	0	0	0	0	0	0.005	0
Al_2O_3	24.166	24.388	24.883	25.003	24.649	24.92	25.506	25.574	25.259	25.392
FeO	0.134	0.145	0.168	0.125	0.195	0.15	0.188	0.157	0.163	0.134
MgO	0.003	0.017	0.001	0.017	0.003	0	0.004	0.006	0.005	0.004
CaO	5.877	6.032	6.582	6.603	6.189	6.575	7.273	7.299	7.11	7.122
Na_2O	7.389	7.269	7.043	6.998	7.195	7.118	6.711	6.702	6.739	6.744
K_2O	0.571	0.532	0.53	0.518	0.536	0.537	0.465	0.429	0.488	0.466
Total	98.571	98.642	98.719	98.488	98.816	98.924	99.056	98.937	98.276	98.422

UoW no.	W150-443	W150-443	W150-443	W150-443	W150-443	W150-443	W150-443	W150-406	W150-406	W150-406
Sample no.	McH1-Plagioclase-7-rim	McH1-Plagioclase-9-centre	McH1-Plagioclase-9-mid	McH1-Plagioclase-9-rim	McH1-Plagioclase-10-mid	McH1-Plagioclase-11-centre	McH1-Plagioclase-11-rim	P-Plagioclase-1P-rim	P-Plagioclase-2-centre	P-Plagioclase-2-rim
SiO_2	58.819	60.647	60.996	59.062	57.299	54.959	66.317	59.539	59.92	59.888
TiO_2	0	0	0	0	0.002	0.008	0.022	0	0	0
Al_2O_3	25.637	24.331	24.098	25.297	26.597	28.218	22.164	25.241	25.217	25.374
FeO	0.212	0.172	0.145	0.109	0.19	0.188	0.233	0.168	0.118	0.174
MgO	0	0.008	0	0	0.009	0	0.023	0.006	0	0.004
CaO	7.256	5.648	5.545	6.734	8.454	10.122	4.516	6.633	6.615	6.772
Na_2O	6.857	7.416	7.546	6.721	6.124	5.439	5.958	6.938	6.781	6.953
K_2O	0.455	0.607	0.618	0.466	0.405	0.308	0.96	0.468	0.523	0.459
Total	99.236	98.829	98.948	98.389	99.08	99.242	100.193	98.993	99.174	99.624

UoW no.	W150-406	W150-406	W150-406	W150-406	W150-406	W150-406	W150-406	W150-406	W150-406	W150-406
Sample no.	P-Plagioclase-3-centre	P-Plagioclase-3-rim	P-Plagioclase-4-centre	P-Plagioclase-11-centre	P-Plagioclase-12-centre	P-Plagioclase-12-rim	P-Plagioclase-13-t4	P-Plagioclase-13-t3	P-Plagioclase-13-t2	P-Plagioclase-13-t1
SiO_2	60.403	60.759	60.637	55.59	60.263	60.168	61.314	60.584	60.864	60.993
TiO_2	0	0	0	0.012	0	0	0	0	0	0.005
Al_2O_3	24.512	24.526	24.504	27.75	24.607	24.833	24.331	24.696	24.496	24.274
FeO	0.127	0.159	0.114	0.321	0.067	0.181	0.1	0.074	0.219	0.123
MgO	0	0	0	0.019	0	0	0	0.014	0.003	0.009
CaO	5.85	5.766	5.894	9.906	5.952	6.167	5.475	5.918	5.743	5.493
Na_2O	7.194	7.196	7.142	5.368	7.28	6.976	7.36	7.09	7.205	7.364
K_2O	0.581	0.567	0.546	0.138	0.526	0.513	0.659	0.572	0.657	0.62
Total	98.667	98.973	98.837	99.104	98.695	98.838	99.239	98.948	99.187	98.881

UoW no.	W150-406	W150-406	W150-406	W150-406	W150-406	W150-406	W150-406	W150-406	W150-406	W150-406
Sample no.	P-Plagioclase-14-centre	OF2-2-Plagioclase-1-rim	OF2-2-Plagioclase-3-centre	OF2-2-Plagioclase-3-rim	OF2-2-Plagioclase-4-centre	OF2-2-Plagioclase-4-rim	OF2-2-Plagioclase-5	OF2-2-Plagioclase-6-centre	OF2-2-Plagioclase-6-rim	OF2-2-Plagioclase-7-cluster-SEcenter
SiO_2	60.205	56.12	55.755	60.778	59.092	58.866	59.216	60.284	59.265	60.137
TiO_2	0	0	0	0	0.004	0	0	0	0	0
Al_2O_3	24.947	27.57	24.047	24.42	25.798	25.7	25.52	24.74	25.182	25.198
FeO	0.156	0.277	0.138	0.183	0.179	0.192	0.179	0.112	0.141	0.15
MgO	0	0.022	0.014	0.01	0	0.005	0	0.007	0.003	0
CaO	6.284	9.728	6.751	5.92	7.164	7.096	6.964	6.2	6.658	6.443
Na_2O	7.006	5.485	6.932	6.075	6.759	6.791	6.778	6.915	7.032	7.013
K_2O	0.483	0.303	0.52	0.572	0.448	0.473	0.483	0.589	0.529	0.492
Total	99.081	99.505	94.157	97.958	99.444	99.123	99.14	98.847	98.81	99.433

UoW no.	W150-406	W150-406	W150-406	W150-406	W150-406	W150-406
Sample no.	OF2-2-Plagioclase-7-cluster-lowercenter	OF2-2-Plagioclase-7-cluster-topmidcente	OF2-2-Plagioclase-8-center	OF2-2-Plagioclase-8-rim	OF2-2-Plagioclase-Z-Left	OF2-2-Plagioclase-Z-right
SiO_2	60.942	59.881	57.147	58.669	59.17	57.8
TiO_2	0	0	0.008	0.007	0	0.003
Al_2O_3	24.664	25.131	27.163	25.94	25.581	25.048
FeO	0.069	0.246	0.237	0.252	0.234	0.564
MgO	0	0.011	0.001	0	0.01	0.008
CaO	5.734	6.434	8.684	7.35	7.094	7.109
Na_2O	7.302	7.065	6.131	6.766	6.539	6.695
K_2O	0.61	0.47	0.339	0.434	0.407	0.43
Total	99.321	99.238	99.71	99.418	99.035	97.657

Raw biotite analysis

Raw data for the biotite crystals within the Owharoa and Waikino Ignimbrites from the Electron microprobe								
UoW no.	**W150-406**	**W150-443**	**W150-443**	**W150-407**	**W150-407**	**W150-407**	**W150-440**	**W150-440**
Sample name	**OF2-1-Biotite-1**	**McH 1 a**	**McH-Biotite-or-opaque**	**OF2-2-Biotite-1a**	**OF2-2-Biotite-1b**	**OF2-2-Biotite-1c**	**WAI1-Biotite-1**	**WAI1-Biotite-1a**
SiO_2	35.453	63.377	60.968	35.66	36.021	34.804	48.261	45.216
TiO_2	3.896	0.047	0.046	3.532	3.638	3.898	0.03	0.04
Al_2O_3	14.038	10.657	19.947	14.546	14.425	13.777	18.661	18.397
FeO	25.097	0.274	1.25	22.935	24.497	25.187	19.499	18.589
MnO	0.138	0.022	0.032	0.135	0.138	0.088	0.004	0
MgO	8.217	0.093	0.091	7.993	8.506	8.226	0.293	0.287
CaO	0.347	26.534	10.471	0.901	0.615	0.238	16.103	17.951
Na_2O	1.306	3.441	3.76	1.054	1.14	1.166	0.09	0.106
K_2O	12.71	2.779	3.737	11.874	12.836	12.686	0.335	0.299
Total	101.202	107.224	100.302	98.63	101.816	100.07	103.276	100.885

Raw opaque minerals analysis within the Owharoa and Waikino ignimbrites

UoW no.	-	-	W150-440	W150-440	W150-440	W150-440	W150-440	W150-440	W150-406	W150-440	W150-440
Opaque Sample	Magnetite -01 Standard	Ilmenite 1 Standard	WAI1-1-center	WAI1-1.1-center	WAI1-4-center	WAI1-6-center	WAI1-9-center	WAI1-10-center	OF2-1-4	W3-2	W3- -6
SiO_2	0.007	0.005	9.589	20.003	23.425	0.028	0	16.62	0.958	75.141	0.117
TiO_2	0.158	45.989	8.129	14.803	28.284	47.911	50.166	29.234	17.208	13.087	22.491
Al_2O_3	0.008	0.004	0.486	0.438	0.229	0.054	0.003	0.326	1.483	3.58	0.402
FeO	91.13	45.563	71.457	57.068	41.624	47.55	44.955	46.545	69.848	5.166	66.094
MnO	0.06	4.616	0.535	0.558	0.975	0.852	1.138	0.978	0.398	0.131	0.992
MgO	0.077	0.304	0.271	0.422	0.76	0.558	0.658	0.753	0.356	0.14	0.819
Cr_2O_3	0.323	0.015	0.051	0.018	0.006	0	0.08	0.002	0.074	0	0
Total	91.763	96.496	90.518	93.31	95.303	96.953	97	94.458	90.325	97.245	90.915

UoW no. sample	W150-443 McH1-Opaque-4-center	W150-406 P-Opaque-2-center	W150-406 P-Opaque-2-rim	W150-406 P-Opaque-3-Westside	W150-406 P-Opaque-8-east	W150-406 P-Opaque-9
SiO_2	0.031	0.032	0.247	0	0.024	0
TiO_2	48.35	48.484	48.637	48.928	48.605	48.608
Al_2O_3	0.065	0.093	0.079	0.076	0.054	0.088
FeO	47.502	47.178	46.179	47.201	46.982	46.986
MgO	0.767	0.762	0.779	0.76	0.75	0.778
MnO	0.676	0.689	0.692	0.756	0.716	0.749
Cr_2O_3	0.008	0.021	0.029	0.001	0.023	0.03
Total	97.399	97.259	96.642	97.722	97.154	97.239